

3-29-2018


Sab Concentration Determines the Chemotherapeutic Efficacy in Gynecological Cancer

Iru Paudel

Florida International University, ipaud001@fiu.edu

DOI: 10.25148/etd.FIDC006535

Follow this and additional works at: <https://digitalcommons.fiu.edu/etd>

 Part of the [Analytical, Diagnostic and Therapeutic Techniques and Equipment Commons](#),
[Biology Commons](#), [Chemicals and Drugs Commons](#), and the [Medical Molecular Biology Commons](#)

Recommended Citation

Paudel, Iru, "Sab Concentration Determines the Chemotherapeutic Efficacy in Gynecological Cancer" (2018). *FIU Electronic Theses and Dissertations*. 3707.

<https://digitalcommons.fiu.edu/etd/3707>

This work is brought to you for free and open access by the University Graduate School at FIU Digital Commons. It has been accepted for inclusion in FIU Electronic Theses and Dissertations by an authorized administrator of FIU Digital Commons. For more information, please contact dcc@fiu.edu.

FLORIDA INTERNATIONAL UNIVERSITY

Miami, Florida

SAB CONCENTRATION DETERMINES THE CHEMOTHERAPEUTIC EFFICACY
IN GYNECOLOGICAL CANCER

A dissertation submitted in partial fulfillment of

the requirements for the degree of

DOCTOR OF PHILOSOPHY

in

BIOMEDICAL SCIENCES

by

Iru Paudel

2018

To: Dean John Rock
College of Medicine

This dissertation, written by Iru Paudel, and entitled Sab concentration determines chemotherapeutic efficacy in gynecological cancer, having been approved in respect to style and intellectual content, is referred to you for judgment.

We have read this dissertation and recommend that it be approved.

Fenfei Leng

Helen Tempest

Dietrich Lorke

Jeremy W. Chambers, Major Professor

Date of Defense: March 29 2018.

The dissertation of Iru Paudel is approved.

Dean John Rock
College of Medicine

Andrés G. Gil
Vice President for Research and Economic Development
and Dean of the University Graduate School

Florida International University, 2018

© Copyright 2018 by Iru Paudel

All rights reserved.

DEDICATION

Dedicated to my wonderful family.

ACKNOWLEDGMENTS

I would like to express my sincere gratitude to my advisor Dr. Jeremy W. Chambers for his continuous support, inspiration, and guidance. It has been a great learning experience under his mentorship. In addition to being extremely helpful with the studies and research, Dr. Chambers was tremendously supportive in every aspect of life. Having a baby in the final year and finishing graduate school was extremely challenging which would not have been possible without Dr. Chambers support and encouragement. I could not have imagined a better advisor and mentor for my Ph.D. Thank you, Dr. Chambers!

I would like to thank all my committee members Drs. Fenfei Leng, Helen Tempest and Dietrich Lorke who pointed me in the right direction of my graduate research. I would also like to thank College of Medicine for the funding provided during my Ph.D.

It would not have been possible without my husband's help, who took care of our newborn while I was writing my dissertation. Thank you, Amrit for being always there for me.

Supurna, you were there when I was happy or when I needed to complain about so many things, when I was frustrated with my research and when my experiments were not working. Thank you for the friendship.

Lastly, I am grateful to my parents for their unwavering support and inspiration, my sister Luna and brother Shaishab for their support and love and my sweetheart Serene, who would sleep during night letting her mamma finish this dissertation.

ABSTRACT OF THE DISSERTATION
SAB CONCENTRATION DETERMINES THE CHEMOTHERAPEUTIC EFFICACY
IN GYNECOLOGICAL CANCER

by

Iru Paudel

Florida International University, 2018

Miami, Florida

Professor Jeremy W. Chambers, Major Professor

The American Cancer Society predicts there will be 110,070 new cases and 32,120 deaths due to gynecological malignancies in 2018. A major contributing factor to the high mortality associated with gynecological cancers is the recurrence of treatment-resistant tumors. Ovarian cancer (OC) remains the most lethal gynecological malignancy, yet the mechanisms responsible for regulating tumor resistance and vulnerability are largely unknown or undruggable. Therefore, the goal of this research is to identify mechanisms responsible for therapeutic resistance in gynecological cancers and discover innovative approaches to circumvent these molecular alterations. Our efforts began in OC where secondary analysis of gene expression data from OC studies revealed that Sab, an outer mitochondrial membrane (OMM) scaffold protein, was down-regulated in OC tumors compared to normal tissue controls. Our previous studies demonstrate that Sab-mediated OMM signaling induces cell death in cervical cancer. In the current study, we found that Sab concentrations corresponded to chemoresponsiveness in a panel of OC cells; wherein, OC cells with low Sab levels were chemoresistant. Dynamic BH3 profiling revealed that

cells with high Sab expression were primed for apoptosis. Furthermore, over-expression of Sab in chemoresistant cells enhanced apoptotic priming and restored cellular vulnerability to cisplatin/paclitaxel treatment. Additionally, an examination of treatment-resistant metastatic uterine cancer (UC) cells were found to have low Sab concentrations compared to vulnerable primary site-derived UC cells. Ectopic expression of Sab in chemoresistant UC cells enhanced the susceptibility towards megestrol acetate and BH3-mimetic ABT-737. To exploit the relationship between Sab concentrations and chemo-responsiveness in gynecological cancer cells, we developed a high-throughput screening assay to detect Sab levels in chemo-resistant OC cells. In collaboration with the Torrey Pines Institute for molecular studies, we have identified compounds that can increase Sab levels in resistant OC cells. The identified compounds improved the effectiveness of cisplatin/paclitaxel therapy. We propose that Sab may be a prognostic marker to discern personalized treatments for gynecological cancer patients. Furthermore, pharmacologically enhancing Sab-mediated signaling may increase the efficacy of chemotherapeutic agents, which would mean lower doses that would limit toxic side-effects.

TABLE OF CONTENTS

CHAPTER	PAGE
CHAPTER 1	1
LITERATURE REVIEW	1
Gynecological cancer	2
1. Ovarian cancer	2
1.1. OC Statistics.....	2
1.2. Clinical Stages of OC	3
1.3. Types of OC	3
1.4. Common OC features	5
1.5. OC chemotherapy mechanism of action and the involvement of JNK signaling	6
2. Uterine/Endometrial cancer	8
3. Cervical Cancer	8
4. c-Jun N-terminal kinase (JNK)	9
5. Bcl-2 superfamily of proteins	12
5.1. Interactions between Bcl-2 proteins	13
5.2. Bax activation	15
5.3. Bcl-2 proteins	16
5.3.1. Bcl-2.....	16
5.3.2. Bcl-xL	18
5.3.3. Mcl-1	20
5.3.4. Bim/Bmf	21
5.3.5. DP5/Hrk	23
5.3.6. PUMA.....	24
5.3.7. Bad	25
5.3.8. Bax and Bak.....	25
6. Mitochondrial permeabilization.....	26
7. Mitochondrial priming and BH3 profiling.....	27
8. SH3BP5 (Sab).....	28
8.1. Sab and JNK interaction	29
9. Conclusion	30
References.....	31
 CHAPTER 2	 47
HYPOTHESIS and RATIONALE	47
1. Problem statement.....	48
2. Hypothesis and rationale.....	48
3. Project Aims	49
4. Chapter Abstracts.....	49
5. References.....	53

CHAPTER 3	54
SAB CONCENTRATIONS INDICATE CHEMOTHERAPEUTIC SUSCEPTIBILITY IN OVARIAN CANCER CELL LINES	54
1. Introduction.....	55
2. Experimental procedures	58
3. Results.....	67
3.1.Sab expression is reduced in ovarian cancer.....	67
3.2.Ovarian cancer cell lines have distinct levels of Sab expression and mitochondrial JNK signaling.	70
3.3.Ovarian cancer cell lines with low Sab levels are resistant to chemotherapy agents	75
3.4.Ovarian cancer cell mitochondria with high Sab expression are primed for apoptosis	78
3.5.Ectopic expression of Sab induces apoptotic priming	79
3.6.Increasing Sab expression sensitizes SK-OV-3 cells to chemotherapies	83
4. Discussion.....	87
References.....	91
 CHAPTER 4	 99
SAB-MEDIATED SIGNALING SENSITIZES UTERINE CANCER CELLS TO CHEMOTHERAPY	99
1. Introduction.....	100
2. Materials and methods	103
3. Results.....	108
3.1.Sab expression is diminished in late-stage uterine cancer and recurrent disease	108
3.2.Metastatic AN-3-Ca cells have reduced chemosusceptibility	109
3.3.AN-3-Ca cells have diminished Sab concentrations	110
3.4.AN-3-Ca cells have increased anti-apoptotic Bcl-2 proteins resulting from diminished Sab levels	114
3.5.Silencing Sab expression in SKUT-1 cells induces chemoresistance	114
4. Discussion.....	119
References.....	123
 CHAPTER 5	 131
A HIGH-THROUGHPUT ASSAY TO SCREEN FOR COMPOUNDS ELEVATING SAB CONCENTRATIONS IN CHEMO-RESISTANT HUMAN OVARIAN CANCER CELLS	131
1. Introduction.....	132
2. Methods.....	135
3. Results.....	139
3.1.Development of a reliable ICW to detect Sab levels in human cell lines and	

OC cells	139
3.2.Pilot studies reveal that mitochondrial toxins and estrogens increase Sab expression	142
3.3.Examination of the scaffold ranking library from Torrey Pines Institute for Molecular Studies (TPIMS)	144
4. Discussion.....	148
References.....	152
 CHAPTER 6	 157
CONCLUSION.....	158
 APPENDICES	 162
 VITA.....	 171

LIST OF FIGURES

FIGURE	PAGE
1.1. JNK phosphorylation and activation occurs in response to the activation of upstream kinases, MKK and MKKK	10
1.2. Bcl-2 family of proteins with specific domains	13
1.3. BH-3 only proteins have multiple roles	17
3.1. Summary of Sab expression levels in six OC gene expression studies	70
3.2. The levels of Sab differ among OC cell lines and correspond to stress-induced mitochondrial JNK recruitment	73
3.3. Cisplatin/Paclitaxel treatment affects OC cell lines differently	77
3.4. OC cell lines with high Sab expression are primed for apoptosis and chemosensitive	80
3.5. Artificially elevating Sab expression in resistant OC cell increases vulnerability to chemotherapy	82
3.6. Inhibiting Sab mediated signaling in sensitive OC cells enhances resistance	85
4.1. Secondary analysis of Sab expression from uterine cancer microarray studies	109
4.2. Mitochondrial metabolism differs between AN-3-Ca and SKUT-1 cells	111
4.3. Sab concentrations are distinct in a metastatic cell line and a primary site-derived UC cell line	112
4.4. Increasing Sab concentrations restore chemosensitivity in AN-3-Ca cells	113
4.5. Silencing Sab in SKUT-1 cells make them chemoresistant	117
5.1. Validation of Sab specific antibody for assay development	140
5.2. Optimizing the ICW for detection of distinct levels of Sab in cells	141
5.3. A preliminary screen to examine Sab levels following pharmacological treatments	142
5.4. A redeveloped ICW for Sab detection in chemoresistant SK-OV-3 cells	143
5.5. A feasibility screen for detecting changes in Sab levels in SK-OV-3 cells	144
5.6. A scaffold ranking screen and compound criteria for the TPIMS library	146
5.7. A positional scanning screen to identify best-in-class compounds from the TPIMS library	147
5.8. Evaluation of family 1661 in SK-OV-3 cells	148

LIST OF TABLES

TABLE	PAGE
1.1. Gynecological cancer statistics	2
3.1. Summary of ovarian cancer expression studies and observed changes in Sab expression	68
3.2. Cell-based IC ₅₀ values (μm) for chemotherapeutic agents in OC cell lines	76
4.1. IC ₅₀ values for Common Chemotherapy agents for UC cell lines	111
4.2. IC ₅₀ values for Chemotherapy agents in AN-3-Ca cells with increasing Sab expression	116
4.3. IC ₅₀ values for chemotherapy agents in SKUT-1 cells with diminished Sab expression	119

ABBREVIATIONS AND ACRONYMS

ACRONYM/ ABBREVIATION	TERM
ACS	American Cancer Society
APAF-1	Apoptotic protease activating factor-1
BC	Bcl-2 core
CDC	Center for Disease Control
CDK	Cyclin-dependent kinase
DMF	Dimethylformamide
DMSO	Dimethyl sulfoxide
DNA	Deoxy-ribonucleic acid
EOC	Epithelial ovarian carcinoma
ERK	Extracellular related kinase
FCCP	Trifluoromethoxy carbonylcyanide phenylhydrazone
FIGO	Federation of Gynecological Oncologists
FRET	Fluorescence resonance energy transfer
G2-M	Gap 2 to mitosis
JNK	c-Jun N-terminal kinase
ICW	In-cell western
IL-3	Interleukin-3
IMM	Inner mitochondrial membrane

KIM	Kinase interaction motif
MAPK	Mitogen-activated protein kinase
MEF	Mouse embryonic fibroblast
MMP	Mitochondrial membrane potential
MMR	Mismatch repair
OMMP	Mitochondrial outer membrane permeabilization
NER	Nucleotide excision repair
NGF	Nerve growth factor
NMR	Nuclear magnetic resonance
OC	Ovarian Cancer
OMM	Outer mitochondrial membrane
PBS	Phosphate buffered saline
PBST	Phosphate buffered saline with tween-20
PCR	Polymerase chain reaction
PI3K	Phosphoinositide 3-kinase
PKA	Protein kinase A
SMAC	Second mitochondria-derived activator of caspase
STS	Staurosporine
TNF- α	Tumor necrosis factor alpha
UC	Uterine cancer

Chapter 1
LITERATURE REVIEW

Gynecological cancer

Five different types of cancer arise within the reproductive organs of women are termed together as gynecological cancer. These include cervical, ovarian, uterine, vaginal and vulvar cancers. Each gynecological malignancy is uniquely characterized by different diagnostic signatures, symptoms, and pathogenesis (CDC). The projected statistics for gynecological cancer for 2018 is enlisted in table 1.1 [1]. Ovarian cancer is the most lethal gynecological malignancy [2], and we will focus mostly on it.

1. Ovarian Cancer

1.1. OC Statistics: Ovarian cancer (OC) is the gynecological malignancy with the greatest mortality. OC accounts for approximately 4% of all cancer in the women and is the seventh most common cancer worldwide [2]. In the United States, according to American Cancer Society (ACS), the estimated number of new cases of OC in 2017 was 22,440, and the estimated number of deaths was 14,080. The overall five-year survival rate for OC is 46.5% (2007-2013). In a woman's lifetime, the risk of developing an invasive form of OC is 1 in 79, and the resulting risk of death is 1 in 109 [2]. These statistics demonstrate gravity associated with OC and the demand for better treatment.

Table 1.1: Gynecological cancer statistics

2018 Cancer Projections	Incidence (cases)	Mortality (cases)
Uterine (Endometrium)	63,230	11,350
Ovarian	22,240	14,070
Cervical	13,240	4,170
Vaginal	5,170	1,330
Vulvar	6,190	1,200

1.2. Clinical Stages of OC: For effective treatment, OC is divided into different stages based on how far it has spread and what organs are affected in patients. It is called the FIGO (Federation of Gynecological Oncologists) system.

- A. Stage 1: The cancer is confined to the ovaries (primary site tumors).
- B. Stage 2: Cancerous cells have gone beyond ovaries, it has spread to the pelvis and sometimes even to the abdomen.
- C. Stage 3: Cancer has crossed the pelvis and spread to the abdominal cavity
- D. Stage 4: Cancer has spread to distant organs like liver and lungs.

The staging may also be classified as local (referred as stage 1 and confined to primary sites), regional (spread to regional lymph nodes), distant (cancer has metastasized) and unknown. Approximately, 14.8% of OC are diagnosed at the local stage, and the five-year survival for these patients is 92.5%. However, 60% of women in the United States are diagnosed with late-stage OC. More than half of the patients diagnosed with late-stage OC will relapse within 18 months after initial therapy [3].

1.3. Types of OC: OC is classified into three types based on the etiology of the malignancy: epithelial ovarian cancer (EOC), germline ovarian cancer and stromal cell ovarian cancer [4]. EOC is the most common and highly heterogeneous form of ovarian cancer [4]. Histologically EOC can be further divided into different subtypes; the four most common includes Serous, Endometrioid, Mucinous and Clear Cell carcinoma [5]. Histological classification of OC is based on the tumor cell origin and morphology [6].

1.3.1. Serous ovarian carcinoma (SOC): Serous carcinomas are considered to develop from ovarian surface epithelium or inclusion cysts [7]. SOC comprise most ovarian carcinomas and are further classified into low-grade and high-grade. Low-grade carcinomas are less

common than high-grade. The high grade and low-grade carcinomas are characterized by different underlying pathogeneses, molecular events, behavior and prognosis [8]. These two are distinguished based on morphology, the degree of nuclear atypia (abnormal appearance of cell nuclei), and the amount of mitotic activity. Low-grade serous carcinomas have mild to moderate nuclear atypia with less than 12 mitoses per 10 high-power field images. High-grade have, in contrast, nuclear atypia greater than 12 mitoses per 10 high-power field images [8]. In both grades of serous carcinomas, diverse cellular architectural patterns, such as nested, papillary, glandular, cribriform, solid and single can be present. Laminated psammoma bodies are usually present in both tumor types [8].

1.3.2. Mucinous ovarian carcinomas (MOC): These are the less common type of ovarian carcinomas, only 5-10% of EOC [9]. Mucinous carcinomas are of so-called intestinal or enteric subtype with cystic unilocular neoplasm with a thin space wall and filled with watery mucinous fluid. MOCs are confined to the ovary at diagnosis. They have solid and necrotic areas which histologically may be borderline or malignant [10]. MOCs have the worst prognosis and poor response to chemotherapy compared to other subtypes [11].

1.3.3. Endometrioid ovarian carcinoma: Endometrioid carcinomas have been reported to develop from endometriotic tissues [12]. Endometrioid carcinomas are commonly characterized by an epithelium composed of single layer of large polygonal cells with abundant eosinophils and large hyperchromatic, smudged nuclei [10,12]. Advanced endometrioid carcinoma normally responds to platinum-taxane combination treatment. However, the relapse rate is high with poor prognosis [13].

1.2.4. Clear cell carcinoma: This is a rare epithelial ovarian carcinoma which makes less than 10% of EOC [10,12]. They are characterized by a clear peg-shaped cell with abundant

cytoplasm. The cells can be observed either alone or in combination [10]. Clear cell carcinomas are usually chemoresistant malignancies with a poor prognosis [14].

1.4. Common OC features: Cancers cells are typified by the occurrence of ten traits, which are termed hallmarks of cancer. OC hallmarks include the capabilities for sustaining proliferative signaling, resisting cell death, evading growth suppressors, activating invasion and metastasis, enabling replicative immortality, inducing angiogenesis, avoiding immune destruction, tumor-promoting inflammation, genome instability, and mutation and deregulating cellular energetics [15]. These features allow cancer cells to survive, proliferate, and disseminate. In addition to these hallmarks, tumors have other characteristics like evading immune destruction, the presence of genomic instability and mutation, and reprogramming of energy metabolism. Somatic mutations in the ovarian tumors, which can activate downstream pathways; for example, mutations in the *BRAF* proto-oncogene can engage mitogen-activated protein kinase (MAPK) signaling pathways. Alterations in MAPK pathways are observed during cancer progression. Inhibition of the c-Jun N-terminal Kinase (JNK)-induced apoptotic death is one of the mechanisms developed during OC [16]. Tumors have a complex environmental dynamics including the presence of heterogeneous cell populations. This includes the cells that make up the tumor and those in the surrounding tumor microenvironment, wherein both areas play a significant role in tumor development and progression. Normal cells, including immune cells, may contribute to tumorigenesis by providing various growth factors to tumors [15]. The cell types and tumor microenvironment are crucial to the development and outcomes of individual tumors including tumor size and therapeutic resistance.

The hallmarks of cancer are present in OC, and these hallmarks represent potential, enticing targets for OC drug discovery. Metastasis is one crucial hallmark, which accounts for the high morbidity and mortality by OC because the spread of the tumor beyond ovaries increases the difficulty of treating cancer [17]. There are two prevailing reasons behind the absence of an effective treatment for OC: late diagnosis and resistance to available therapeutic approaches [3]. Complicating the difficulties in treating OC is the fact that the origins and pathogeneses of OCs are poorly understood. There are numerous treatment options available for the attempted management of OC; however, each one has its benefits and drawbacks. For example, radiation targets specifically the cancer cells; however, it damages the DNA of cells instead of killing cells while chemotherapy is given to entire body and kills cancer as well as other dividing cells. The most prominent problem with OC treatment is its relapse or recurrence because of the return of the disease following treatment is typified by the presence of highly resistant tumor cells. One important cause of characteristic of these resistant cells is their ability to withstand a variety of cell death mechanisms. The heterogeneous cell population and absence of a prevailing cell death pathway are evidence of the urgent need for novel and aggressive therapies for OC [17].

1.5. OC chemotherapy mechanisms of action and the involvement of JNK signaling

The standard of care for OC patients is the combination of surgery and radio/chemotherapy [18]. Surgery removes the local tumor mass (or those that are visible) [19], and surgery may be followed by a chemotherapeutic regimen comprised of a platinum-based compound, such as cisplatin, and a taxane, like paclitaxel [17]. Based on individual responses to chemotherapy, OC patients are classified into platinum-sensitive (recurs after

six months of treatment), platinum-resistant (recurs within six months after treatment) and platinum-refractory (recurs during treatment) [17].

Platinum compounds, like cisplatin and carboplatin, form active species by aqueous hydrolysis (i.e., these compounds react with water and form reactive species). These species can interact with DNA, RNA, and proteins. Most of the cytotoxic effects of platinum compounds result from the formation of DNA inter-stand and intra-stand crosslinks because these disturb DNA replication. Consequently, the cell engages repair processes such as nucleotide-excision repair (NER) and mismatch repair (MMR) [20]. NER solely repairs the damage, whereas MMR can induce apoptosis in addition to repair. It has been observed that in response to cisplatin, MMR-related signaling pathways; specifically, c-Abl protein tyrosine kinase and JNK are activated. In the cells lacking MMR, both signaling pathways are not initiated [21]. This evidence suggests that JNK is involved in cisplatin-induced cell death. Further studies reveal that sustained activation of JNK pathway by cisplatin occurs in the OC cell line 2008, while in its cisplatin-resistant clone 2008c13 did not display JNK activation [22]. This suggests that a failure to robustly induce apoptotic signaling may be a contributing factor to platinum resistance in OC.

Taxols act by binding to β -tubulin of microtubules causing microtubule stabilization, leading to cell cycle arrest (specifically arresting cells at G2-M) and ultimately apoptosis [23]. Paclitaxel regulates MAPK signaling and promotes phosphorylation of Bcl-2 and dephosphorylation of Bad triggering apoptosis [24]. Additional research suggests that paclitaxel promotes apoptosis in OC cells. Woo et al., demonstrate that JNK activity contributes to paclitaxel-induced apoptosis [25]. Further, the Ras-related nuclear protein (Ran) impairs JNK-mediated phosphorylation in U373MG cells preventing the

phosphorylation of downstream pro-apoptotic Bcl-2 proteins and induction of apoptosis [25]. Additionally, Lee and colleagues show that JNK is phosphorylated after paclitaxel exposure in a dose-dependent manner before cell death [26]. These studies collectively fundamentally implicate JNK in chemotherapy-induced apoptosis in OC cells.

2. Uterine/Endometrial Cancer

Uterine or endometrial cancer is the fourth most common cancer in the United States. Endometrial cancer is the most commonly diagnosed gynecological malignancy. ACS estimates 63,230 new cases and 11,350 death from the cancer of uterine body in 2018. The 5-year survival for uterine cancer is 82% [1]. It is the sixth most common cause of cancer death among women in the USA [2]. The most common treatment approach for endometrial cancer is surgery [27], and it has been found to be effective for tumors confined to the uterus [28]. However, surgery alone cannot treat advanced or recurrent endometrial cancer. A combination of radiotherapy with platinum-based chemotherapy is employed for progression-free survival in endometrial cancer [29].

3. Cervical Cancer

Cervical cancer is caused by the development of cancer in the uterine cervix. ACS estimates 13,240 new cases and 4,170 deaths from the cancer of the cervix in 2018. Cervical cancer is the second leading cause of cancer death in women aged 20 to 39 years [1]. The prognosis of the cervical cancer patient with an advanced or metastatic malignancies is poor. A common form of treatment is surgery followed by cisplatin or carboplatin. Cisplatin-paclitaxel combination may be an improved chemotherapeutic modality for advanced cervical cancer [30]. Bevacizumab is a humanized vascular endothelial growth factor (VEGF)- neutralizing antibody, and the addition of bevacizumab

to combination chemotherapy increases disease-free survival in cases of advanced or metastasized cervical cancer [31].

4. c-Jun N-terminal kinase (JNK)

Mitogen-activated protein kinases (MAPKs) are critical modulators of numerous cellular processes, namely proliferation, differentiation and apoptosis [32]. JNK is a member of the MAPK superfamily and is an effector kinase. JNK has a profound impact on cellular viability, as it is a critical regulator of apoptosis. JNK is a serine/threonine (Ser/Thr) protein kinase that modulates cell survival pathways by targeting transcription factors and other non-nuclear substrates [32-34]. JNK activation and function is regulated by phosphorelay cascade (Figure 1.1). JNK activation occurs in response to both extracellular and intracellular stimuli, which may influence JNK function in a cell and stress-dependent manner by activating specific MKKKs. These MAPKKKs, in turn, activate two MAPKKs, MKK7 and MKK4. MKK7 and MKK4 phosphorylate JNK on threonine 183 (Thr183) and tyrosine 185 (Tyr185) of the activation loop respectively [32,34]. Although phosphorylation of both sites is required for full activation, it is suggested that Thr183 is the critical residue and Tyr185 gives fine tuning in TNF- α induced JNK activation [35]. Active JNK then phosphorylates downstream substrates, such as c-Jun, ATF-2, c-Myc, p53, and Bcl-2 proteins; this protein alteration determines the biological outcomes of specific stimuli [32,33,36].

The role of JNK in apoptosis is well-established [32,37], and JNK-mediated apoptosis has been observed in numbers of stresses including anisomycin, dexamethasone, phorbol ester, acetaminophen-induced liver injury, DNA damaging agents, paclitaxel and in disease models of cardiac stress, cerebral ischemia, and aging [26,38-44]. JNK-mediated apoptosis

was first identified in rat PC-12 pheochromocytoma cells following nerve growth factor (NGF) withdrawal. This apoptotic cell death was suppressed by inhibition of JNK pathway by using dominant negative form of the JNK substrate c-jun.

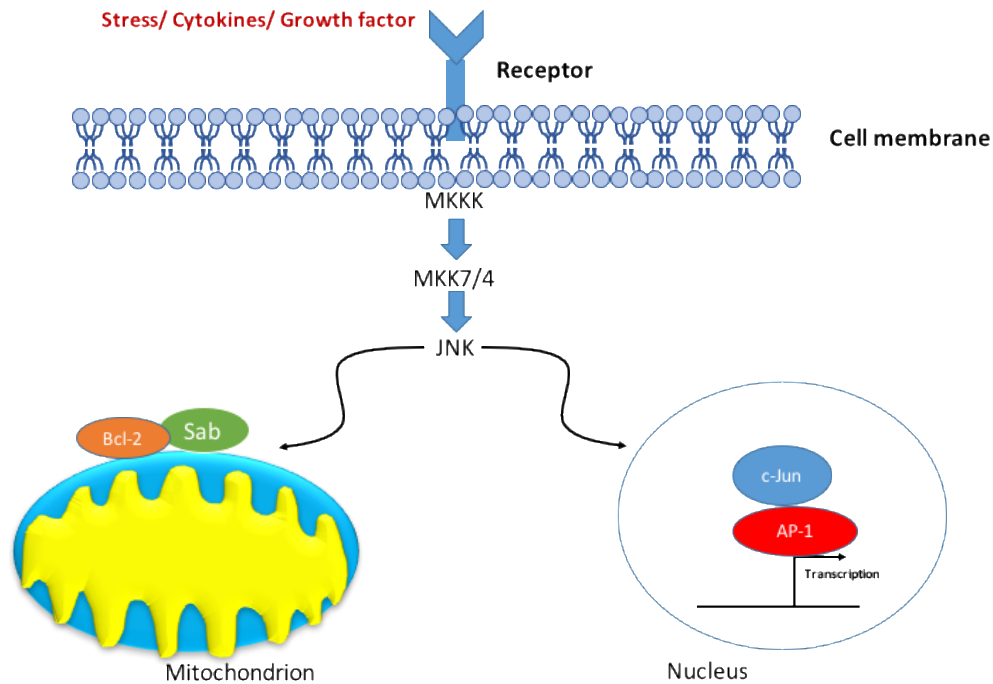


Figure 1.1: JNK phosphorylation and activation occurs in response to the activation of upstream kinases, MKK and MKKK. In response to different signals, the upstream kinase MKKK gets phosphorylated, which phosphorylates MKK7 and MKK4. MKK7/4 activation causes the phosphorylation of JNK. JNK activation can lead to nuclear-JNK or mitochondrial-JNK signaling depending on the signal and cell type.

Further, constitutively active mitogen-activated protein kinase kinase 1 (MEKK1) induced apoptosis, implicating JNK as a pro-apoptotic kinase [45]. Additionally, genetic ablation of JNK prevents apoptosis as well. Hippocampal neurons in *JNK3*^{-/-} mice were resistant to kainic acid-induced apoptosis [46]. Suppression of cell death in response to ultra-violet light and anisomycin in *JNK1*^{-/-} *JNK2*^{-/-} and *MKK4*^{-/-} *MKK7*^{-/-} mouse embryonic fibroblasts (MEFs) also demonstrate the significance of JNK in apoptosis [35,47]. It was

shown that the absence of JNK prevented the release of cytochrome c from the mitochondria, in *JNK1^{-/-} JNK2^{-/-}* MEF following UV exposure; while cytochrome c release was observed in WT-MEF (wild-type). Again demonstrating JNK as an important component of the mitochondria-mediated apoptosis [47]. Recently, the interaction of JNK with mitochondrial scaffold protein Sab (or SH3-binding protein 5 – SH3BP5) during stress was revealed to have a significant impact on apoptosis; the association of JNK with Sab promotes JNK-mediated phosphorylation of anti-apoptotic protein Bcl-2 on Ser-70. JNK phosphorylation of Bcl-2 leads to emigration of the protein from the outer mitochondrial membrane (OMM) ultimately promoting apoptosis [48].

Despite an abundance of data implicating JNK in apoptosis, other studies suggest JNK signaling may have pro-survival functions. JNK can facilitate IL-3-mediated survival of hematopoietic pro-B FL5.12 cells [49]. JNK generates this survival response by phosphorylating and inactivating pro-apoptotic protein Bad at Thr-201; inhibition of JNK caused an increase in IL-3 withdrawal-induced apoptosis. Meanwhile, expression of a constitutively active MEKK1 suppressed cell death [49]. Sabapathy *et al.*, have shown both the pro-apoptotic and anti-apoptotic role of JNK in the development of fetal brain using *JNK1^{-/-} JNK2^{-/-}* double knockout fetuses. JNK1 and JNK2 positively regulate apoptosis in hindbrain region at E9.25 (embryonic day); whereas, there was a decrease in apoptosis in the double-knockout animals. The overall effect of the double-knockout is defective neural morphogenesis and defective neural tube closure [50]. Inhibition of cell proliferation and inhibition of cell cycle progression was observed in cultured KB-3 human cells with JNK inhibitor (SP600125), and JNK-specific anti-sense oligonucleotides, supported the role of JNK in cellular proliferation [51]. Thus, JNK activity can be a pro-apoptotic and a pro-

survival kinase, depending on the stress, physiologic conditions, localization, and potentially the activity of distinct JNK isoforms.

The involvement of mitochondrial JNK signaling in improving the chemotherapeutic efficacy in gynecological cancer was observed following low-dose sub-chronic administration of LY294002 in HeLa cells (cervical cancer) [52]. The prolonged exposure of HeLa cells to LY294002 increases phospho-JNK (active kinase) on the mitochondria of HeLa cells [52]. Blocking the accumulation of JNK on mitochondria was found to reduce the sensitivity of HeLa cells towards common chemotherapeutic agents [52]. Mitochondrial JNK also regulates mitochondria-mediated intrinsic apoptosis by regulating Bcl-2 family of proteins [53]. These studies demonstrate that mitochondrial JNK may be a crucial driver of apoptosis in cancer cells.

5. Bcl-2 superfamily of proteins

B-cell lymphoma-2 (Bcl-2) family of proteins includes both pro-survival and pro-apoptotic proteins with a profound impact on cell death and survival. This family of proteins has four domains BH1, BH2, BH3 and BH4; and subfamilies are identified by the specific domains that are present within the proteins (Figure 1.2). Anti-apoptotic or pro-survival Bcl-2 proteins have all four BH domains and include, Bcl-2, Bcl-xL, Mcl-1, Bcl-w, Bcl-B, Bfl-1/A1. Pro-apoptotic Bcl-2 proteins are further divided into pro-apoptotic BH3 only proteins and multi-domain proteins. BH3 only pro-apoptotic proteins include Bid, Bad, Bim, Bmf, Bik, Hrk/DP5, Blk, Nip3, BNip3/Nix, Puma, Noxa. These proteins assist the executor proteins in apoptosis and sequester anti-apoptotic proteins (Figure 1.3). Bid and Bim act as major ‘direct activators’ which are responsible for the induction of activation of Bax and Bak via their BH3 domain whereas Bad and Puma are also called sensitizers or de-

repressors, because of their ability to bind anti-apoptotic protein [54,55]. Multi-domain proteins have BH1, BH2, and BH3 domains. These are executor apoptotic proteins and are also called effectors, which include Bax, Bak, and lesser known protein Bok [56,57].

Bax and Bak's oligomerization leads to MOMP (mitochondrial outer membrane permeabilization), pore formation and release of cytochrome c and other factors into the cytoplasm. This ultimately starts the cell death process by activating apoptotic protease activating factor-1 (APAF-1) which further stimulates caspases [58].

Antiapoptotic Bcl-2 protein



Pro-apoptotic Bcl-2 protein

1. BH3- only protein



2. Multidomain BH1, 2, 3 effector protein



Figure 1.2: Bcl-2 family of proteins with specific domains. Anti-apoptotic proteins have all four domains (BH1, BH2, BH3 and BH4), whereas BH-3 only pro-apoptotic have BH3 domain, and effector proteins have three domains (BH1, BH2, and BH3).

5.1. Interaction between Bcl-2 proteins

Bcl-2 family is classified into two groups, folded globular and intrinsically unstructured proteins (IUPs). Globular proteins, which include antiapoptotic and effector protein, share a core structure of the protein called 'Bcl-2 core'. The first study of the structure of these

proteins was done in Bcl-xL, which is a 20KD globular protein, using NMR based spectroscopy and X-ray crystallography[59]. Three-dimensional structure of 'Bcl-2 core' contains seven or eight amphipathic alpha helices, surrounding central helix, $\alpha 5$ and $\alpha 6$. Both helices are highly hydrophobic and are flanked by $\alpha 3$ and $\alpha 4$ on one side and $\alpha 1$ and $\alpha 2$ on the other. This hydrophobic groove is termed as BC groove. The BH4 (conserved $\alpha 1$ positioned along $\alpha 6$) domain stabilizes BH1-BH3 regions. BC groove and $\alpha 1/\alpha 6$ makes up the 'Bcl-2 core'[60,61].

The hydrophobic groove is the interaction site of anti-apoptotic proteins and BH3 domain of both the effector and BH3 only proteins, which was first observed between Bcl-xL and Bak. This interaction was detected by co-immunoprecipitation and two-hybrid interaction in the yeast; which was supported by NMR spectroscopy between Bcl-xL/Bak peptide complexes. Heterodimerization was observed, which was because of electrostatic and hydrophobic interaction between these two proteins [56]. Mutation on BH3 domain led to the termination of this interaction which suggests that there is conserved amino acid in the BH3 domain.

The BH3 domain consists of between 9 and 16 amino acids, of which seven were found to be core amino acids by phylogenetic studies. The sequence is LXXXXGDE, where X is any amino acid [62]. Recently, a 13-residue consensus motif has been proposed based on structural studies and sequence analysis. The consensus motif is $\Phi_1\Sigma XX\Phi_2XX\Phi_3\Sigma'DZ\Phi_4r$; where Φ represents a hydrophobic residue (Φ_2 is often leucine), Σ is a small residue (G, A, S), Z is usually an acidic residue and r is a hydrophilic residue [63]. The most conserved residues are leucine and aspartic acid residues which have an important role in interaction with the anti-apoptotic protein. The leucine residue is

buried in the protein-protein interface and packs against the conserved residue of anti-apoptotic protein whereas aspartate forms ionic interaction with conserved arginine in the BH1 domain of pro-survival protein [56,64]. Other binding interactions like Vander Waals, hydrophobic and hydrophilic interaction play equally important role [63].

As different BH3 proteins have diverse amino acids in their BH3 domains, this could be affecting their binding preference for anti-apoptotic proteins. In vitro analysis was performed using recombinant anti-apoptotic proteins and synthetic BH3 peptides of the BH3 only protein to determine the binding specificity of this BH3 only proteins. This revealed that there is preference shown by BH3 domains for binding anti-apoptotic proteins [65]. Among eight BH3 peptides, BIM and Puma had the affinity for all the anti-apoptotic Bcl-2 proteins whereas others were specific. It could be said that the observed selectivity was relying on the BH3 motif; any mutational change could change the specificity easily [66].

5.2. Bax activation

While there are many BH3-only proteins having the ability to bind to anti-apoptotic proteins, only few can bind to effector pro-apoptotic proteins. Activators BH3 proteins, Bim and Bid, can induce oligomerization of Bax and Bak, OMMP formation and cytochrome c release [67].

Bid also has the affinity for anti-apoptotic Bcl-2 and Bcl-xL. There are two different theories for activation of Bax by Bid. Bid can either directly activate full-length Bax or t-Bid, a cleaved form of Bid activates Bax differently. t-Bid has been described as the direct activator of Bax. However, the exact mechanism of Bax activation was not clear. Bid can be cleaved by caspase 8 forming t-Bid, which is unable to interact with full-length Bax or

Bcl-xL in solution [68]. Following cleavage, N-terminus Bid (N-Bid) remains attached with C-terminus Bid (C-Bid), forming BH3 domain. In the presence of lipid bilayer; mimicking OMM, C-Bid inserts into the membrane, while the N-Bid remains in the solution. Once in the membrane, it can recruit Bax into the membrane, which was shown by fluorescence resonance energy transfer (FRET) [68]. This emphasizes the importance of lipid membrane for Bax activation. tBID also can cause an allosteric conformational change of Bak followed by its homo-oligomerization and the release of cytochrome c [69]. To understand the mechanism of Bax activation by Bid, the α -helix of Bid was stabilized by a chemical modification called ‘hydrocarbon stapling’ [70]. The C terminal α -helix 9 of Bax is embedded into the hydrophobic groove, making it problematic for BH3 protein binding; as this is the site where BH3 domain binds to the anti-apoptotic protein [71]. With the modification of BH3 Bid helix, it could bind to the groove by displacing intramolecular Bax α -helix. This led to the conformational change of Bax and cytochrome c release was observed in both *in vitro* and *in vivo* experiments. A similar result was observed with the modification of Bim peptide. However, modified Bad BH3 didn’t show any ability to bind Bax [70]. According to the NMR studies, Bax interaction with Bim causes the conformational change in α -helix 1 & 2, from closed to an open conformation which causes the release of α -helix 9 hydrophobic grooves exposing the groove for BH3 binding [72].

5.3. Bcl-2 proteins: The individual member of the Bcl-2 family will be discussed further below.

5.3.1. Bcl-2: B-cell lymphoma-2 (Bcl-2) is a 26kD anti-apoptotic protein. Bcl-2 is a membrane-associated protein embedded in the endoplasmic reticulum, the nuclear envelope, and the outer mitochondrial membrane [73]. Bcl-2 can be modified by several

kinases and phosphatases, and these modifications play significant roles in cellular survival/death [36].

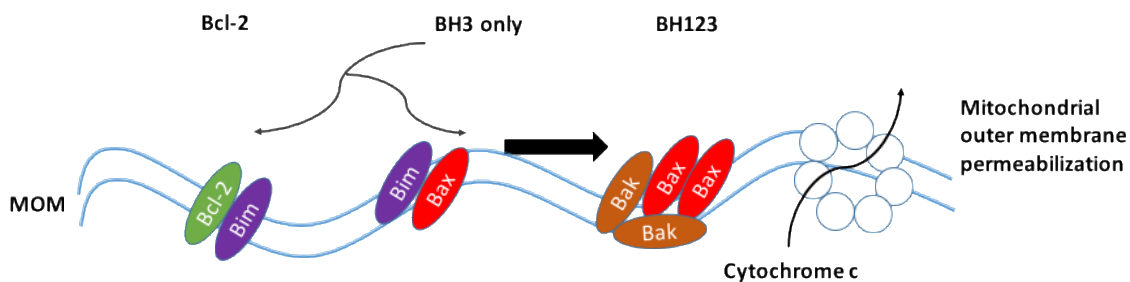


Figure 1.3: BH3 only proteins have multiple roles. They can neutralize the pro-survival proteins causing the release of Bax and Bak or directly activate effector proteins by a conformational change of Bax and Bak. Both events lead to the translocation of Bax to OMM, oligomerization with mitochondria located Bak, which eventually causes OMM permeabilization, the release of cytochrome c and initiation of apoptosis.

The microtubule damaging agent, paclitaxel induces phosphorylation of Bcl-2 in unstructured loop regions where residues Ser70, Ser87, and Thr69 were phosphorylated in Jurkat-Bcl-2 cells [36]. This is further supported by other observations where deletion of Bcl-2 loop regions completely blocked paclitaxel-induced apoptosis [74,75]. Mutations of these sites enhance the anti-apoptotic function of Bcl-2 [36]. Ser-70 is the principal site of phosphorylation of Bcl-2 during various stress conditions, including paclitaxel, vinblastine, and anisomycin [48,76,77]. This phosphorylation was found to be mediated by JNK [36]. Ser-70 phosphorylation suppresses the pro-survival function of Bcl-2, and mutation in this site improves the anti-apoptotic function of Bcl-2 indicating the importance of this site in Bcl-2 function [36]. In contrast, same site phosphorylation could lead to inhibition of cell death pathway. JNK-mediated Ser-70 phosphorylation was found to enhance cell survival during various stress conditions including IL-3 withdrawal and a low dose of okadaic treatment in murine wild-type [78].

With the treatment of paclitaxel, the active form of JNK (Phospho-Thr-Tyr) and phosphorylated Bcl-2 (Ser-70) were found in the mitochondria of HeLa (cervical cancer) and MCF-7 (breast cancer) cells. This was also observed in cell-free mitochondria when treated with cytosolic activated JNK, which was extracted from HeLa cell treated with paclitaxel. Preincubation of a cytosolic extract from paclitaxel-treated HeLa cells with CEP11004, a proposed JNK inhibitor, did not show any phosphorylation of Bcl-2 [79].

Conversely, Park *et al.* have shown the regulation of JNK1 activity by Bcl-2 protein. Apoptosis is activated in N18TG neuroglioma cells in response to various apoptotic stresses. However, in N18TG cells expressing Bcl-2 (N18 cells transfected with Bcl-2) were resistant to etoposide, staurosporine, anisomycin, and UV mediated cell death. It was found that Bcl-2 inhibits the activation of MEKK1, the upstream activator of JNK signaling pathway [80]. Expression of JNK1 in N18/ Bcl-2 cells neutralized or counteracted the anti-apoptotic effect of Bcl-2; making N18/Bcl-2 cells as sensitive as the control cells [80]. Bcl-2 was also shown to inhibit the activation of JNK in response to nerve growth factor withdrawal in PC12 cells [81]. These observations suggest that JNK1 and Bcl-2 protein can regulate each other depending on the cellular context.

5.3.2. Bcl-xL: B-cell lymphoma extra-large (Bcl-xL) is an anti-apoptotic transmembrane protein present in the mitochondria. Bcl-xL is a 20kD globular protein and was the first protein of the family in which structural detail was studied [82]. Bcl-xL can inhibit the formation of OMMP and release of cytochrome c. Even though many cell lines express both Bcl-2 and Bcl-xL, an inverse association in the expression pattern of these two proteins have been found in thirty-four cell lines derived from colon, breast, ovary, central nervous system, and renal cancers [83].

Petros and colleagues have suggested that the characteristic feature of Bcl-xL and Bcl-2 to heterodimerize with Bax, Bak, and other BH3 only proteins keeps the apoptotic balance of the cells [84]. Letai and colleagues proposed that the antiapoptotic protein binds to the BH3 domain of activator protein and sequesters them before they could activate Bax and Bak [85].

In response to ionizing radiation, Kharbanda *et al.* have shown the translocation of JNK to mitochondria in U-937 (lymphoma) cells, using fluorescence image analyzer, microscopy, and immunoblotting. At mitochondria, JNK was found to interact with Bcl-xL, which was shown by a co-localization assay. JNK phosphorylates Bcl-xL on Threonine-47 (Thr-47) and Threonine 115 (Thr-115) in U-937 cells [86]. Further, the effect of tetradecanoyl phorbol-13-acetate (TPA) on JNK and Bcl-xL was studied on U-937 cells, where no significant effect of Bcl-xL was found on the JNK translocation to mitochondria; however, TPA-induced the interaction of JNK and Bcl-xL. Overexpression of Bcl-xL mutated at sites of JNK phosphorylation (T47A and T115A) caused a substantial decrease in the release of cytochrome c and apoptosis compared to the overexpression of normal Bcl-xL; signifying the importance of these two sites in Bcl-xL function [40]. JNK was also found to phosphorylate Bcl-xL in 293T cells [86]. JNK mediated phosphorylation in Ser-62, within the unstructured loop region of Bcl-xL was observed in response to taxol or 2-methoxyestradiol in DU145 human prostate cancer cells [87].

Phosphorylation of Bcl-2 and Bcl-xL by JNK has been observed in KB-3 sarcoma cells following treatment with vinblastine. When JNK-1 and JNK-2 expression were inhibited using antisense oligonucleotides, there was a decrease in the phosphorylation of Bcl-2 by 85% and Bcl-xl by 65% [76]. Similarly, Du *et al.* have shown phosphorylation of Bcl-2

and Bcl-xL with the treatment of vinblastine in KB-3 carcinomas. Even though the phosphorylation of both proteins was shown to be dependent on the same kinase, they were not able to identify the kinase responsible. They showed that there was no effect in phosphorylation event with the use of JNK, ERK and CDK inhibitors [88]. Taken together, JNK has a significant role in post-translational modification of pro-survival proteins Bcl-2 and Bcl-xL resulting in different outcomes.

5.3.3. Mcl-1: Myeloid cell leukemia-1 (Mcl-1) is a 40kD pro-survival Bcl-2 protein, expressed in many cell types [61]. Mcl-1 is regulated at the transcriptional, translational and post-translational level [89,90]. Mcl-1 has an important role in proliferating cells and early embryonic development [91]. Mcl-1 contributes to pro-survival function by inhibiting the formation of OMMP and release of cytochrome c, which is done either by inactivating Bax and Bak or sequestering the BH3 only activator protein Bim [61].

Mcl-1 is regulated by phosphorylation at various sites. Enhancement of the antiapoptotic function of Mcl-1 occurs when it is phosphorylated at Ser-64 in a cell-cycle-dependent manner by CDK1, CDK2, and JNK1. Instead of affecting the Mcl-1 turnover, Ser-64 phosphorylation enhances the binding of Mcl-1 to pro-apoptotic Bcl-2 protein. The requirement of Ser64 phosphorylation of Mcl-1 in TNF-related apoptosis-inducing ligand (TRAIL)-mediated apoptosis was shown in KMCH cholangiocarcinoma cell by silencing endogenous Mcl-1 and transfecting with S64A, S64E and wild-type Mcl-1. Cells with silenced Mcl-1 and S64A were quite sensitive to TRAIL while S64E, which mimics phosphorylation, and wild-type were resistant [92].

JNK facilitates the UV-mediated degradation of Mcl-1. In wild-type fibroblasts, there was a significant decrease of Mcl-1 while there was no change in JNK1^{-/-}, JNK2^{-/-} fibroblasts.

This degradation of Mcl-1 occurs via the GSK-3 mediated proteasomal pathway. JNK phosphorylates Mcl-1 at Thr-163 and primes Mcl-1 for GSK3 phosphorylation. GSK3 phosphorylates Mcl-1 at Ser-159 leading to its ubiquitination and degradation [90]. Mcl-1 half-life and turn-over rate are regulated by the proteasomal degradation pathway [93,94]. Phosphorylation of Ser-121 and Thr-163 in Mcl-1 by JNK has shown opposing effects in two different cell lines. In hepatocytes, it stabilizes Mcl-1 whereas, in endothelial cells, it causes a reduction in the anti-apoptotic effect of Mcl-1 mediated by oxidative damage [61,95,96]. JNK signaling pathway is involved in phosphorylation of Mcl-1, which could enhance its pro-survival function or inhibit its pro-survival function and initiate the degradation of the protein.

5.3.4. Bim/ Bmf: Bcl-2 interacting mediator of cell death (Bim) and the closely related Bim-related molecule (Bmf) are BH3-only pro-apoptotic proteins that are normally sequestered by binding to motor complexes. Transcriptional and post-translational regulation plays an important role in their apoptotic activity [58]. Bim exists in three isoforms produced as a result of alternative splicing; BimS (short isoform), BimL (long isoform) and BimEL (extra-long isoform) [97]. BimL and BimEL are present in normal cells while BimS is transiently present in cells undergoing apoptosis. The presence of short peptide motif (DKSTQTP) in BimL and BimEL mediates their binding to Dynein motor complex via dynein light chain (DLC1); whereas, BimS doesn't have this motif and can potentially show apoptotic activity [98]. Bmf also contains a similar motif (DKATQTLSP) that binds to DLC2, a component of the myosin V motor complex [98].

The apoptotic activity of Bim is sequestered by binding of this protein to DLC1 of dynein motor complex under normal condition. However, with the exposure to UV radiation, Bim

gets detached from the DLC1 and is activated because of the phosphorylation caused by JNK at Ser-44, Thr-56, and Ser-58 [58]. JNK mediated phosphorylation of Bim was observed both *in vivo* and *in vitro*. Exposure to UV caused an increase in phosphorylation of BimL in cells labeled with [32P]phosphate [58]. It was also observed that Thr-56 phosphorylation inhibits the binding of BimL to DLC1 and increases apoptotic activity [58]. TRAIL facilitated JNK mediated phosphorylation of Bim and caused Fas-induced liver damage. JNK and Bim deficient thymocytes were protected against TRAIL-mediated Fas-induced damage [99].

Bim is involved in neuronal apoptosis under trophic factor withdrawal. Induction of Bim is considered a hallmark of neuronal apoptosis. Potassium withdrawal in cerebral granule neurons caused a five-fold increase in mRNA levels of Bim. However, with the use of CEP-1347, the mRNA level of these BH3-only proteins were not increased to that level even in the absence of potassium. CEP-1347 is a mixed lineage kinase inhibitor which blocks c-Jun phosphorylation and inhibits activation under trophic factor withdrawal. The mRNA level of Bim was upregulated by 2.8 folds. This shows that inhibiting JNK pathway reduces the induction of Bim mRNA by ~55%. A similar trend was observed in sympathetic neurons during nerve growth factor (NGF) deprivation [100]. However, Putcha *et al.* have shown that JNK is not required for BIM induction in NGF-deprived superior cervical ganglions. They observed that JNK signaling pathway activation is not required for NGF-deprivation induced Bim-EL expression in sympathetic neurons. They suggest two pathways for apoptotic cell death of NGF deprived neurons; one caused by activation of JNK pathway and another by induction of Bim and Dp5 BH3 only proteins. Both of them act upstream of Bax activation, so both of these pathways are required for

NGF deprived neuronal apoptosis which acts in parallel [101]. Activation of JNK pathway is required for, but not sufficient for, Bim-mediated death in NGF deprived neuronal apoptosis.

Bmf, which is a related protein to Bim is also regulated by JNK, and the phosphorylation site is the same (Thr56 and Ser58) as Bim, which is conserved in Bmf. Bmf is detached from DLC2 when phosphorylated by JNK. JNK deficient and Bim deficient thymocytes show a similar deficiency in apoptosis [58].

5.3.5. DP5/Hrk: Death protein 5/ harakiri (DP5, Hrk) is a BH3 only apoptotic protein involved mostly in neuronal apoptosis [102,103]. DP5 was originally identified in rat sympathetic neurons, during screening for genes induced after nerve growth factor (NGF) withdrawal [104]. Hrk is a human DP5 homolog, which interacts specifically with Bcl-2 and Bcl-xL [105]. Harris *et al.* have shown DP5 induced neuronal apoptosis to be Bax dependent [100]. Thus, it can be suggested that like other BH3 only protein, Hrk promotes apoptosis either by neutralizing anti-apoptotic proteins or activating Bax.

The DP5 gene is transcriptionally regulated by JNK. This is mediated via phosphorylation of c-Jun by JNK. It was observed that DP5/Hrk was upregulated with potassium deprivation in cerebellar granule neurons (CGNs) [102]. DIV7 cells were cultured in 25mM or 5mM KCl containing media for different times. The increase in phospho-JNK was observed followed by phospho-c-Jun which was further followed by an increase in DP5 in the cells grown in 5mM KCl. Inhibition of JNK using SP600125 resulted in a decrease in DP5 by 62%, showing that the JNK pathway is involved in transcription regulation of DP5 under potassium deprivation [102]. Polyglutamine- repeat expansion in the androgen receptor (PolyQ-AR) induces neurotoxicity which results in

neurodegeneration and apoptosis in various disorders. This apoptotic cell death was found to be mediated by Hrk, regulated by JNK via c-Jun [106].

JNK is also involved in Hrk manipulation during ceramide-mediated mitochondrial dysfunction, as evident by the release of cytochrome c and a decrease in OMMP in human corneal stromal fibroblasts (HCSF) [107]. JNK plays a significant role in neuronal apoptosis by regulation of Bim/Bmf and DP5/Hrk proteins.

5.3.6. PUMA: The p53-upregulated modulator of apoptosis (PUMA), identified as a target of p53 is a pro-apoptotic member of the Bcl-2 family of proteins [108]. It is localized to mitochondria with a hydrophobic groove on its C-terminal domain [108,109]. PUMA binds to anti-apoptotic proteins via the BH3 domain and activates the induction of apoptosis [108]. PUMA is transcriptionally regulated mostly by p53 (tumor suppressor gene); there are few observations showing regulation of PUMA by JNK.

Palmitate-induced PUMA expression was found to be JNK-dependent. In Huh-7 (hepatocarcinoma) cells treated with palmitate, an increase in JNK phosphorylation and PUMA mRNA leading to lipoapoptosis was observed. Whereas, SP600125 caused significant decrease in JNK phosphorylation and 70% decrease in PUMA mRNA and protein level even with the treatment of palmitate [110]. PUMA was found to be involved in apoptosis of cerebral granule neurons under potassium withdrawal. JNK was involved in the induction of PUMA mRNA and increase in PUMA protein. A decrease in PUMA protein was observed with the use of SP600125 [111].

5.3.7. Bad: Bcl-2 associated death promoter (Bad) is a pro-apoptotic protein involved in initiating the apoptotic pathway. Once activated, it can form a heterodimer with anti-apoptotic proteins (Bcl-2 and Bcl-xL) and prevent them from inhibiting apoptosis [54,112].

Phosphorylation at different sites determines the activity of Bad. Phosphorylation of Bad at Ser-136 or Ser-112 or both by survival factors causes the binding and sequestration of the 14-3-3 protein, whereas phosphorylation at Ser-128 on 14-3-3 promotes the release of Bad [113-115].

In contrast, JNK is found to be inhibiting apoptosis by phosphorylation of pro-apoptotic protein Bad in IL-3 mediated hematopoietic cells (FL5.12) [49,116]. Unphosphorylated Bad heterodimerizes with Bcl-xL at a non-membrane site causing inactivation of this antiapoptotic protein. Whereas phosphorylated Bad binds to 14-3-3, causing the sequestration of Bad in the cytosol in hematopoietic pro-B FL5.12 cells [113]. IL-3 mediated phosphorylation of Bad by JNK occurs at the Thr-201 residue. This phosphorylation was found to reduce the association of Bad with Bcl-xL. The importance of the Thr-201 residue of Bad in JNK mediated cell survival was shown by the generation of a mutant, which under IL-3 withdrawal could show higher apoptotic activity compared to wild type [49]. JNK mediated phosphorylation of Bad results in a commitment to either death or survival under different contexts.

5.3.8. Bax and Bak: Bcl-2 associated X- protein is a cardinal member of the Bcl-2 family. Bax regulates the critical balance between life and death [117]. Bax is predominantly a cytosolic protein, which translocates to mitochondria by various modifications including stress. Another reason is a conformational change in Bax with the interaction of BH3 proteins like BID and Bim, which causes its insertion into the mitochondrial membrane [117]. Bax heterodimerizes with B-cell associated killer protein (Bak) present on mitochondrial membrane, leading to oligomerization of Bax and Bak and initiates pore formation in the outer mitochondrial membrane [118].

Bax protein is sequestered in the cytoplasm by various mechanisms; one of which is binding of Bax by 14-3-3, a cytoplasmic anchor protein [119]. Under stress, Bax dissociates from 14-3-3 and translocates to mitochondria. JNK plays a significant role during this translocation process, which was shown in COS-1 cells treated with anisomycin or staurosporine. It was also shown that SP600125 or JNK binding peptide (JBP) prevented Bax translocation. JNK phosphorylation of 14-3-3 ζ at Ser-184 and 14-3-3 σ at Ser-186 causes the dissociation of Bax. This phosphorylation was found both *in vitro* and *in vivo* in HTC116 (colon carcinoma) cells following anisomycin treatment [120]. Another stress shows the phosphorylation of Bax on Thr-167 by JNK and p38 kinase in response to treatment with staurosporine, UV light, and H₂O₂ in HepG2, human hepatoma cell line. They suggest that this phosphorylation causes the conformational change in Bax which leads to the translocation of Bax to mitochondrion [118]. JNK induced apoptosis requires Bax and Bak, which was shown in Bax/Bak double knock out MEFs. Apoptosis was observed with the activation of JNK in WTMEFs whereas there was no apoptosis in DKO MEFs [121]. JNK favors apoptosis by direct modification of Bax or modification of anchor protein ultimately resulting in translocation of Bax to mitochondria.

6. Mitochondrial permeabilization

Mitochondria are comprised of two membranes, the inner mitochondrial membrane (IMM) and the outer mitochondrial membrane (OMM). In the space between these two membranes (dubbed the intermembrane space), cytochrome c and various other factors are found [122]. Executor apoptotic proteins, Bax which are present in the cytosol of the normal cells translocate to the OMM when activated. Similarly Bak is constitutively targeted to the mitochondria after activation [55]. The activation of Bax and Bak occurs either by direct

activators or by other proteins or non-protein factors, like mild heat, high pH and detergents [55]. Due to the change in the structure, these proteins homo-oligomerize leading to the formation of proteolipid pores in the OMM; OMM permeabilization occurs after a critical number beyond the capacity of recovery has occurred. OMMP is considered the point of no return and is the crucial event in programmed cell death [64,123]. This leads to the release of cytochrome c, SMAC/DIABLO, endonuclease G, apoptosis-inducing factor (AIF), adenylate kinase, Ser protease OMI, deafness dystonia protein (DDP) and OPA1, some of which are also involved in caspase-independent cell death [65,122].

7. Mitochondrial priming and BH3 profiling

Apoptosis is a complex process regulated by several proteins; the intrinsic apoptotic pathway is mostly regulated by Bcl-2 proteins. As mentioned before, this group of proteins contains many members, making it difficult to analyze the complex pattern of interaction of individual proteins. However, Letai group developed a mechanism to find the ultimate result of this interaction. Cells are usually classified as dead or alive; they termed a third term called ‘primed for death’ [124]. Priming determines the dependence of cells on anti-apoptotic proteins for survival [125]. In response to death signaling received, these ‘primed cells’ have pro-apoptotic proteins sequestered by anti-apoptotic Bcl-2 proteins. Mitochondrial priming is used to reveal the degree of proximity to death. It correlates with the clinical response to chemotherapy. It can be used to characterize patients’ tissue into chemo-resistant and chemo-sensitive [126].

The Letai group developed a technique to measure priming called BH3-profiling. BH3-profiling is proposed to measure mitochondrial priming in patients to guide a personalized selection of the best chemotherapeutic regimen for a patient. BH3-profiling not only

determines if the tumor cells are primed for death, but it can also determine which anti-apoptotic proteins promote the survival of resistant samples [124,127]. Letai group have developed different ways of BH3-profiling. In this technique, mitochondria are isolated and treated with a panel of BH3-peptides and as a measure of the formation of OMMP release of cytochrome c or change in MMP is assessed. A fluorescent-associated cell sorting (FACS) for the measurement of MMP or cytochrome c can be utilized. However, a plate-based assay is commonly used for homogeneous cell population whereas FACS can be used in heterogeneous cell population [125].

Using B-cell lymphoma as a model, the Letai group classified cancer cell into three classes. Class A has suppression of pro-apoptotic activator BH3 proteins, Class B has lost Bax and Bak, effector Bcl-2 protein and Class C has high expression of anti-apoptotic Bcl-2 protein. Further class C cells which were sensitive to ABT-737, a BH3-mimetics, the anti-apoptotic protein particularly responsible for survival was identified [127]. This method can be used to find the dependency of on anti-apoptotic protein for survival. For example, a tumor it could be dependent on either Bcl-2 or Mcl-1 and Bcl-2 antagonists ABT-263 or ABT-199 could be used in that patient [125]. This classification helps in determining the chemotherapeutic drug that will work best in the patient.

8. SH3BP5 (Sab)

Sab (also called SH3 binding protein 5 or SH3BP5) was first identified as a novel molecule binding to SH3-domain of Bruton's tyrosine kinase (Btk) using protein interaction cloning method [128]. Sab is a scaffold protein present on the OMM [129]. Sab has three interaction motifs; kinase interaction motifs (KIM-1 and KIM-2) and SH3-binding motif [130,131]. A yeast-two hybrid screening method showed that C-terminus of Sab binds to

JNK [130]. C-terminus also has potential phosphorylation sites that can be assigned to MAPKs. The C-terminus is present on the outside of the mitochondria facing cytoplasm while N-terminal lies in between inner and outer membrane coil-like structure similar to myosin heavy chain [131]. Sab has been shown to facilitate pro-apoptotic signaling events in response to cytotoxic stress. One of the major known interacting partners of Sab is JNK; the interaction between these two have been shown to be involved in mitochondrial dysfunction and cell death in few studies. However, other mechanisms regulating Sab is not known yet.

8.1. Sab and JNK interaction

Sustained activation of JNK leads to its translocation to mitochondria [48,129]. The interaction between JNK and Sab was found to ‘prime the mitochondria’ for JNK signaling in the presence of 25µm of anisomycin for 30 minutes. It was observed that interaction of Sab with JNK results in initiation of the apoptotic pathway which occurs via KIM-1 motif. While inhibition of Mito-JNK signaling which was mediated by Sab, no mitochondrial dysfunction was observed [48]. It was shown that JNK-Sab interaction leads to phosphorylation of the anti-apoptotic protein Bcl-2, which leads to its emigration from mitochondria and favors the accumulation of pro-apoptotic BH3 only proteins [48]. The interaction between Sab and JNK leads to inhibition of respiration, increased reactive oxygen species (ROS) which further endures JNK activation and causes cell death [48,52,132,133]. JNK-Sab interaction leading to cell death has been observed in different disease models, which are inhibited by inhibiting JNK-Sab interaction or silencing of Sab. Acetaminophen or tumor-necrosis factor-induced liver injury requires JNK-Sab interaction [129]. In addition to this, the JNK-Sab nexus is involved in palmitic acid-induced

hepatocyte lipotoxicity, tunicamycin ER-stress induced apoptosis [134,135] This highlights the importance of the JNK interaction with scaffold protein Sab for causing mitochondria-mediated cell death.

The potential for the levels of Sab on the OMM to indicate the robustness of apoptotic induction was first illustrated by sub-chronic administration of LY294002 in HeLa cells [52]. Increasing Sab-levels by subchronic exposure to LY294002 could enhance the efficacy of cisplatin and paclitaxel in HeLa cells. While silencing of Sab or inhibition of JNK-Sab interaction did not increase the efficacy of these agents but rather promoted resistance [52]. We suggest that this technique of increasing Mito-JNK signaling by increasing Sab could be used to restore or enhance apoptosis in drug-resistant cancer cells.

9. Conclusion

Few investigations have examined the involvement of Mito-JNK in chemotherapeutic-induced death in OC cells; even though, a broad inhibition of JNK reveals a contribution to cisplatin- and paclitaxel-mediated apoptosis. There is even less information regarding the role of Sab in chemotherapeutic responses. The Chambers and Kaplowitz groups' collective research demonstrates the importance of Sab in mediating toxic JNK signaling events under different stress conditions. Increasing Sab concentration increases Mito-JNK signaling and consequently the potential to induce apoptosis through the manipulation of Bcl-2 proteins; however, the molecular mechanisms relating chemotherapeutic efficacy and Sab concentration have not been explored in gynecological cancers. This endeavor will be the subject of my dissertation research.

References:

- 1 Siegel, R. L., Miller, K. D. and Jemal, A. (2018) Cancer statistics, 2018. *CA: A Cancer Journal for Clinicians* **68**, 7–30.
- 2 Siegel, R. L., Miller, K. D. and Jemal, A. (2015) Cancer statistics, 2015. *CA: A Cancer Journal for Clinicians* **65**, 5–29.
- 3 Holmes, D. (2015) The problem with platinum. *Nature* **527**, S218–9.
- 4 Agarwal, R. and Kaye, S. B. (2003) Ovarian cancer: strategies for overcoming resistance to chemotherapy. *Nature Reviews Cancer*, Nature Publishing Group **3**, 502–516.
- 5 Tavassoli, F. A. and Devilee, P. (2003) Pathology and genetics of tumours of the breast and female genital organs.
- 6 Vaughan, S., Coward, J. I., Bast, R. C., Berchuck, A., Berek, J. S., Brenton, J. D., Coukos, G., Crum, C. C., Drapkin, R., Etemadmoghadam, D., et al. (2011) Rethinking ovarian cancer: recommendations for improving outcomes. *Nature Reviews Cancer*, Nature Publishing Group **11**, 719–725.
- 7 Seidman, J. D. and Kurman, R. J. (2000) Ovarian serous borderline tumors: A critical review of the literature with emphasis on prognostic indicators. *Human Pathology*, Elsevier **31**, 539–557.
- 8 McCluggage, W. G. (2011) Morphological subtypes of ovarian carcinoma. *Pathology* **43**, 420–432.
- 9 Heinzelmann-Schwarz, V. A., Gardiner-Garden, M., Henshall, S. M., Scurry, J. P., Scolyer, R. A., Smith, A. N., Bali, A., Bergh, P. V., Baron-Hay, S., Scott, C., et al. (2006) A distinct molecular profile associated with mucinous epithelial ovarian cancer. *British Journal of Cancer*, Nature Publishing Group **94**, 904–913.
- 10 Kaku, T., Ogawa, S., Kawano, Y., Ohishi, Y., Kobayashi, H., Hirakawa, T. and Nakano, H. (2003) Histological classification of ovarian cancer. *Med Electron Microsc*, Springer-Verlag **36**, 9–17.

- 11 Pignata, S., Ferrandina, G., Scarfone, G., Scollo, P., Odicino, F., Cormio, G., Katsaros, D., Villa, A., Mereu, L., Ghezzi, F., et al. (2008) Activity of chemotherapy in mucinous ovarian cancer with a recurrence free interval of more than 6 months: results from the SOCRATES retrospective study. *BMC Cancer* 2008 8:1, *BioMed Central* **8**, 252.
- 12 Bell, D. A. (2005) Origins and molecular pathology of ovarian cancer. *Modern Pathology* 2005 18:S2, Nature Publishing Group **18**, S19–S32.
- 13 Cont, N. T., Ferrero, A., Peccatori, F. A., D’Alonzo, M., Codacci-Pisanelli, G., Colombo, N. and Biglia, N. (2015) Medical treatment of early stage and rare histological variants of epithelial ovarian cancer. *ecancer, Cancer Intelligence* **9**, 584.
- 14 Petrillo, M., Nero, C., Amadio, G., Gallo, D., Fagotti, A. and Scambia, G. (2016) Targeting the hallmarks of ovarian cancer: The big picture. *Gynecologic Oncology, Elsevier Inc.* **142**, 176–183.
- 15 Hanahan, D. and Weinberg, R. A. (2011) Hallmarks of Cancer: The Next Generation. *Cell, Elsevier Inc.* **144**, 646–674.
- 16 Fodale, V., Pierobon, M., Liotta, L. and Petricoin, E. (2011) Mechanism of cell adaptation: when and how do cancer cells develop chemoresistance? *Cancer J, The Cancer Journal* **17**, 89–95.
- 17 Yap, T. A., Carden, C. P. and Kaye, S. B. (2009) Beyond chemotherapy: targeted therapies in ovarian cancer. *Nature Reviews Cancer* **9**, 167–181.
- 18 Dasari, S. and Tchounwou, P. B. (2014) Cisplatin in cancer therapy_ Molecular mechanisms of action. *European Journal of Pharmacology, Elsevier* **740**, 364–378.
- 19 Mutch, D. G. (2002) Surgical management of ovarian cancer. *Seminars in Oncology, Elsevier* **29**, 3–8.
- 20 Kartalou, M. and Essigmann, J. M. (2001) Recognition of cisplatin adducts by cellular proteins. *Mutation Research/Fundamental and Molecular Mechanisms of Mutagenesis* **478**, 1–21.

- 21 Nehmé, A., Baskaran, R., Aebi, S., Fink, D., Nebel, S., Cenni, B., Wang, J. Y. J., Howell, S. B. and Christen, R. D. (1997) Differential Induction of c-Jun NH2-Terminal Kinase and c-Abl Kinase in DNA Mismatch Repair-proficient and -deficient Cells Exposed to Cisplatin. *Cancer Research*, American Association for Cancer Research **57**, 3253–3257.
- 22 Mansouri, A., Ridgway, L. D., Korapati, A. L., Zhang, Q., Tian, L., Wang, Y., Siddik, Z. H., Mills, G. B. and Claret, F. X. (2003) Sustained activation of JNK/p38 MAPK pathways in response to cisplatin leads to Fas ligand induction and cell death in ovarian carcinoma cells. *Journal of Biological Chemistry*, American Society for Biochemistry and Molecular Biology **278**, 19245–19256.
- 23 Dumontet, C. and Sikic, B. I. (1999) Mechanisms of action of and resistance to antitubulin agents: microtubule dynamics, drug transport, and cell death. *J. Clin. Oncol.* **17**, 1061–1070.
- 24 Haldar, S., Basu, A. and Croce, C. M. (1997) Bcl2 is the guardian of microtubule integrity. *Cancer Research*, American Association for Cancer Research **57**, 229–233.
- 25 Woo, I. S., Jang, H.-S., Eun, S. Y., Kim, H. J., Ham, S. A., Kim, H. J., Lee, J. H., Chang, K. C., Kim, J.-H., Han, C. W., et al. (2008) Ran suppresses paclitaxel-induced apoptosis in human glioblastoma cells. *Apoptosis*, Springer US **13**, 1223–1231.
- 26 Lee, L.-F., Lee, L.-F., Li, G., Li, G., Templeton, D. J. and Ting, J. P. Y. (1998) Paclitaxel (Taxol)-induced Gene Expression and Cell Death Are Both Mediated by the Activation of c-Jun NH2-terminal Kinase (JNK/SAPK). *Journal of Biological Chemistry*, American Society for Biochemistry and Molecular Biology **273**, 28253–28260.
- 27 Amant, F., Moerman, P., Neven, P., Timmerman, D., Van Limbergen, E. and Vergote, I. (2005) Endometrial cancer. *The Lancet*, Elsevier **366**, 491–505.
- 28 Tangjitgamol, S., See, H. T. and Kavanagh, J. (2011) Adjuvant Chemotherapy for Endometrial Cancer. *International Journal of Gynecological Cancer* **21**, 885–895.
- 29 Högberg, T., Signorelli, M., de Oliveira, C. F., Fossati, R., Lissoni, A. A., Sorbe, B., Andersson, H., Grenman, S., Lundgren, C., Rosenberg, P., et al. (2010)

Sequential adjuvant chemotherapy and radiotherapy in endometrial cancer - Results from two randomised studies. *European Journal of Cancer*; 46(13), pp 2422-2431 (2010), IFAC & Elsevier Ltd. **46**, 2422–2431.

- 30 Lorusso, D., Petrelli, F., Coinu, A., Raspagliesi, F. and Barni, S. (2014) A systematic review comparing cisplatin and carboplatin plus paclitaxel-based chemotherapy for recurrent or metastatic cervical cancer. *Gynecologic Oncology*, Elsevier Inc. **133**, 117–123.
- 31 Tewari, K. S., Sill, M. W., Long, H. J. I., Penson, R. T., Huang, H., Ramondetta, L. M., Landrum, L. M., Oaknin, A., Reid, T. J., Leitao, M. M., et al. (2014) Improved Survival with Bevacizumab in Advanced Cervical Cancer. <http://dx.doi.org/10.1056/NEJMoa1309748>, *Massachusetts Medical Society* **370**, 734–743.
- 32 Davis, R. J. (2000) Signal transduction by the JNK group of MAP kinases. In *Inflammatory Processes: Molecular Mechanisms and Therapeutic Opportunities*, pp 13–21, Birkhäuser Basel, Basel.
- 33 Hibi, M., Lin, A., Smeal, T., Minden, A. and Karin, M. (1993) Identification of an oncoprotein- and UV-responsive protein kinase that binds and potentiates the c-Jun activation domain. *Genes & Development* **7**, 2135–2148.
- 34 Johnson, G. L. and Lapadat, R. (2002) Mitogen-activated protein kinase pathways mediated by ERK, JNK, and p38 protein kinases. *Science, American Association for the Advancement of Science* **298**, 1911–1912.
- 35 Tournier, C., Dong, C., Turner, T. K., Jones, S. N., Flavell, R. A. and Davis, R. J. (2001) MKK7 is an essential component of the JNK signal transduction pathway activated by proinflammatory cytokines. *Genes & Development, Cold Spring Harbor Lab* **15**, 1419–1426.
- 36 Yamamoto, K., Ichijo, H. and Korsmeyer, S. J. (1999) BCL-2 is phosphorylated and inactivated by an ASK1/Jun N-terminal protein kinase pathway normally activated at G(2)/M. *Molecular and Cellular Biology, American Society for Microbiology* **19**, 8469–8478.
- 37 Weston, C. R. and Davis, R. J. (2007) The JNK signal transduction pathway. *Current Opinion in Cell Biology* **19**, 142–149.

- 38 Zhou, Q., Lam, P. Y., Han, D. and Cadenas, E. (2008) c-Jun N-terminal kinase regulates mitochondrial bioenergetics by modulating pyruvate dehydrogenase activity in primary cortical neurons. *Journal of Neurochemistry*, Blackwell Publishing Ltd **104**, 325–335.
- 39 Minden, A., Lin, A., Smeal, T., Derijard, B., Cobb, M., Davis, R. and Karin, M. (1994) c-Jun N-terminal phosphorylation correlates with activation of the JNK subgroup but not the ERK subgroup of mitogen-activated protein kinases. *Molecular and Cellular Biology*, American Society for Microbiology **14**, 6683–6688.
- 40 Ito, Y., Mishra, N. C., Yoshida, K., Kharbanda, S., Saxena, S. and Kufe, D. (2001) Mitochondrial targeting of JNK/SAPK in the phorbol ester response of myeloid leukemia cells. *Cell death and differentiation* **8**, 794–800.
- 41 Hanawa, N., Shinohara, M., Saberi, B., Gaarde, W. A., Han, D. and Kaplowitz, N. (2008) Role of JNK translocation to mitochondria leading to inhibition of mitochondria bioenergetics in acetaminophen-induced liver injury. *Journal of Biological Chemistry*, American Society for Biochemistry and Molecular Biology **283**, 13565–13577.
- 42 Aoki, H., Kang, P. M., Hampe, J., Yoshimura, K., Noma, T., Matsuzaki, M. and Izumo, S. (2002) Direct activation of mitochondrial apoptosis machinery by c-Jun N-terminal kinase in adult cardiac myocytes. *Journal of Biological Chemistry*, American Society for Biochemistry and Molecular Biology **277**, 10244–10250.
- 43 Zhao, Y. and Herdegen, T. (2009) Cerebral ischemia provokes a profound exchange of activated JNK isoforms in brain mitochondria. *Molecular and Cellular Neuroscience* **41**, 186–195.
- 44 Zhou, Q., Lam, P. Y., Han, D. and Cadenas, E. (2009) Activation of c-Jun-N-terminal kinase and decline of mitochondrial pyruvate dehydrogenase activity during brain aging. *FEBS Letters* **583**, 1132–1140.
- 45 Xia, Z., Dickens, M., Raingeaud, J., Davis, R. J. and Greenberg, M. E. (1995) Opposing effects of ERK and JNK-p38 MAP kinases on apoptosis. *Science* **270**, 1326–1331.

- 46 Yang, D. D., Kuan, C.-Y., Whitmarsh, A. J., Rinócn, M., Zheng, T. S., Davis, R. J., Rakic, P. and Flavell, R. A. (1997) Absence of excitotoxicity-induced apoptosis in the hippocampus of mice lacking the *Jnk3* gene. *Nature*, Nature Publishing Group **389**, 865–870.
- 47 Tournier, C., Hess, P., Yang, D. D., Xu, J., Turner, T. K., Nimmual, A., Bar-Sagi, D., Jones, S. N., Flavell, R. A. and Davis, R. J. (2000) Requirement of JNK for stress-induced activation of the cytochrome c-mediated death pathway. *Science*, American Association for the Advancement of Science **288**, 870–874.
- 48 Chambers, J. W., Cherry, L., Laughlin, J. D., Figuera-Losada, M. and LoGrasso, P. V. (2011) Selective Inhibition of Mitochondrial JNK Signaling Achieved Using Peptide Mimicry of the Sab Kinase Interacting Motif-1 (KIM1). *ACS Chemical Biology* **6**, 808–818.
- 49 Yu, C., Minemoto, Y., Zhang, J., Liu, J., Tang, F., Bui, T. N., Xiang, J. and Lin, A. (2004) JNK Suppresses Apoptosis via Phosphorylation of the Proapoptotic Bcl-2 Family Protein BAD. *Molecular Cell* **13**, 329–340.
- 50 Sabapathy, K., Jochum, W., Hochedlinger, K., Chang, L., Karin, M. and Wagner, E. F. (1999) Defective neural tube morphogenesis and altered apoptosis in the absence of both JNK1 and JNK2. *Mechanisms of Development* **89**, 115–124.
- 51 Du, L., Lyle, C. S., Obey, T. B., Gaarde, W. A., Muir, J. A., Bennett, B. L. and Chambers, T. C. (2004) Inhibition of cell proliferation and cell cycle progression by specific inhibition of basal JNK activity: evidence that mitotic Bcl-2 phosphorylation is JNK-independent. *Journal of Biological Chemistry*, American Society for Biochemistry and Molecular Biology **279**, 11957–11966.
- 52 Chambers, T. P., Portalatin, G. M., Paudel, I., Robbins, C. J. and Chambers, J. W. (2015) Sub-chronic administration of LY294002 sensitizes cervical cancer cells to chemotherapy by enhancing mitochondrial JNK signaling. *Biochemical and Biophysical Research Communications* **463**, 538–544.
- 53 Dhanasekaran, D. N. and Reddy, E. P. (2008) JNK signaling in apoptosis. *Oncogene*, Nature Publishing Group **27**, 6245–6251.
- 54 Petros, A. M., Nettesheim, D. G., Wang, Y., Olejniczak, E. T., Meadows, R. P., Mack, J., Swift, K., Matayoshi, E. D., Zhang, H., Fesik, S. W., et al. (2000)

Rationale for Bcl-XL/Bad peptide complex formation from structure, mutagenesis, and biophysical studies. *Protein Science*, Cold Spring Harbor Laboratory Press **9**, 2528–2534.

- 55 Chipuk, J. E., Moldoveanu, T., Llambi, F., Parsons, M. J. and Green, D. R. (2010) The BCL-2 family reunion. *Molecular Cell* **37**, 299–310.
- 56 Serasinghe, M. N., Missert, D. J., Ascioffa, J. J., Podgrabinska, S., Wieder, S. Y., Izadmehr, S., Belbin, G., Skobe, M. and Chipuk, J. E. (2015) Anti-apoptotic BCL-2 proteins govern cellular outcome following B-RAFV600E inhibition and can be targeted to reduce resistance. *Oncogene*, Nature Publishing Group **34**, 857–867.
- 57 Kuwana, T., Bouchier-Hayes, L., Chipuk, J. E., Bonzon, C., Sullivan, B. A., Green, D. R. and Newmeyer, D. D. (2005) BH3 Domains of BH3-Only Proteins Differentially Regulate Bax-Mediated Mitochondrial Membrane Permeabilization Both Directly and Indirectly. *Molecular Cell* **17**, 525–535.
- 58 Lei, K. and Davis, R. J. (2003) JNK phosphorylation of Bim-related members of the Bcl2 family induces Bax-dependent apoptosis. *Proceedings of the National Academy of Sciences* 2432–2437.
- 59 Letai, A., Bassik, M. C., Walensky, L. D., Sorcinelli, M. D., Weiler, S. and Korsmeyer, S. J. (2002) Distinct BH3 domains either sensitize or activate mitochondrial apoptosis, serving as prototype cancer therapeutics. *Cancer Cell* **2**, 183–192.
- 60 Green, D. R., Galluzzi, L. and Kroemer, G. (2014) Cell biology. Metabolic control of cell death. *Science*, American Association for the Advancement of Science **345**, 1250256–1250256.
- 61 Mojsa, B., Lassot, I. and Desagher, S. (2014) Mcl-1 Ubiquitination: Unique Regulation of an Essential Survival Protein **3**, 418–437.
- 62 Youle, R. J. and Strasser, A. (2008) The BCL-2 protein family: opposing activities that mediate cell death. *Nature Reviews Molecular Cell Biology* **9**, 47–59.
- 63 Chen, L., Willis, S. N., Wei, A., Smith, B. J., Fletcher, J. I., Hinds, M. G., Colman, P. M., Day, C. L., Adams, J. M. and Huang, D. C. S. (2005) Differential targeting

of prosurvival Bcl-2 proteins by their BH3-only ligands allows complementary apoptotic function. *Molecular Cell* **17**, 393–403.

- 64 Letai, A. G. (2008) Diagnosing and exploiting cancer's addiction to blocks in apoptosis. *Nature Reviews Cancer*, Nature Publishing Group **8**, 121–132.
- 65 Leist, M. and Jäätelä, M. (2001) Four deaths and a funeral: from caspases to alternative mechanisms. *Nature Reviews Molecular Cell Biology*, Nature Publishing Group **2**, 589–598.
- 66 Hirsch, T., Susin, S. A., Marzo, I., Marchetti, P., Zamzami, N. and Kroemer, G. (1998) Mitochondrial permeability transition in apoptosis and necrosis. *Cell Biol Toxicol*, Kluwer Academic Publishers **14**, 141–145.
- 67 Green, D. R. (2006) At the gates of death. *Cancer Cell* **9**, 328–330.
- 68 Ricci, J.-E., Waterhouse, N. and Green, D. R. (2003, May) Mitochondrial functions during cell death, a complex (I-V) dilemma. *Cell Death Differ*.
- 69 Archer, S. L. (2013) Mitochondrial Dynamics — Mitochondrial Fission and Fusion in Human Diseases. *N Engl J Med* (Longo, D. L., ed.) **369**, 2236–2251.
- 70 Leboucher, G. P., Tsai, Y. C., Yang, M., Shaw, K. C. and Zhou, M. (2012) Stress-induced phosphorylation and proteasomal degradation of mitofusin 2 facilitates mitochondrial fragmentation and apoptosis. *Molecular Cell*.
- 71 Rojo, M., Legros, F., Chateau, D. and Lombès, A. (2002) Membrane topology and mitochondrial targeting of mitofusins, ubiquitous mammalian homologs of the transmembrane GTPase Fzo. *Journal of Cell Science*, The Company of Biologists Ltd **115**, 1663–1674.
- 72 Perfettini, J.-L., Roumier, T. and Kroemer, G. (2005) Mitochondrial fusion and fission in the control of apoptosis. *Trends in Cell Biology*, Elsevier Current Trends **15**, 179–183.
- 73 Lithgow, T., Van Driel, R., Bertram, J. F. and Strasser, A. (1994) The protein product of the oncogene bcl-2 is a component of the nuclear envelope, the

endoplasmic reticulum, and the outer mitochondrial membrane. *Cell growth & differentiation* **5**, 411–417.

- 74 Srivastava, R. K., Mi, Q. S., Hardwick, J. M. and Longo, D. L. (1999) Deletion of the loop region of Bcl-2 completely blocks paclitaxel-induced apoptosis. *Proceedings of the National Academy of Sciences, National Acad Sciences* **96**, 3775–3780.
- 75 Fang, G., Chang, B. S., Kim, C. N., Perkins, C., Thompson, C. B. and Bhalla, K. N. (1998) “Loop” domain is necessary for taxol-induced mobility shift and phosphorylation of Bcl-2 as well as for inhibiting taxol-induced cytosolic accumulation of cytochrome c and apoptosis. *Cancer Research, American Association for Cancer Research* **58**, 3202–3208.
- 76 Fan, M., Goodwin, M., Vu, T., Brantley-Finley, C., Gaarde, W. A. and Chambers, T. C. (2000) Vinblastine-induced Phosphorylation of Bcl-2 and Bcl-XL Is Mediated by JNK and Occurs in Parallel with Inactivation of the Raf-1/MEK/ERK Cascade. *Journal of Biological Chemistry* **275**, 29980–29985.
- 77 Haldar, S., Jena, N. and Croce, C. M. (1995) Inactivation of Bcl-2 by phosphorylation. *Proceedings of the National Academy of Sciences, National Acad Sciences* **92**, 4507–4511.
- 78 Deng, X., Xiao, L., Lang, W., Gao, F., Ruvolo, P. and May, W. S. (2001) Novel role for JNK as a stress-activated Bcl2 kinase. *Journal of Biological Chemistry* **276**, 23681–23688.
- 79 Brichese, L., Cazettes, G. and Valette, A. (2004) JNK is Associated with Bcl-2 and PP1 in Mitochondria: Paclitaxel Induces Its Activation and Its Association with the Phosphorylated Form of Bcl-2. *Cell Cycle, Taylor & Francis* **3**, 1312–1319.
- 80 Park, J., Kim, I., Oh, Y. J., Lee, K.-W., Han, P.-L. and Choi, E.-J. (1997) Activation of c-Jun N-terminal Kinase Antagonizes an Anti-apoptotic Action of Bcl-2. *Journal of Biological Chemistry, American Society for Biochemistry and Molecular Biology* **272**, 16725–16728.
- 81 Park, D. S., Stefanis, L., Yan, C. Y., Farinelli, S. E. and Greene, L. A. (1996) Ordering the cell death pathway. Differential effects of BCL2, an interleukin-1-converting enzyme family protease inhibitor, and other survival agents on JNK

- activation in serum/nerve growth factor-deprived PC12 cells. *Journal of Biological Chemistry, American Society for Biochemistry and Molecular Biology* **271**, 21898–21905.
- 82 Muchmore, S. W., Sattler, M., Liang, H., Meadows, R. P., Harlan, J. E., Yoon, H. S., Nettlesheim, D. G., Chang, B. S., Thompson, C. B., Wong, S.-L., et al. (1996) X-ray and NMR structure of human Bcl-xL, an inhibitor of programmed cell death. *Nature* **381**, 335–341.
- 83 Kroemer, G., Zamzami, N. and Susin, S. A. (1997) Mitochondrial control of apoptosis. *Immunology Today* **18**, 44–51.
- 84 Petros, A. M., Olejniczak, E. T. and Fesik, S. W. (2004) Structural biology of the Bcl-2 family of proteins. *Biochimica et Biophysica Acta (BBA) - Molecular Cell Research* **1644**, 83–94.
- 85 Letai, A. G. (2008) Diagnosing and exploiting cancer's addiction to blocks in apoptosis. *Nature Reviews Cancer, Nature Publishing Group* **8**, 121–132.
- 86 Kharbanda, S., Saxena, S., Yoshida, K., Pandey, P., Kaneki, M., Wang, Q., Cheng, K., Chen, Y. N., Campbell, A., Sudha, T., et al. (2000) Translocation of SAPK/JNK to Mitochondria and Interaction with Bcl-xL in Response to DNA Damage. *Journal of Biological Chemistry, American Society for Biochemistry and Molecular Biology* **275**, 322–327.
- 87 Basu, A. and Haldar, S. (2003) Identification of a novel Bcl-xL phosphorylation site regulating the sensitivity of taxol- or 2-methoxyestradiol-induced apoptosis. *FEBS Letters* **538**, 41–47.
- 88 Du, L., Lyle, C. S. and Chambers, T. C. (2004) Characterization of vinblastine-induced Bcl-xL and Bcl-2 phosphorylation: evidence for a novel protein kinase and a coordinated phosphorylation/dephosphorylation cycle associated with apoptosis induction. *Oncogene* **24**, 107–117.
- 89 Opferman, J. T. (2007) Life and death during hematopoietic differentiation. *Current opinion in immunology* **19**, 497–502.

- 90 Morel, C., Carlson, S. M., White, F. M. and Davis, R. J. (2009) Mcl-1 Integrates the Opposing Actions of Signaling Pathways That Mediate Survival and Apoptosis. *Molecular and Cellular Biology* **29**, 3845–3852.
- 91 Krajewski, S., Bodrug, S., Krajewska, M., Shabaik, A., Gascoyne, R., Berean, K. and Reed, J. C. (1995) Immunohistochemical analysis of Mcl-1 protein in human tissues. Differential regulation of Mcl-1 and Bcl-2 protein production suggests a unique role for Mcl-1 in control of programmed cell death in vivo. *The American Journal of Pathology, American Society for Investigative Pathology* **146**, 1309–1319.
- 92 Kobayashi, S., Lee, S.-H., Meng, X. W., Mott, J. L., Bronk, S. F., Werneburg, N. W., Craig, R. W., Kaufmann, S. H. and Gores, G. J. (2007) Serine 64 Phosphorylation Enhances the Antiapoptotic Function of Mcl-1. *Journal of Biological Chemistry* **282**, 18407–18417.
- 93 Michels, J., Johnson, P. W. M. and Packham, G. (2005) Mcl-1. **37**, 267–271.
- 94 Maurer, U., Charvet, C., Wagman, A. S., Dejardin, E. and Green, D. R. (2006) Glycogen synthase kinase-3 regulates mitochondrial outer membrane permeabilization and apoptosis by destabilization of MCL-1. *Molecular Cell* **21**, 749–760.
- 95 Inoshita, S., Takeda, K., Hatai, T., Terada, Y., Sano, M., Hata, J., Umezawa, A. and Ichijo, H. (2002) Phosphorylation and Inactivation of Myeloid Cell Leukemia 1 by JNK in Response to Oxidative Stress. *Journal of Biological Chemistry* **277**, 43730–43734.
- 96 Kodama, Y., Taura, K., Miura, K., Schnabl, B., Osawa, Y. and Brenner, D. A. (2009) Antiapoptotic Effect of c-Jun N-terminal Kinase-1 through Mcl-1 Stabilization in TNF-Induced Hepatocyte Apoptosis. *Gastroenterology* **136**, 1423–1434.
- 97 O'Reilly, L. A., Cullen, L., Visvader, J., Lindeman, G. J., Print, C., Bath, M. L., Huang, D. C. S. and Strasser, A. (2000) The Proapoptotic BH3-Only Protein Bim Is Expressed in Hematopoietic, Epithelial, Neuronal, and Germ Cells. *The American Journal of Pathology* **157**, 449–461.

- 98 Puthalakath, H., Huang, D. C. S., O'Reilly, L. A., King, S. M. and Strasser, A. (1999) The Proapoptotic Activity of the Bcl-2 Family Member Bim Is Regulated by Interaction with the Dynein Motor Complex. *Molecular Cell* **3**, 287–296.
- 99 Corazza, N., Jakob, S., Schaer, C., Frese, S., Keogh, A., Stroka, D., Kassahn, D., Torgler, R., Mueller, C., Schneider, P., et al. (2006) TRAIL receptor-mediated JNK activation and Bim phosphorylation critically regulate Fas-mediated liver damage and lethality. *Journal of Clinical Investigation, American Society for Clinical Investigation* **116**, 2493–2499.
- 100 Harris, C. A. and Eugene M Johnson, J. (2001) BH3-only Bcl-2 Family Members Are Coordinately Regulated by the JNK Pathway and Require Bax to Induce Apoptosis in Neurons. *Journal of Biological Chemistry, American Society for Biochemistry and Molecular Biology* **276**, 37754–37760.
- 101 Putcha, G. V., Moulder, K. L., Golden, J. P., Bouillet, P., Adams, J. A., Strasser, A. and Johnson, E. M., Jr. (2001) Induction of BIM, a Proapoptotic BH3-Only BCL-2 Family Member, Is Critical for Neuronal Apoptosis. *Neuron* **29**, 615–628.
- 102 Ma, C., Ying, C., Yuan, Z., Song, B., Li, D., Liu, Y., Lai, B., Li, W., Chen, R., Ching, Y.-P., et al. (2007) dp5/HRK is a c-Jun target gene and required for apoptosis induced by potassium deprivation in cerebellar granule neurons. *Journal of Biological Chemistry, American Society for Biochemistry and Molecular Biology* **282**, 30901–30909.
- 103 Guan, Q.-H., Pei, D.-S., Xu, T.-L. and Zhang, G.-Y. (2006) Brain ischemia/reperfusion-induced expression of DP5 and its interaction with Bcl-2, thus freeing Bax from Bcl-2/Bax dimmers are mediated by c-Jun N-terminal kinase (JNK) pathway. *Neuroscience Letters* **393**, 226–230.
- 104 Imaizumi, K., Tsuda, M., Imai, Y., Wanaka, A., Takagi, T. and Tohyama, M. (1997) Molecular Cloning of a Novel Polypeptide, DP5, Induced during Programmed Neuronal Death. *Journal of Biological Chemistry, American Society for Biochemistry and Molecular Biology* **272**, 18842–18848.
- 105 Inohara, N., Ding, L., Chen, S. and Núñez, G. (1997) *harakiri*, a novel regulator of cell death, encodes a protein that activates apoptosis and interacts selectively with survival-promoting proteins Bcl-2 and Bcl-XL. *The EMBO Journal, EMBO Press* **16**, 1686–1694.

- 106 Young, J. E., Garden, G. A., Martinez, R. A., Tanaka, F., Sandoval, C. M., Smith, A. C., Sopher, B. L., Lin, A., Fischbeck, K. H., Ellerby, L. M., et al. (2009) Polyglutamine-expanded androgen receptor truncation fragments activate a Bax-dependent apoptotic cascade mediated by DP5/Hrk. *The Journal of Neuroscience, Society for Neuroscience* **29**, 1987–1997.
- 107 Rizvi, F., Heimann, T., Herrnreiter, A. and O'Brien, W. J. (2011) Mitochondrial Dysfunction Links Ceramide Activated HRK Expression and Cell Death. *PLOS ONE* (El-Rifai, W., ed.), Public Library of Science **6**, e18137.
- 108 Nakano, K. and Vousden, K. H. (2001) PUMA, a novel proapoptotic gene, is induced by p53. *Molecular Cell, Elsevier* **7**, 683–694.
- 109 Yu, J., Wang, Z., Kinzler, K. W., Vogelstein, B. and Zhang, L. (2003) PUMA mediates the apoptotic response to p53 in colorectal cancer cells. *Proceedings of the National Academy of Sciences, National Acad Sciences* **100**, 1931–1936.
- 110 Cazanave, S. C., Mott, J. L., Elmi, N. A., Bronk, S. F., Werneburg, N. W., Akazawa, Y., Kahraman, A., Garrison, S. P., Zambetti, G. P., Charlton, M. R., et al. (2009) JNK1-dependent PUMA expression contributes to hepatocyte lipoapoptosis. *Journal of Biological Chemistry, American Society for Biochemistry and Molecular Biology* **284**, 26591–26602.
- 111 Ambacher, K. K., Pitzul, K. B., Karajgikar, M., Hamilton, A., Ferguson, S. S. and Cregan, S. P. (2012) The JNK- and AKT/GSK3 β - signaling pathways converge to regulate Puma induction and neuronal apoptosis induced by trophic factor deprivation. *PLOS ONE* (Hetman, M., ed.) **7**, e46885.
- 112 Yang, E., Zha, J., Jockel, J., Boise, L. H., Thompson, C. B. and Korsmeyer, S. J. (1995) Bad, a heterodimeric partner for Bcl-xL and Bcl-2, displaces bax and promotes cell death. *Cell* **80**, 285–291.
- 113 Zha, J., Zha, Harada, H., Yang, E., Jockel, J. and Korsmeyer, S. J. (1996) Serine Phosphorylation of Death Agonist BAD in Response to Survival Factor Results in Binding to 14-3-3 Not BCL-X_L. *Cell* **87**, 619–628.
- 114 Konishi, Y., Lehtinen, M., Donovan, N. and Bonni, A. (2002) Cdc2 Phosphorylation of BAD Links the Cell Cycle to the Cell Death Machinery. *Molecular Cell* **9**, 1005–1016.

- 115 Donovan, N., Becker, E. B. E., Konishi, Y. and Bonni, A. (2002) JNK phosphorylation and activation of BAD couples the stress-activated signaling pathway to the cell death machinery. *Journal of Biological Chemistry*, American Society for Biochemistry and Molecular Biology **277**, 40944–40949.
- 116 Liu, J. and Lin, A. (2005) Role of JNK activation in apoptosis: A double-edged sword. *Cell Research*, Nature Publishing Group **15**, 36–42.
- 117 Walensky, L. D. and Gavathiotis, E. (2011) BAX unleashed: the biochemical transformation of an inactive cytosolic monomer into a toxic mitochondrial pore. *Trends in Biochemical Sciences* **36**, 642–652.
- 118 Kim, B. J., Ryu, S. W. and Song, B. J. (2006) JNK- and p38 Kinase-mediated Phosphorylation of Bax Leads to Its Activation and Mitochondrial Translocation and to Apoptosis of Human Hepatoma HepG2 Cells. *Journal of Biological Chemistry* **281**, 21256–21265.
- 119 Samuel, T., Weber, H. O., Rauch, P., Verdoodt, B., Eppel, J. T., McShea, A., Hermeking, H. and Funk, J. O. (2001) The G2/M regulator 14-3-3sigma prevents apoptosis through sequestration of Bax. *Journal of Biological Chemistry*, American Society for Biochemistry and Molecular Biology **276**, 45201–45206.
- 120 Tsuruta, F., Sunayama, J., Mori, Y., Hattori, S., Shimizu, S., Tsujimoto, Y., Yoshioka, K., Masumaya, N. and Gotoh, Y. (2004) JNK promotes Bax translocation to mitochondria through phosphorylation of 14-3-3 proteins. *The EMBO Journal* **23**, 1889–1899.
- 121 Whitmarsh, A. J., Cavanagh, J., Tournier, C., Yasuda, J. and Davis, R. J. (1998) A Mammalian Scaffold Complex That Selectively Mediates MAP Kinase Activation. *Science* **281**, 1671–1674.
- 122 Newmeyer, D. D. and Ferguson-Miller, S. (2003) Mitochondria: Releasing Power for Life and Unleashing the Machineries of Death. *Cell*, Cell Press **112**, 481–490.
- 123 Chipuk, J. E., Bouchier-Hayes, L. and Green, D. R. (2006) Mitochondrial outer membrane permeabilization during apoptosis: the innocent bystander scenario. *Cell Death Differ*, Nature Publishing Group **13**, 1396–1402.

- 124 Certo, M., Moore, V. D. G., Nishino, M., Wei, G., Korsmeyer, S., Armstrong, S. A. and Letai, A. (2006) Mitochondria primed by death signals determine cellular addiction to antiapoptotic BCL-2 family members. *Cancer Cell* **9**, 351–365.
- 125 Ryan, J. and Letai, A. (2013) BH3 profiling in whole cells by fluorimeter or FACS. *Methods* **61**, 156–164.
- 126 Chonghaile, T. N., Sarosiek, K. A., Vo, T.-T., Ryan, J. A., Tammareddi, A., Del Gaizo Moore, V., Deng, J., Anderson, K. C., Richardson, P., Tai, Y.-T., et al. (2011) Pretreatment Mitochondrial Priming Correlates with Clinical Response to Cytotoxic Chemotherapy. *Science, American Association for the Advancement of Science* **334**, 1129–1133.
- 127 Deng, J., Carlson, N., Takeyama, K., Dal Cin, P., Shipp, M. and Letai, A. (2007) BH3 Profiling Identifies Three Distinct Classes of Apoptotic Blocks to Predict Response to ABT-737 and Conventional Chemotherapeutic Agents. *Cancer Cell, Cell Press* **12**, 171–185.
- 128 Matsushita, M., Yamadori, T., Kato, S., Takemoto, Y., Inazawa, J., Baba, Y., Hashimoto, S., Sekine, S., Arai, S., Kunikata, T., et al. (1998) Identification and Characterization of a Novel SH3-Domain Binding Protein, Sab, Which Preferentially Associates with Bruton's Tyrosine Kinase (Btk). *Biochemical and Biophysical Research Communications* **245**, 337–343.
- 129 Win, S., Than, T. A., Han, D., Petrovic, L. M. and Kaplowitz, N. (2011) c-Jun N-terminal Kinase (JNK)-dependent Acute Liver Injury from Acetaminophen or Tumor Necrosis Factor (TNF) Requires Mitochondrial Sab Protein Expression in Mice. *Journal of Biological Chemistry, American Society for Biochemistry and Molecular Biology* **286**, 35071–35078.
- 130 Wiltshire, C., Matsushita, M., Tsukada, S., Gillespie, D. A. F. and May, G. H. W. (2002) A new c-Jun N-terminal kinase (JNK)-interacting protein, Sab (SH3BP5), associates with mitochondria. *Biochemical Journal, Portland Press Limited* **367**, 577–585.
- 131 Wiltshire, C., Gillespie, D. A. F. and May, G. H. W. (2004) Sab (SH3BP5), a novel mitochondria-localized JNK-interacting protein. *Biochemical Society Transactions, Portland Press Limited* **32**, 1075–1077.

- 132 Win, S., Than, T. A., Le, B. H. A., García-Ruiz, C., Fernandez-Checa, J. C. and Kaplowitz, N. (2015) Sab (SH3BP5) dependence of JNK mediated inhibition of mitochondrial respiration in palmitic acid induced hepatocyte lipotoxicity. *Journal of Hepatology* **62**, 1367–1374.
- 133 Chambers, J. W. and LoGrasso, P. V. (2011) Mitochondrial c-Jun N-terminal Kinase (JNK) Signaling Initiates Physiological Changes Resulting in Amplification of Reactive Oxygen Species Generation. *Journal of Biological Chemistry* **286**, 16052–16062.
- 134 Win, S., Than, T. A., Min, R. W. M., Agahajan, M. and Kaplowitz, N. (2016) c-Jun N-Terminal Kinase Mediates Mouse Liver Injury Through a Novel Sab (SH3BP5)-Dependent Pathway Leading to Inactivation of Intramitochondrial Src. *Hepatology* **63**, 1987–2003.
- 135 Win, S., Than, T. A., Fernandez-Checa, J. C. and Kaplowitz, N. (2014) JNK interaction with Sab mediates ER stress induced inhibition of mitochondrial respiration and cell death. *Cell Death and Disease* **5**, e989–e989.

CHAPTER 2
HYPOTHESIS AND RATIONALE

1. Problem Statement

Gynecological cancer mortality can be attributed to the presence of recurrent, highly metastatic, and resistant disease [1]. Unfortunately, the molecular mechanisms responsible for the resistance to conventional therapies are not thoroughly defined. Because of this knowledge gap, treatment-resistant gynecological cancers are responsible for diminished survival in late-stage ovarian and uterine cancer patients [2]. Thus, until the mechanisms driving therapeutic resistance are defined, effective therapies for advanced gynecological cancers will likely remain elusive. Therefore, it is the goal of this research to identify and characterize molecular events responsible for therapeutic resistance in gynecological cancers. By elucidating these events, one anticipates that new treatments targeting these specific molecular alterations can be developed to reestablish cell death induction in many difficult to treat tumors.

2. Hypothesis and Rationale

The inability of tumor cells to induce cell death mechanisms is a hallmark of cancer [3]. A recent study demonstrated that treatment with a chemosensitizer (LY294002) altered cell death signaling on the mitochondrial surface, the site for induction of apoptosis [4]. Sub-chronic, low-dose treatment with LY294002 increased the concentration of the outer mitochondrial scaffold protein Sab. Because the concentration of scaffold proteins dictate the biological outcomes of signaling pathways at discrete subcellular locales [5, 6], one could propose that increased Sab levels on mitochondria would correspond to enhanced c-Jun N-terminal Kinase (JNK) signaling on the organelle. Indeed, chemosensitization did increase the drug-induced translocation of JNK to mitochondria and lowered the threshold for apoptosis in a Sab-dependent manner [4]. Based on this study and other relevant

literature (See Chapter 1), the *over-arching hypothesis* of this project is that decreased Sab expression in gynecological cancers is in part responsible for chemotherapeutic resistance in late-stage disease. Furthermore, therapeutic strategies aimed at elevating the local concentrations of Sab on mitochondria may represent useful approaches to restore cell death induction in treatment-resistant gynecological tumors. The rationale for this research is once approaches are found to restore apoptotic pathways in gynecological tumors efficacious treatments can eliminate the disease resulting in increased patient survival and improve quality of life.

3. Project Aims

To investigate the hypothesis, and accomplish the research goal, the approach for this project is to understand the role of mitochondrial signaling in drug resistance for gynecological cancers and develop an approach to restore mitochondrial JNK signaling and induction of apoptosis in tumor cells. For this purpose, the following specific aims are proposed.

- a. Identify the role of Sab in mitochondrial JNK signaling and mitochondrial priming in gynecological cancers.
- b. Identify and characterize compounds that increase Sab concentrations in treatment-resistant gynecological cancer cells.

4. Chapter Abstracts

The project has resulted in three submitted manuscripts, which will comprise Chapters 3, 4, and 5 of the dissertation. To preview these chapters, the abstracts from these manuscripts/chapters appear below:

Chapter 3 - Sab Concentrations Indicate Chemotherapeutic Susceptibility in Ovarian Cancer Cell Lines

The occurrence of chemotherapy-resistant tumors makes ovarian cancer (OC) the most lethal gynecological malignancy. While many factors may contribute to chemoresistance in OC, the mechanisms responsible for regulating tumor vulnerability are under investigation. Our analysis of gene expression data from OC studies revealed that Sab, a mitochondrial outer membrane (OMM) scaffold protein, was down-regulated in OC patients. Our previous studies demonstrate that Sab-mediated signaling on the OMM induces cell death suggesting that this apoptotic pathway may be diminished in OC. In the current study, we examined Sab expression in a panel of OC cell lines and found that the magnitude of Sab expression correlated to chemo-responsiveness; wherein, OC cells with high Sab concentrations were vulnerable to chemotherapy, while cells with low Sab levels were chemoresistant. The Sab levels were reflected by a complementary amount of the c-Jun N-terminal kinase (JNK) on the OMM in response to cytotoxic stress. Dynamic BH3 profiling and examination of Bcl-2 and BH3-only protein concentrations revealed that cells with high Sab expression were primed for apoptosis, as determined by the decrease in pro-survival Bcl-2 proteins and an increase in pro-apoptotic BH3-only proteins on mitochondria. Furthermore, over-expression of Sab in chemoresistant cells enhanced apoptotic priming and restored cellular vulnerability to a combination treatment of cisplatin and paclitaxel. Contrariwise, inhibiting Sab-mediated signaling or silencing Sab expression in a chemosensitive cell line resulted in decreased apoptotic priming and increased resistance to cisplatin/paclitaxel treatment. We propose that Sab may be a prognostic biomarker to discern personalized treatments for OC patients.

Chapter 4 – Sab Concentrations Indicate Chemotherapeutic Susceptibility in Uterine Cancer Cell Lines

Metastatic uterine cancer (UC) has a 5-year survival less than 8%. This mortality is associated with treatment resistance in metastatic UC cells. There is an urgent need to identify the mechanisms contributing to resistance in UC patients with metastatic disease to improve the patient survival. Mitochondria control cell death responses, yet cancer cells can develop mechanisms to avoid apoptosis and evade therapeutic approaches. We propose communication between the cell and mitochondria becomes altered during metastasis, and metastatic UC cells have mitochondria that can no longer process cell death signals. To address if mitochondrial-cell communication was altered during metastasis, we compared a human cell line derived from a primary site tumor (SK-UT-1) and another isolated from a metastatic site (AN-3-Ca). Analysis of the signaling proteins on the surface of the mitochondria in these two cell lines revealed that a scaffold protein, Sab, was down-regulated in metastatic AN-3-Ca cells compared to SK-UT-1. Our previous research demonstrated that elevated levels of Sab induced mitochondrial dysfunction and apoptosis, ultimately enhancing chemo-responsiveness in gynecological tumors. We examined the apoptotic potential of SK-UT-1 and AN-3-Ca cells by measuring the levels of pro-survival Bcl-2 proteins and pro-death BH-3 only proteins. Our results indicate that metastatic AN-3-Ca cells had considerably higher levels of Bcl-2 proteins, while SK-UT-1 cells had higher levels of BH-3 only proteins. We found that AN-3-Ca cells were more resistant to taxane and platinum treatment than SK-UT-1 cells. To determine if diminished Sab-mediated signaling played a role chemo-resistance, we ectopically expressed Sab in AN-3-Ca cells. Elevating Sab levels in AN-3-Ca cells rescued chemo-responsiveness by

decreasing Bcl-2 protein levels and increasing BH-3 only protein concentrations. We surmise that Sab-mediated signaling plays a critical role in treatment responsiveness in UC and that inhibiting Sab expression is a critical event in metastasis and chemo-resistance.

Chapter 5 - A high-throughput Assay to Screen for Compounds Elevating Sab Concentrations in Chemoresistant Human Ovarian Cancer Cells.

Ovarian cancer (OC) is the most lethal gynecological malignancy. OC mortality is associated with the high rate of recurrence, which stands at approximately 80%. Recurrence is typified by the presence of treatment-resistant cells; consequently, conventional therapies, including chemotherapy, are often ineffective. Therefore, it is imperative to find novel therapeutic options to eliminate treatment-resistant OC cells. We propose that targeting mitochondrial-cell communication in resistant OC cells will increase their susceptibility to established chemotherapies. Previous studies from our lab demonstrate that increasing the concentration of the outer mitochondrial scaffold protein Sab sensitizes OC cells to paclitaxel by inducing apoptotic priming. These studies suggest that increasing Sab levels in OC will induce a pre-apoptotic state and sensitize the tumor cells to conventional chemotherapies, thus rendering resistant OC cells sensitive. We have developed a high-throughput assay, an in-cell western (ICW), to detect changes in Sab protein concentrations following chemical exposures. The ICW approach was developed in HEK-293 cells and validated using Sab silencing and overexpression. A trail screen of known compounds found that mitochondrial toxins were the most potent enhancers of Sab levels, while antioxidants were the greatest suppressors of Sab levels. The ICW assay was re-optimized in SK-OV-3 cells (z- score of 0.81), a chemoresistant cell line. The Sab ICW

was co-stained with the TO-PRO-3 DNA stain for normalization and as an index of viability. We screened a scaffold-ranking and positional-scanning library (provided by the Torrey Pines Institute for Molecular Studies) to identify novel compounds that increase Sab expression in OC cells. Fifty (50) chemical scaffolds were screened for SK-OV-3 cells. Scaffolds selected for further testing increased Sab expression greater than 30% and demonstrated minimal toxicity in SK-OV-3 cells. Using this method we have identified six candidate scaffolds. Individual compounds derived from this scaffold are currently being evaluated to identify the best compounds for OC studies. We predict that this approach will identify novel drugs that will improve OC treatment and mortality.

References

- 1 Ferlay, J., Soerjomataram, I., Dikshit, R., Eser, S., Mathers, C., Rebelo, M., Parkin, D. M., Forman, D. and Bray, F. (2015) Cancer incidence and mortality worldwide: sources, methods and major patterns in GLOBOCAN 2012. *Int J Cancer*. **136**, E359-386
- 2 Montero, J., Sarosiek, Kristopher A., DeAngelo, Joseph D., Maertens, O., Ryan, J., Ercan, D., Piao, H., Horowitz, Neil S., Berkowitz, Ross S., Matulonis, U., Jänne, Pasi A., Amrein, Philip C., Cichowski, K., Drapkin, R. and Letai, A. (2015) Drug-Induced Death Signaling Strategy Rapidly Predicts Cancer Response to Chemotherapy. *Cell*. **160**, 977-989
- 3 Hanahan, D. and Weinberg, R. A. (2011) Hallmarks of cancer: the next generation. *Cell*. **144**, 646-674
- 4 Chambers, T. P., Portalatin, G. M., Paudel, I., Robbins, C. J. and Chambers, J. W. (2015) Sub-chronic administration of LY294002 sensitizes cervical cancer cells to chemotherapy by enhancing mitochondrial JNK signaling. *Biochem Biophys Res Commun*. **463**, 538-544

- 5 Good, M. C., Zalatan, J. G. and Lim, W. A. (2011) Scaffold Proteins: Hubs for Controlling the Flow of Cellular Information. *Science*. **332**, 680-686
- 6 Zeke, A., Lukács, M., Lim, W. A. and Reményi, A. (2009) Scaffolds: interaction platforms for cellular signalling circuits. *Trends in Cell Biology*. **19**, 364-374

Chapter 3

**SAB CONCENTRATIONS INDICATE CHEMOTHERAPEUTIC
SUSCEPTIBILITY IN OVARIAN CANCER CELL LINES.**

1. Introduction

Ovarian cancer (OC) is the most lethal gynecological malignancy [1]. While the overall 5-year survival for OC is approximately 45%, 60% of OC patients suffer from the metastatic disease, which has a survival rate of nearly 28%; whereas, locally detected OC cases have a 92% survival rate [2]. The high mortality associated with OC is attributed to a combination of poor detection and an extremely high recurrence rate (~80%) [3]. Recurrent OC is typified by the presence of treatment-resistant tumor cells [4]. Specifically, OC patients are often characterized by their relative responsiveness to platinum-based drugs, which are commonly used chemotherapy agents for OC [4, 5]. Patients are classified as platinum-sensitive (recurrence after six months), platinum-resistant (recurrence in less than six months) or platinum-refractory (recurrence during or upon completion of chemotherapy) [6], and this patient stratification is used, in part, to determine treatment options. In fact, the front-line treatment of paclitaxel and a platinum agent, such as cisplatin, only provides a modest improvement in survival among OC patients [7, 8]. Thus, the molecular mechanisms driving chemoresistance need to be defined and targeted to enhance treatment responsiveness in OC patients. To date, many factors have been implicated and targeted in platinum-resistant/refractory OC to improve therapeutic efficacy. These include angiogenesis [9, 10], perturbations in cellular signal transduction [11-15], DNA maintenance and repair machinery [7, 16], folate metabolism [17, 18], and mitochondrial physiology [19-21].

Recent research has demonstrated that changes in the apoptotic potential (ability to induce cell death) is altered in advanced OC patients [22, 23]. Specifically, a decrease in the

relative abundance of pro-apoptotic BH3-only proteins is linked to chemoresistance in OC. BH3-only proteins (Bad, Bid, Bik, Bim, Noxa, and Puma) are members of the Bcl-2 superfamily of proteins and facilitate apoptosis by sequestering pro-survival Bcl-2 proteins or enhancing mitochondrial outer membrane permeabilization (OMMP) by catalyzing the assembly of Bax-Bak pores [24, 25]. Because of the association among BH3-only proteins, apoptosis, and chemo-responsiveness, BH3 profiling, a reproducible, high-throughput assessment of BH3-only protein levels, has been proposed to be an index for chemo-responsiveness in solid tumors, including OC tumors [26-28]. Recent BH3 profiling efforts have found that indeed OC cells with high levels of BH3-only proteins were sensitive to chemotherapy [22, 23]. Moreover, increasing BH3-only protein concentrations, emulating BH3-only functions with chemical mimetics (ABT-737), and inhibiting pro-survival Bcl-2 proteins have been found to enhance chemotherapeutic efficacy in resistant OC cells [23, 24, 29]. However, the precise molecular mechanisms controlling the relative levels of BH3-only proteins on mitochondria in OC are currently being investigated and may represent new therapeutic and prognostic targets.

The outer mitochondrial membrane (OMM) is the interface between mitochondria and the rest of the cell. The OMM is not only the primary site of signal integration for mitochondria [30], but the OMM is also the location of Bcl-2 superfamily proteins, including several BH3-only proteins [31, 32]. Signaling complexes on the OMM may influence many aspects of mitochondrial physiology, including the recruitment, function, and retention of BH3-only proteins. Previously, we found that the OMM scaffold protein Sab organized pro-apoptotic signaling cascades in response to cytotoxic stress [33-35]. Specifically, the

c-Jun N-terminal kinase (JNK) translocated to the mitochondria and interacted with Sab in human cervical cancer (HeLa) cells treated with anisomycin [34]. Selective inhibition of the JNK-Sab interaction using a small, cell-permeable peptide (Tat-Sab_{KIMI}) prevented JNK-induced apoptotic events such as phosphorylation and emigration of Bcl-2 from the OMM [33]. Recently, we reported that sub-chronic treatment of HeLa cells with a chemosensitizer, LY294002, increased Sab expression and chemosensitivity towards cisplatin and paclitaxel, two drugs commonly used in combination to treat OC [35]. In general, enhanced Sab-mediated signaling may increase the sensitivity of cells to toxic stress [36], including OC tumors. However, we have yet to determine the precise molecular mechanisms by which Sab-mediated signaling may reduce chemoresistance.

In our current study, we examined the role of Sab-mediated signaling in OC chemoresponsiveness. Analysis of gene expression data from six, independent OC patient studies shows that Sab expression is reduced more than five-fold on average across 970 OC samples when compared to normal tissue. Profiling four commercially available OC cell lines revealed that cells with high Sab expression are sensitive to common chemotherapy agents and that Sab levels reflect the concentrations of BH3-only proteins on mitochondria. Additionally, over-expression of Sab in the chemoresistant SK-OV-3 cell line increased BH3-only protein levels and chemosensitivity to cisplatin and paclitaxel treatment. Conversely, inhibition of Sab-mediated signaling in a chemosensitive cell line, PA-1, was sufficient to enhance chemoresistance to paclitaxel and cisplatin. Our studies demonstrate that manipulation of OMM signaling, such as increasing Sab-mediated signaling events,

may be a useful strategy to determine viable, personalized treatment options for OC patients.

2. Experimental procedures

Materials: Cell lines were purchased from American Type Culture Collection (ATCC, Manassas, VA). Human Ovarian Epithelium Cells were obtained from ScienCell Research Laboratories (Carlsbad, CA). Chemotherapeutic agents ABT-737, carboplatin, cisplatin, docetaxel, doxorubicin, etoposide, and paclitaxel were purchased from Sigma-Aldrich (St. Louis, MO). Antibodies were purchased from vendors as listed below. General laboratory supplies were purchased from Fisher Scientific (Pittsburgh, PA).

Gene Expression Analysis: Secondary data analysis was performed to determine the relative levels of Sab expression in normal and OC tissue samples. The expression of Sab (SH3-binding protein 5; SH3BP5) was examined using the Oncomine database (<http://www.oncomine.org>) in March 2017 [37]. By querying six datasets available for OC that included Sab as part of past studies [38-43], we compared experimental data for normal tissue and OC samples. The data were compiled from across six independent studies, which contained a total of 41 normal tissue samples and 970 OC samples (1,011 samples in total). The data were presented as medians with error bars with limits of the 90th and 10th percentiles. All of the OC samples were from surgically removed primary site tumors (summarized in Table 1).

Cell Culture: OC cell lines CaOV-3 (HTB-75), PA-1 (CRL-1572), SW-626 (HTB-78), and SK-OV-3 (HTB-77) cells were cultured according to the suppliers instructions in

Dulbecco's Minimal Essential Medium (DMEM), Eagle's Minimal Essential Medium (EMEM), Lebovitz L15 medium, and McCoy's 5a medium, respectively. Each medium was supplemented with 10% fetal bovine serum (FBS), 1,000 U/mL penicillin, 100mg/mL streptomycin, and 5µg/mL plasmocin. For experiments, cells between passages 3 and 20 were used. To account for media-induced effects, cells were also adapted to DMEM and analyzed as described below. Human ovarian epithelium cells were cultured under normal cell culture conditions on poly-L-lysine-coated plates according to manufacturer's instructions using Ovarian Epithelial Cell Medium (ScienCell Research Laboratories) for no more than five passages.

Immunoblotting: To isolate proteins from cells for analysis, cells were plated at 2.5×10^5 cells/well in six-well plates and 60-mm dishes. Following treatment, cells were lysed, and proteins were harvested as previously described. Briefly, cells were washed twice in phosphate buffered saline (PBS; 137mM NaCl, 2.7mM KCl, 10mM Na₂HPO₄, and 1.8mM KH₂PO₄) and lysed in radioimmunoprecipitation assay buffer (RIPA; 50mM Tris-HCl, pH 8.0, 150mM NaCl, 1% Nonidet P-40, 0.5% deoxycholate, 0.1% SDS) supplemented with 1mM phenylmethanesulfonyl fluoride (PMSF) and Halt Protease and Phosphatase Inhibitor Cocktails (Thermo Scientific). Cells were incubated while gently rocking at 4°C for five minutes, and then transferred to a sterile microcentrifuge tube. After two minutes on ice, cell disruption was completed using sonication. The lysate was cleared by centrifuging at $14,000 \times g$ for 15 minutes. Supernatant protein concentrations were measured using the Pierce BCA Assay kit. Proteins (25µg) were resolved by SDS-PAGE and transferred onto low-fluorescence PVDF membranes. Membranes were placed in

blocking buffer comprised of PBS with 5% bovine serum albumin (BSA) and incubated for one hour at room temperature. The membranes were incubated in PBS containing 0.1% Tween 20 (PBST) and 5% BSA in the presence of primary antibodies overnight (4°C) while gently rocking. Primary antibodies specific for Sab (Novus Biologicals, H00009467-M01), Phospho-JNK (Thr183/Tyr185, Cell Signaling Technology (CST), 4668), JNK (Cell Signaling Technology, 9252), Phospho-c-Jun (Ser73, CST, 3270), c-Jun (CST, 9165), Phospho-Bcl-2 (Ser70) (CST, 2827), Bcl-2 (CST, 2870), Bcl-xL (CST, 2764), Mcl-1 (CST, 5453), Bad (CST, 9239), Bik (CST, 4592), Bim (CST, 2933), Bid (CST, 2002), PUMA (CST, 12450), Bax (CST, 5023), Bak (CST, 12105) Actin (CST, 4970), α -tubulin (CST, 2144), COX-IV (CST, 4850), GAPDH (CST, 5174), Calnexin (CST, 2679), Histone H3 (CST, 4499), TOM20 (Abcam, ab115746), TIMM23 (Abcam, ab116329), and PEX19 (Abcam, ab137072) were used at dilutions of 1:1000. Membranes were washed three times for five minutes in PBST and were incubated with secondary antibodies in the appropriate blocking buffer at a ratio of 1:20,000 for one hour at RT gently rocking. The following secondary antibodies were used in the experiments below: IRDye 680RD goat anti-rabbit (926-32211) and IRDye 800CW goat anti-mouse (926-68070) (Licor Biosciences). Membranes were again washed three times for five minutes in PBST. Membranes were analyzed using fluorescence detection using the Odyssey CLx near infrared scanner (Licor Biosciences). The corresponding bands on the immunoblots were quantified and normalized using the Image Studio 2.0 software (Licor Biosciences). The fluorescence of specific bands of interest was divided by the fluorescence of the loading control band to equilibrate signal strength and loading. The resulting signal was then normalized by dividing the signals from treated samples by untreated controls for each experiment.

Cell-based IC₅₀s of Chemotherapeutic Agents: To determine the relative chemo-sensitivity of the OC cell lines, cells were treated with increasing concentrations (generally 0-100 μ M) of drugs approved for the treatment of OC. Cells were plated at 1.5×10^4 cells per well in black-walled, clear bottom plates (Perkin Elmer) and grown overnight. The cells were then treated with chemotherapeutic agents for 48 hours. The cells were washed three times with PBS and fixed in 4% paraformaldehyde/PBS. The cells were then stained with 5 μ M TO-PRO-3 for 45 minutes at RT [35, 36]. The cells were then washed three times in Hank's Buffered Saline Solution (HBSS). The plate was imaged using the Odyssey CLx scanner (Licor Biosciences) and analyzed using the Image Studio 2.0 software (Licor Biosciences). The IC₅₀s were then calculated using the GraphPad Prism7© software.

Mitochondrial Isolation: To determine the relative abundance of proteins located on or within mitochondria, we isolated mitochondria as described in our previous work [33, 36]. Mitochondrial preparations with greater than 75% purity were used for our studies. Mitochondria purity was determined by immunoblotting for proteins from other subcellular compartments. For protein analyses, a total of 50 μ g protein was loaded for each mitochondrial sample.

JNK Activity Assay: We have previously used a luciferase-based kinase activity assay (Promega's Kinase-Glo Assay) to determine cellular JNK activity [33, 63]. In this study, mitochondria were isolated from each cell type, and the organelles were lysed using a native lysis buffer (25mM Tris-HCl [pH 7.5], 150mM NaCl, 1mM EGTA, 1mM EDTA, 1% TritonX-100) supplemented with protease and phosphatase inhibitors (Halt Cocktails – Thermo Fisher Scientific). Next, the mitochondrial lysate was placed in JNK activity

buffer (25mM HEPES, pH 7.4, 10mM MgCl₂, 2mM dithiothreitol (DTT), 1mg/mL BSA, and 1μM ATP). Then, 1μM of peptide substrate: either c-Jun (1-79) peptide, recombinant Sab polypeptide (335-435), or mutant Sab polypeptide (335-435) with mutated JNK binding sites to prevent kinase docking (Sab^{KIM1/2L-A}(335-435)) was added. Sab peptides were expressed and purified as previously described [33, 64]. As a control for JNK activity, specific lysates were pretreated fifteen minutes with 10μM SR-3306 (Tocris) to inhibit JNK. The assays were incubated for one hour at 30°C, and the reaction was stopped by the addition of 50mM EDTA. The reaction was combined with an equivalent volume of Kinase-Glo reagent and incubated at room temperature for ten minutes. Luminescence was measured on the BioTek Synergy H1 microplate reader with 500ms integration. ATP concentrations were determined by interpolating results onto an ATP standard curve acquired during each kinase reaction replicate. The data are reported as mean relative luminescence and normalized to protein concentration (mg) with error bars representing one standard deviation of the mean.

Apoptotic Priming Assay: To examine the potential for OC cell lines to induce apoptosis, we employed dynamic BH3-profiling, a high-throughput technique to predict the responsiveness of tumors to therapy [23, 26, 29, 65]. First, 2.0x10⁴ cells were used for the analysis of each cell line. The cells were trypsinized and dispersed into single cell suspensions, as determined by microscopy, in Trehalose Experiment Buffer (T-EB, 300mM Trehalose, 10mM HEPES-KOH (pH 7.7), 80mM KCl, 1mM EGTA, 1mM EDTA, 0.1% BSA, and 5mM succinate) at four times the final density. Bim BH3-peptide (MRPEIWIAQELRRIGDEFNA) was prepared as ten distinct concentrations over a three

log margin ranging in concentrations from 0.01mM to 100mM to determine the optimal conditions of the assay. A concentration of 500nM was determined to be the optimal concentration of Bim BH3 assays in HeLa cells and later used for our profiling of OC cell lines. Next, 15 μ L of Bim BH3-peptide was placed in a black 384-well plate (Nunc 262260). One volume (7.5 μ L) of the cell suspension was combined with one volume (7.5 μ L) of JC-1/Digitonin Mastermix (4mM JC-1, 40 μ g/mL oligomycin, 20mM β -mercaptoethanol, and 0.02% digitonin in T-EB). The cells were permeabilized for 10 minutes at room temperature. The 15 μ L of cell/dye solution was then added to the Bim BH3-peptide in the respective well of the 384-well plate. When completed, the plate was placed inside a BioTek Synergy H1 plate reader and shaken for 15 seconds. The fluorescence was then monitored at 590nm (excitation 545nm; with 20nm bandwidths) every five minutes for 120 minutes. As a positive control for complete depolarization, cells were treated with 3 μ M Carbonyl-cyanide-p-trifluoro-methoxy-phenylhydrazone (FCCP) and 250nM valinomycin. For each biological replicate, experimental conditions were performed in replicates of five for each cell line; experiments with a standard deviation of less than 10% were used for our analysis. The percent priming (% priming) was found by subtracting the mean maximum depolarization (FCCP/Valinomycin) from the mean depolarization from Bim BH3-peptide treatment across replicates. The change in priming (Δ % priming) refers to the difference in priming between non-treated, and Bim BH3-peptide-treated cells [22].

Mitochondrial outer membrane permeabilization: To evaluate the integrity of the OMM, we chose to quantify the amount of cytosolic cytochrome c [36]. Extra-mitochondrial

cytochrome c concentrations were assessed using immunoblotting of subcellular fractions (mitochondria and S100 (cytosol)). Briefly, 5×10^7 cells were grown in two 150-mm dishes. The cells were resuspended in 800 μ L of ice-cold homogenization buffer (250 mM sucrose, 20 mM HEPES, 10 mM KCl, 1.5 mM $MgCl_2$, 1 mM EDTA, 1 mM EGTA, 1 mM DTT, pH 7.4 and Halt protease inhibitor cocktail). The cells were homogenized and centrifuged (750xg, 10 minutes, 4°C) to remove nuclei and intact cells. The supernatant was centrifuged (10,000xg, 10 minutes, 4°C). The resulting supernatant was transferred to a new tube, and the pellet (or mitochondria-containing fraction) was resuspended in homogenization buffer. The supernatant was centrifuged at 100,00xg (4°C) for 60 minutes yielding the cytosolic fraction. Finally, 50 μ g of protein was resolved by SDS-PAGE, and cytochrome c was detected by immunoblotting as described above.

Manipulation of Sab-mediated signaling: We transiently transfected SK-OV-3 (a low Sab expressing OC line) with plasmids designed to express Sab (pLOC: Sab), red fluorescent protein (RFP; pLOC: RFP), or a Sab mutant lacking MAPK binding motifs (Sab^{KIM-2L/A}; pLOC: Sab^{KIM-2L/A}) [35, 36] to evaluate the impact of increased Sab levels. Plasmid DNA and FugeneHD (Promega) were combined in Optimem (Invitrogen) at a ratio of 1:3 and incubated for 15 minutes at RT before addition to culture. Eight hours after the addition of the transfection complex to media, the media was exchanged. Protein levels were assessed at 72 hours post-transfection. For drug-related studies, chemotherapeutic agents were added at 48 hours post-transfection, and cell viability was measured at 96 hours post-transfection (48 hours after drug).

To reduce Sab-mediated signaling in a high Sab-expressing OC cell line (PA-1), we used

peptide-based inhibition of protein-protein interactions on Sab as described in our prior studies. Cells were treated with up to 10 μ M of Tat-Sab_{KIM1} (a cell-permeable, inhibitory peptide) [33], scrambled control peptide (Tat-Scramble), or a variant of Tat-Sab_{KIM1} lacking the intact MAPK binding site (Tat-Sab_{KIM1L/A}). Cells were plated as described above and then treated with peptide for thirty minutes before drug treatment.

To decrease Sab expression, PA-1 cells were transiently transfected with pLKO.1 plasmids containing shRNAs either a luciferase-specific shRNA (control) or a shRNA for Sab that demonstrated over 85% silencing in 72 hours (Supplemental Figure 3). Ectopic expression of a shRNA-resistant form of Sab (previously described in [35]) was used to rescue Sab levels in PA-1 cells silencing Sab. Briefly, 1.5x10⁴ cells were plated in a 96-well plate, or 1.5x10⁵ cells were plated a day before transfection in 35-mm dishes for experiments. Plasmids were mixed with FugeneHD (Promega) at a 3:1 ratio per manufacturer's recommendations and added to cells for up to 72 hours. Protein levels were determined by immunoblotting as described above.

Cell Viability: To determine the extent of cell death, we utilized two methods: 1) Annexin-V with propidium iodide (PI) analyzed by fluorescent microscopy and 2) Caspase 3/7 fluorescent activity assay [66-68]. For the Annexin-V/PI assays (Cayman Chemical), 1.5x10⁴ cells were plated in a black-walled optically-clear bottom 96-well plate (Nunc), and the cells were treated with the chemotherapy agents as described above. The plate was centrifuged at 400xg for five minutes, and the media was removed. The cells were then placed in 100 μ L of Binding Buffer; the plate was centrifuged again (400xg, 5 minutes) and the buffer was removed. The cells were then incubated in 50mL of Annexin-FITC/PI

solution for ten minutes at room temperature, and the solution was removed following centrifugation (400xg, 5 minutes). The cells were placed in 100 μ L of HBSS, and the cells were imaged by fluorescent microscopy using the Applied Precision DeltaVision Elite Imaging System. Images were analyzed by counting cells stained only with unstained, Annexin-V-FITC stained (early apoptosis), and double labeled, Annexin-V/PI stained cells (late apoptosis). As a positive control, cells were treated with 1 μ M staurosporine (STS) to induce significant cell death at 24 hours. Images were assembled using Adobe Photoshop.

For the cell-based caspase 3/7 activity assay, cells were grown in a clear 96-well plate as described for the Annexin-V/PI assay. The plate was centrifuged (400xg) for five minutes, and the supernatant was removed. The cells were placed in 150 μ L of PBS and centrifuged (400xg for 5 minutes). After removing the buffer, the cells were placed in 100 μ L of PBS supplemented with 1% TritonX-100 to lyse the cells. After thirty minutes of incubation on a room temperature orbital shaker, the plate was centrifuged at 800xg for ten minutes, and 90 μ L of the cleared lysate was transferred to a black 96-well plate. Next, either 10 μ L of PBS or 10 μ L of a caspase inhibitor (Ac-DEVD-CHO; 10 μ M) was added to the lysate. Then, 100 μ L of caspase substrate Ac-DEVD-AMC (100 μ M) in PBS supplemented with 20mM DTT was added to the well. The assay was incubated at 37°C for thirty minutes, and fluorescence was measured (excitation: 488nm; emission: 535nm) using the BioTek Synergy H1 plate reader. Each assay was performed in triplicate for each condition for a minimum of four biological replicates. Data are presented as mean relative fluorescent units.

Biological Replicates and Statistics: A minimum of five biological replicates were used for cell-based studies, while a minimum of six experimental replicates was evaluated for biochemical, fluorescence, and other measurements. To determine statistical significance, the Mann-Whitney test was employed for significance between treatments. Statistical significance is indicated by an asterisk in figures in which the p-value is *less* than 0.05. Data are displayed as means with error bars representing plus and minus one standard deviation of the mean.

3. Results

3.1. Sab expression is reduced in OC. Our previous study in HeLa cells demonstrated that increasing the concentration of Sab on the OMM enhanced the sensitivity towards cisplatin and paclitaxel [35]. Because OC is typified by the presence of tumor cells resistant to platinum drugs, such as cisplatin, we wanted to determine if Sab expression may be altered in OC patients. To determine if Sab expression was changed in OC, we queried the Oncomine database [37] for Sab expression in OC samples and normal ovarian tissue. Examination of six independent studies (Table 1) found that Sab levels were reduced on average ~5.5-fold (2.19-fold in log₂ scale) in primary site OC tumors when compared to normal tissue [38-43]. We plotted the medians, 90th percentile values, and 10th percentile values for each study in Figure 1. This analysis of 970 OC samples had a p-value less than 0.001 indicating a difference in Sab expression, at least at the mRNA level, between the normal tissue and OC tumors (Table 3.1)

Table 3.1: Summary of Ovarian Cancer Expression Studies and Observed Changes in Sab Expression.

STUDY	TOTAL SAMPLES	CANCER SAMPLES	NORMAL SAMPLES	OVARIAN CANCER TYPES**	NORMAL TISSUE	GENES ANALYZED	HUMAN GENOME ARRAY(S)	LOG ₂ FOLD CHANGE	AVG. FOLD CHANGE	P	REF.
ABID	16	12	4	Serous Carcinoma	Ovary	8,603	U95A-Av2	-2.331	-5.032	0.003	(38)
BONOME	195	185	10	Ovarian Carcinoma	Ovarian Surface Epithelium	12,624	U133A	-3.776	-13.699	7.18 E-9	(39)
HENDRIX	103	99	4	Multiple**	Ovary	12,624	U133A	-1.446	-2.725	1.43 E-5	(40)
LU	50	45	5	Multiple**	Ovarian Surface Epithelium	17,572	U95A-Av2 U95B U95C U95D U95E	-1.285	-2.437	0.067	(41)
TCGA	594	586	8	Ovarian Serous Cystadenocarcinoma	Ovary	12,624	U113A	-1.684	-3.213	1.17 E-7	(42)
YOSHIHARA	53	43	10	Ovarian Serous Adenocarcinoma	Peritoneum	16,724	Agilent 1A Oligo v2	-2.619	-6.143	2.10 E-9	(43)
TOTALS/MEANS*	1,011	970	41					-2.190	-5.542		

The data presented in the table was obtained from the Oncomine repository and statistically reexamined for Sab (SH3BP5) expression. *The number of samples from each study were added to arrive at the total numbers used for our evaluation. The mean fold changes were generated by averaging the fold changes from the studies. ** The types of OC were provided by the studies; multiple types were used in the Hendrix and Lu studies, and we did not segregate the data based on type. In both studies, the types were clear cell adenocarcinoma, serous adenocarcinoma, endometrioid adenocarcinoma, and mucinous adenocarcinoma.

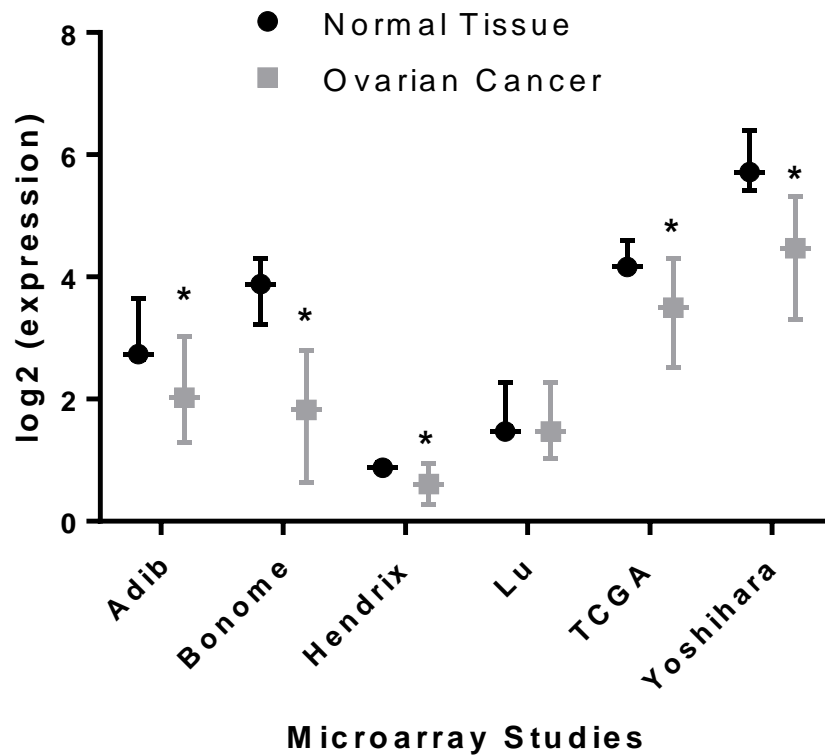


FIGURE 3.1: Summary of Sab expression levels in six OC gene expression studies. Six studies were identified in the Oncomine repository that matched our criteria of a 2-fold decrease in Sab expression and a p-value less than 10^{-4} . The critical data of these studies can be found in Table 1. We plotted the median value for Sab expression in normal tissue (black circles) and ovarian cancer samples (gray squares) for each study, and the error bars represent the 90th and 10th percentiles for each study. An asterisk (*) is used to indicate studies with a p-value < 0.005.

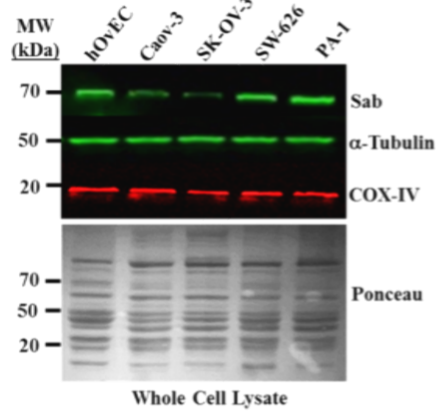
3.2. Ovarian cancer cell lines have distinct levels of Sab expression and mitochondrial

JNK signaling. To determine if the diminished Sab expression in the patient OC samples affects chemosensitivity, we assessed Sab protein levels in OC cell lines. First, we measured Sab expression in four commercially-available OC cell lines, Caov-3, PA-1, SK-OV-3, and SW-626; human ovarian epithelial cells were used as a normal tissue control.

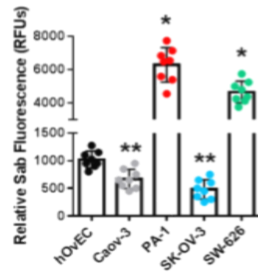
Immunoblot analysis of Sab reveals that Caov-3 and SK-OV-3 lines have lower levels of Sab than that of ovary epithelial cells. Caov-3 and SK-OV-3 had 33% and 48% less expression, respectively (Figure 3.2A and 3.2B). Meanwhile, the expression of Sab was significantly elevated in PA-1 and SW-626 cells (Figure 3.2A, top panel); PA-1 had an average increased Sab expression of 6.7-fold that of ovarian epithelial cells, SW-626 was 4.2-fold higher (Figure 3.2A and 3.2B). α -Tubulin was used as a cellular loading control (Figure 3.2A, middle panel), while COX-IV was used as a control for mitochondrial density (Figure 3.2A, bottom panel). Ponceau S staining of membranes was used to normalize protein levels among cell types (Figure 3.2A). The results of four immunoblotting experiments were quantified and normalized to Ponceau S in Figure 3.2B. To evaluate if the differences in Sab protein levels among the four cell lines occurred on the OMM or elsewhere in the cell, we performed subcellular fractionation to isolate mitochondria and other subcellular compartments [33-35]. Immunoblotting of subcellular fractions reveals that Sab is exclusively in the mitochondrial fraction for each of the four OC cell lines as compared to nuclear, cytosolic, and microsomal fractions (Figure 3.2C). We were unable to detect Sab at substantial levels in the ER, cytosolic or nuclear preparations (Figure 3.2C). Furthermore, the relative purity of each compartment fraction was assessed by monitoring the levels of nuclear (Histone H3), ER (Calnexin), lysosomal (LAMP2), and peroxisomal (PEX19) contamination in the mitochondrial isolates (Figure 3.2C). Only preparations with greater than 80% purity were used in our analysis. The relative levels of Sab were quantified and presented in Figure 3.2D. To examine if the relative Sab levels in the OC cells reflected mitochondrial JNK levels, we performed an immunoblot for JNK. JNK was not detected in any of the OC cell lines under normal

culture conditions (Figure 3.2E). Equivalent mitochondrial loading and OMM loading in each sample was assessed by the signal intensity of COX-IV and TOM20, respectively, (Figure 3.2E). Because previous research has indicated that mitochondrial translocation of JNK is dependent upon activation, we treated each of the four OC lines with 1 μ M staurosporine (STS) for 45 minutes and measured phosphorylated (active) JNK (Thr183/Tyr185) levels in mitochondrial extracts. Upon treatment with 1 μ M STS, phospho-JNK levels on mitochondria increased in all four cell lines (Figure 3.2E); this was reflected by an increase in the amount of total JNK in the mitochondrial isolates (Figure 3.2E). The amount of JNK localized on mitochondria of SK-OV-3 and Caov-3 cells were 62% and 47% less of the amount of JNK on the mitochondria of PA-1 cells (Figure 3.2E; top panel). Also, SW-626 mitochondrial JNK levels were 21% less than JNK on PA-1 mitochondria (Figure 3.2E). Immunoblot analysis of whole cell extracts demonstrates that there was no significant difference in JNK expression among the four OC cell types (Figure 3.2E; bottom panel), suggesting that the amount of JNK on mitochondria was dependent upon the concentrations of Sab. As observed in our previous studies only the higher molecular weight (54kDa) JNK band was present on mitochondria (Figure 3.2E; top panel); accordingly, this band cross-reacted with the phospho-JNK-specific antibody in mitochondrial preps from each of the four OC cell lines (Figure 3.2E, top panel).

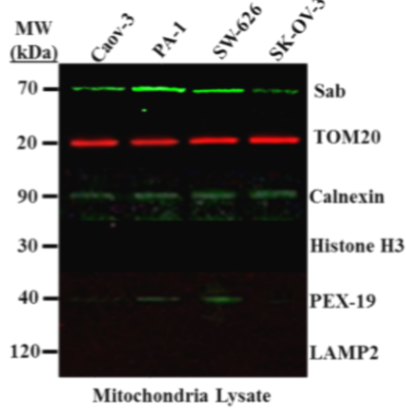
A.



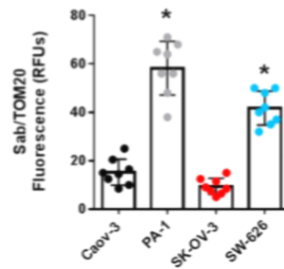
B.



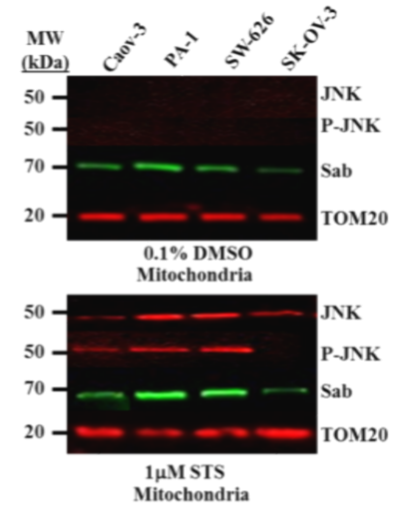
C.



D.



E.



F.

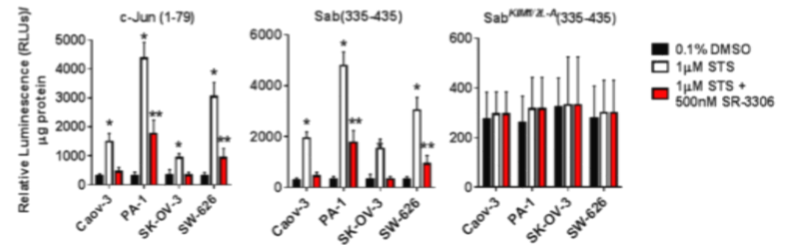


FIGURE 3.2: The levels of Sab differ among OC cell lines and correspond to stress-induced mitochondrial JNK recruitment. (A) OC cell lines were grown under normal cell culture conditions to ~80% confluency. The cells were lysed, and the proteins were resolved by SDS-PAGE. Immunoblotting was performed to determine the relative abundance of Sab with α -Tubulin and COX-IV serving as cellular and mitochondrial loading controls. Ponceau staining of membranes was used to quantify the immunoblotting results. (B) Quantification of Sab abundance from whole cell lysates in Figure 2A. (C) Mitochondrial isolates were prepared from the four OC cell lines and assessed for the levels of Sab by western blot analysis. TOM20 was used as an outer mitochondrial loading control, while the relative contamination of other cellular compartments was assessed by monitoring the levels of Calnexin (ER), Histone H3 (nucleus), PEX-19 (peroxisomes), and LAMP2 (lysosomes). (D) The levels of Sab for each OC cell line were normalized to mitochondria abundance (TOM20 levels) and quantified for seven independent biological replicates. (E) The relative abundance of activated JNK on mitochondria was assessed in the presence and absence of stress. The top panel examines the relative levels of total JNK (JNK), activated JNK (P-JNK), with respect to Sab on mitochondria isolated from untreated OC cells. The bottom panel shows the same proteins following treatment with 1mM staurosporine (STS) for 45 minutes. TOM20 was used as a mitochondrial loading control for both panels. (F) In vitro kinase activity assays for JNK were performed on mitochondria using either a c-Jun (1-79) or a Sab (335-435) peptide containing JNK phosphorylation sites. Additionally, a Sab-peptide lacking JNK binding residues (Sab^{KIM1/2L-A}(335-435)) was used as a negative control substrate. SR-3306 (500nM), a potent JNK inhibitor, was used to impair JNK activity during cellular stress and prevent JNK translocation to mitochondria. An asterisk (*) is used to indicate studies with a p-value <0.01 with respect to controls; meanwhile a double asterisk (**) is used to demark differences between cell types and distinct treatments. Data are plotted as means and error bars represent the standard deviation among at least three biological replicates.

To determine if JNK present on mitochondria following STS treatment was indeed active, we lysed mitochondria isolated from each of the four OC cell lines in non-denaturing conditions and then measured JNK activity towards c-Jun and Sab peptides as well as a Sab mutant peptide (Sab^{KIM1/2L-A}(335-435)) incapable of binding JNK. Following exposure to 1 μ M STS, JNK activity increased on mitochondria from all four cell lines (Figure 3.2F). However, JNK activity with respect to c-Jun and Sab peptides was increased over 10-fold in PA-1 and SW-626 cells, while only a 2.5 and 3.5-fold increase in activity was observed in SK-OV-3 and Caov-3 cells, respectively (Figure 3.2F). No kinase activity was observed with the Sab^{KIM1/2L-A}(335-435) peptide (Figure 3.2F). The activity could be attributed to

JNK as the introduction of 500nM JNK specific inhibitor SR-3306 prevented kinase activity in the assay. Quantitation of western blot analyses can be found in Supplemental Figure 3.2. This reinforces previous observations that imply JNK activation is required for mitochondrial translocation.

To determine if JNK translocation was specific to STS, we treated cells with 25 μ M anisomycin for 30 minutes and measured mitochondrial JNK levels and activity. JNK levels increased in all four OC cell lines, with greater amounts of JNK present on the mitochondria of PA-1 and SW-626 compared to SK-OV-3 and Caov-3 (Supplemental Figure 3). The JNK species on mitochondria cross-reacted with the phospho-specific JNK antibody (Supplemental Figure 3). Similarly, the activity of JNK towards c-Jun and Sab peptides in the mitochondrial fractions was greater in PA-1 and SW-626 cell compared to SK-OV-3 and Caov-3 (Supplemental Figure 3). SR-3306 was used to demonstrate that JNK was the kinase responsible for the activity. Taken together, these results demonstrate that Sab concentrations on the OMM of OC cells may dictate the local magnitude of JNK signaling.

3.3. OC cell lines with low Sab levels are resistant to chemotherapy agents: Because mitochondrial JNK signaling on Sab is linked to apoptosis [33, 44-49], we measured the chemosensitivity of the four OC cell lines to determine if Sab levels correlated to chemoresponsiveness. Using common and clinically relevant chemotherapeutic agents and OC-toxic regimens (Table 3.2), we assessed the potency of each with TO-PRO-3 staining and near-infrared imaging (Supplemental Figure 4). The data presented in Table 3.2 summarizes the chemicals and IC₅₀ values for each of the cells lines. SK-OV-3 and Caov-

3 consistently had higher IC₅₀ values than PA-1 and SW-626 cells. We also examined the potency of paclitaxel/cisplatin treatment, an approach employed for resistant and refractory tumors [5]. Similarly, SK-OV-3 cells and Caov-3 cells had considerably greater cellular viability as assessed by TO-PRO-3

Table 3.2: Cell-based IC₅₀ Values (μM) for Chemotherapeutic Agents in OC Cell

Lines.

CHEMOTHERAPY	CAOV-3	PA-1	SK-OV-3	SW-626
PACLITAXEL	9.7 ± 3.1	0.11 ± 0.05	13.7 ± 4.6	0.57 ± 0.13
DOCETAXEL	0.45 ± 0.19	<0.01	1.22 ± 0.38	0.01 ± 0.004
DOXORUBICIN	0.41 ± 0.13	0.04 ± 0.008	0.5 ± 0.11	0.11 ± 0.007
ETOPOSIDE	28.9 ± 8.17	0.13 ± 0.08	10.9 ± 3.33	8.1 ± 2.67
CARBOPLATIN	48 ± 12.17	1.9 ± 0.93	65 ± 17.6	5.8 ± 2.33
CISPLATIN	34.5 ± 63.3	0.79 ± 0.16	60.2 ± 72.7	3.2 ± 1.61
ABT-263	189 ± 49.1	0.96 ± 0.33	215 ± 67.6	3.2 ± 0.86
ABT-727	8.9 ± 2.67	0.09 ± 0.03	15 ± 4.33	0.47 ± 0.16
OBATOCLAX	1.4 ± 0.67	0.07 ± 0.01	0.6 ± 0.17	0.09 ± 0.02
TW-37	1.69 ± 0.81	0.1 ± 0.05	0.8 ± 0.23	0.4 ± 0.13

Note: IC₅₀ values are presented as means plus or minus one standard deviation of the mean. The IC₅₀s were determined using TO-PRO-3 staining and were confirmed by cell death assays. For each assay, each dose over the range of 10nM to 1mM was performed in quadruplet including the 0.01% DMF control. The means and standard deviations were based on a minimum of three biological replicates.

fluorescence following cisplatin/paclitaxel treatment when compared to PA-1 and SW-626 cells (Figure 3.3). Specifically, SK-OV-3 and Caov-3 had IC₅₀ values greater than 10-fold higher than PA-1 and SW-626 when treated with ABT-737, ABL-263, TW-37, and Obatoclox mesylate (Table 2). To determine if Sab levels correlated to the cellular sensitivities towards chemotherapeutic agents, we derived the Pearson's coefficient with respect to Sab levels (from Figure 3.2A) in the cell lines (Supplemental Figure 5). As presented in Table 3.2, across the four OC cell lines, Sab levels were strongly correlated to chemo sensitivity. The correlation curves and one-sided Pearson's coefficients can be found in Supplemental Figure 5 for each drug presented in Table 3.2.

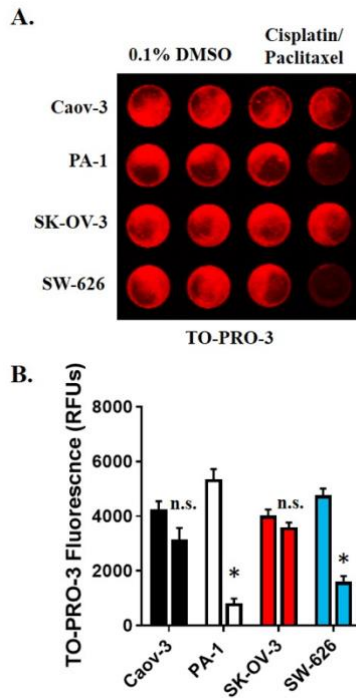


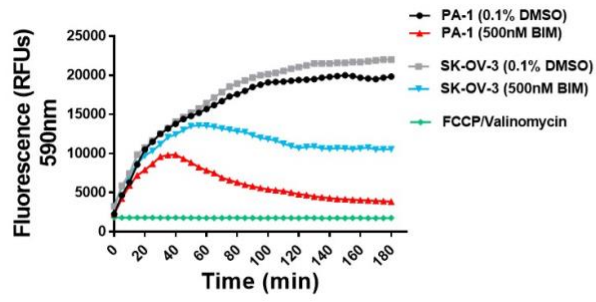
FIGURE 3.3: Cisplatin/Paclitaxel treatment affects OC cell lines differently. (A) TO-PRO-3 staining was used to assess the viability of OC cell types following treatment with vehicle (0.1% DMSO) or a combination of 0.25 μ M cisplatin and 0.1 μ M paclitaxel for 72 hours. A representative experiment with duplicates of each treatment is shown to illustrate the technique. (B) The quantified results of the cell viability are shown for each OC cell line. The vehicle is the left bar, while the right bar represents the relative fluorescence of cells treated with cisplatin and paclitaxel. An asterisk (*) is used to indicate studies with a p-value <0.01. Data are plotted as means and error bars represent the standard deviation among at least three biological replicates.

3.4. OC cell mitochondria with high Sab expression are primed for apoptosis. Because of the Sab-mediated JNK signaling is linked to Bcl-2 levels on mitochondria [33, 45, 49], we measured the apoptotic potential in the four OC cell lines. To examine the extent of apoptotic priming in each of the cancer cell lines, we first performed dynamic BH3 profiling [22, 27, 29] to assess the relative extent of priming. The addition of Bim BH3 peptide caused a rapid depolarization of mitochondrial membrane potential in all four OC cell lines; however, the loss of JC-1 fluorescence was slower in SK-OV-3 cells than PA-1 (Figure 3.4A). Additionally, the PA-1 and SW-626 cells with higher levels of Sab expression were found to have a greater percent depolarization than Caov-3 and SK-OV-3 cells that have relatively low Sab levels (Figure 3.4B). Consequently, the PA-1 and SW-626 cells had a greater change in priming ($\Delta\%$ Priming) compared to Caov-3 and SK-OV-3 cells (Figure 3.4C). Next, we verified the results of the dynamic BH3 profiling by measuring the cytosolic levels of cytochrome c by immunodetection within cytoplasmic subcellular fractions in the presence and absence of 500nM Bim-BH3 peptide (Figure 3.4D; quantified in 3.4E). The extent of cytochrome c present in the cytosol of OC cell lines was modest compared to cells treated with 1 μ M STS for two hours (Figure 3.4D and 3.4E). OC cells with low Sab expression (Caov-3 and SK-OV-3) had decreased cytochrome c release into the cytosol compared to cells with higher Sab expression, PA-1, and SW-626. To examine if the loss of mitochondrial membrane integrity was indeed due to apoptotic priming, the relative levels of Bcl-2 proteins (Bcl-2, Bcl-xL, and Mcl-1), BH3-only proteins (Bid, Bik, Bim, Bad, and Puma), and pro-apoptotic proteins (Bax and Bak)

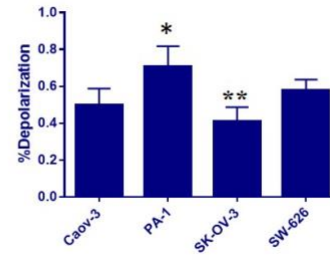
were measured (Figure 3.4F). The quantified data presented in Supplemental Figure 7 indicate that PA-1 and SW-626 cells have higher levels of pro-apoptotic BH3-only proteins than Caov-3 and SK-OV-3 cells, which have higher levels of pro-survival Bcl-2 proteins. This may indicate that ovarian cancer cells with elevated Sab-expression cells may be primed for apoptosis.

3.5. Ectopic expression of Sab induces apoptotic priming. To directly determine if Sab-mediated signaling contributes to apoptotic priming in ovarian cancer cell lines, we ectopically expressed either RFP, Sab, or a Sab mutant incapable of binding JNK (Sab^{KIMIL-A}) [35] (Figure 3.5A) in chemoresistant SK-OV-3 cells over the course of 72 hours (Figure 3.5B). By 72 hours, Sab was expressed five to seven-fold higher than SK-OV-3 cells that are expressing RFP or mock-transfected cells (Figure 3.5B; quantified in Figure 3.5C). Dynamic BH3 profiling reveals that SK-OV-3 cells expressing Sab have a greater percent depolarization and change in depolarization compared to mock-transfected and RFP-expressing cells (Figure 3.5D), an effect that was not observed in cells expressing Sab^{KIMIL-A} (Figure 3.5D). Furthermore, analysis of cytosolic cytochrome c reveals that compared to mock transfected and RFP-expressing SK-OV-3 cells, Sab expressing SK-OV-3 cells have increased cytosolic cytochrome c (Figure 3.5E). This increase is not observed in Sab^{KIMIL-A}-expressing SK-OV-3 cells (Figure 3.5E). Additionally, the mitochondrial levels of Bcl-2 family proteins were assessed (Figure 3.5F). Ectopic expression of Sab in SK-OV-3 cells changed the relative abundance of Bcl-2 and BH3-only proteins on mitochondria when compared to mock transfected, RFP-expressing, and Sab^{KIMIL-A}-expressing cells (Figure 3.5G; quantified in Figure 3.5H).

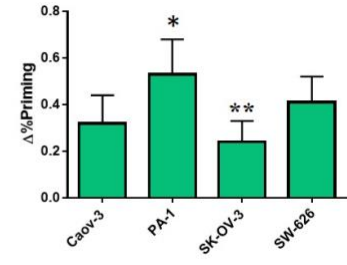
A.



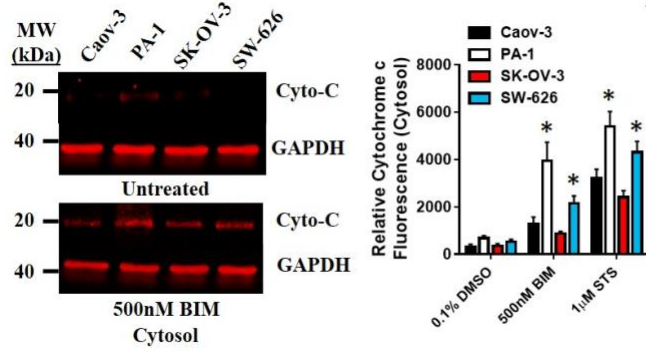
B.



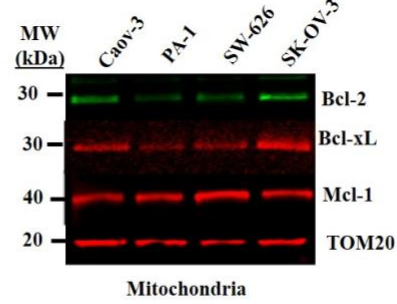
C.



D.



E.



F.

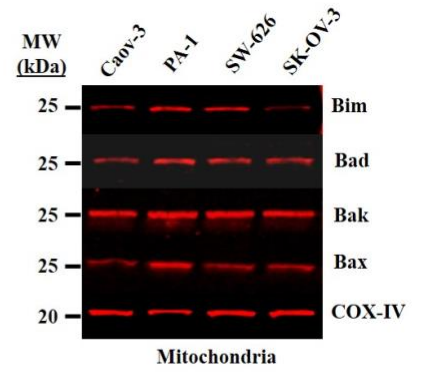
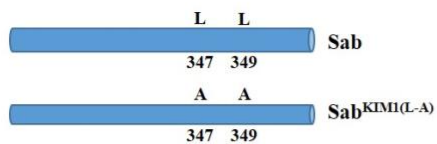
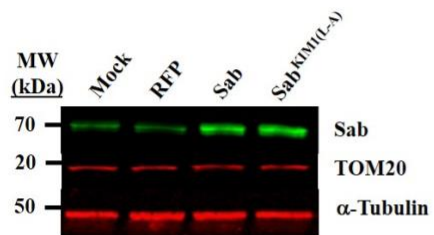


FIGURE 3.4: OC cells with high Sab expression are primed for apoptosis and chemosensitive. (A) Dynamic BH3 profiling was used to evaluate the extent of mitochondrial priming between PA-1 cells with high Sab expression and SK-OV-3 cells with low Sab levels. Cells were treated with vehicle (0.1% DMSO) or 500nM BIM BH3-only peptide and JC-1 fluorescence was monitored. FCCP/Valinomycin was used to depolarize mitochondria in this assay. (B) The percent depolarization and (2) the change relative priming ($\Delta\%$ Priming) were calculated based on the dynamic BH3 profiling for each of the OC cell lines. An asterisk (*) is used to indicate studies with a p-value <0.01. (D) The abundance of cytosolic cytochrome c was measured using western blot analysis of cytosolic fractions taken from OC cells in the absence (top panel) and presence of 500nM BIM peptide (bottom panel). GAPDH was used as a cytosolic loading control. The relative fluorescence of cytosolic cytochrome c was quantified (right panel). An asterisk (*) is used to indicate studies with a p-value <0.01. (E) Pro-survival Bcl-2 protein levels were monitored on isolated mitochondria from each of the four OC cells lines; specifically, Bcl-2, Bcl-xL, and Mcl-1 levels were measured, while TOM20 served as a mitochondrial loading control. (F) Pro-apoptotic protein levels on mitochondrial were measured by western blot analysis. Bim, Bad, Bak, and Bax were detected on isolated mitochondria from the OC cell lines and COX-IV was used as a mitochondrial loading control. Data are plotted as means and error bars represent the standard deviation among at least three biological replicates.

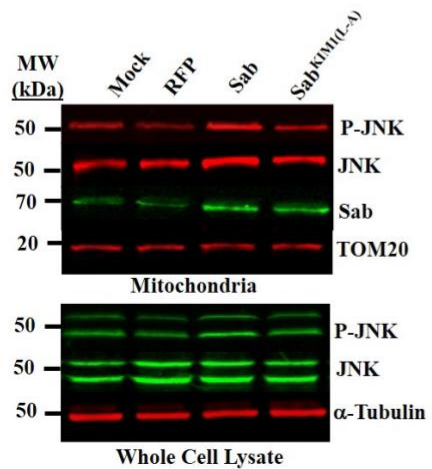
A.



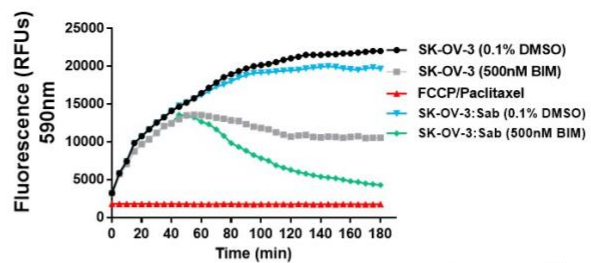
B.



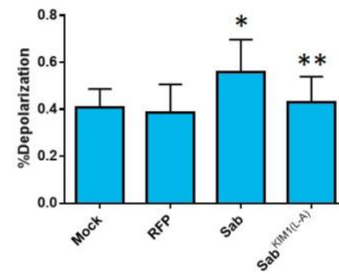
C.



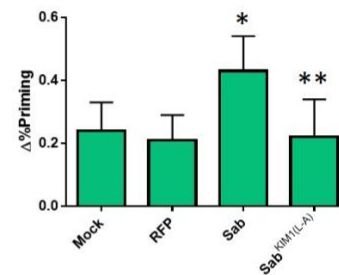
D.



E.



F.



G.

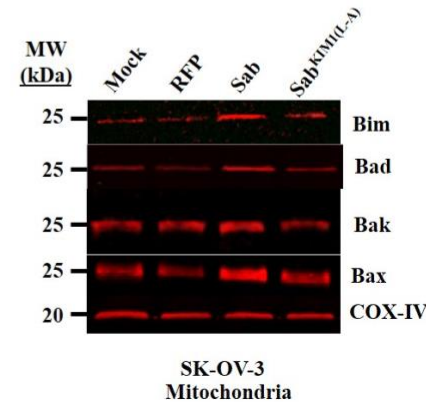
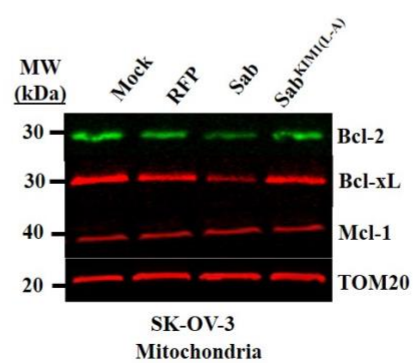


FIGURE 3.5: Artificially elevating Sab expression in resistant OC cells increases vulnerability to chemotherapy. (A) A schematic representation of Sab showing the two leucine residues in the KIM1 motif necessary for JNK binding. The bottom panel shows a Sab-variant (Sab^{KIM1(L-A)}) generated by site-directed mutagenesis that lacks the leucine residues required for JNK binding. (B) Ectopic expression of Sab and Sab^{KIM1(L-A)} in chemoresistant SK-OV-3 cells was assessed using western blot analysis with TOM20 and Tubulin as loading controls for mitochondria and whole cell respectively. (C) The relative levels of activated JNK (P-JNK) and total JNK (JNK) on mitochondria (top panel) and in whole cell lysates (bottom panel) were assessed in SK-OV-3 cells following 45 minutes of 1 μ M STS treatment. (D) Dynamic BH3 profiling of SK-OV-3 cells with and without ectopic expression of Sab was performed in the presence of vehicle or 500nM BIM peptide, and treatment with FCCP/Valinomycin was used as a depolarization control. (E) The %Depolarization and (F) Δ %Priming were calculated from the BH3 profiling for SK-OV-3 cells expressing either RFP, Sab, or Sab^{KIM1(L-A)}. An asterisk (*) is used to indicate studies with a p-value <0.01. (G) Western blot analysis was used to assess the relative abundance of pro-survival (left panel) and pro-apoptotic (right panel) in SK-OV-3 cells expressing either RFP, Sab, or Sab^{KIM1(L-A)}. Data are plotted as means and error bars represent the standard deviation among at least three biological replicates.

3.6. Increasing Sab expression sensitizes SK-OV-3 cells to chemotherapies. Because Sab levels may affect apoptotic priming, and we previously demonstrated that increasing Sab sensitizes HeLa cells to toxic agents [35], we examined whether ectopic expression of Sab enhanced the chemo-responsiveness of resistant SK-OV-3 cells towards cisplatin/paclitaxel treatment. To assess cell death in mock-transfected SK-OV-3 cells, cells transfected with an empty vector, or cells expressing either Sab or Sab^{KIM1(L-A)}, we utilized microscopic analysis of Annexin V and PI staining (Figure 3.6A). Compared to mock-transfected cells and empty vector cells, Sab-expressing SK-OV-3 cells had a considerable increase in the number of apoptotic cells in the presence of 25 μ M cisplatin and 10 μ M paclitaxel after 72 hours (Figure 3.6B). Specifically, these cells had a marked rise in the number of late apoptotic cells (those cells stained with both Annexin V and PI – Figure 3.5B). SK-OV-3 cells expressing the MAPK-binding deficient mutant, Sab^{KIM1(L-A)}, did not differ from mock-transfected and RFP expressing SK-OV-3 cells (Figure 3.6B). To complement the microscopic analysis, we

performed an assay to detect caspase 3 and 7 activity in the cells exposed to 25 μ M cisplatin and 10 μ M paclitaxel. Mock-transfected and empty vector transfected cells had little caspase activation following treatment with cisplatin and paclitaxel (Figure 3.6C); conversely, Sab-expressing cells had a substantial increase in caspase activity in the presence of chemotherapeutic agents, which was comparable to SK-OV-3 cells treated with 1 μ M of STS for 24 hours (Figure 3.6C). Again, expression of Sab^{KIMIL-A} in SK-OV-3 cells did not alter caspase activity levels in response to 25 μ M cisplatin and 10 μ M paclitaxel treatment (Figure 3.6C). To determine if Sab-mediated signaling was involved in cisplatin and paclitaxel-induced death in sensitive cell lines, such as PA-1, we incubated PA-1 with increasing amounts of either Tat-Scramble or Tat-Sab_{KIM1} and measured the extent of cell death following treatment with 0.25 μ M cisplatin and 0.10 μ M paclitaxel (Figure 3.6D). Inhibition of Sab-mediated signaling with the Tat-Sab_{KIM1} peptide prevented PA-1 cell death following cisplatin and paclitaxel administration when compared to untreated and cells treated with Tat-Scramble peptide (Figure 3.6D). PA-1 cells treated with a mutant Sab peptide, Tat-Sab_{KIMIL-A}, which cannot bind MAPKs did not differ from cells treated with the Tat-Scramble peptide (Figure 3.6D). Again, we verified the induction of apoptosis in PA-1 cells following 0.25 μ M cisplatin and 0.10 μ M paclitaxel treatment by using a caspase activity (Figure 3.6E). PA-1 cells treated with 1 μ M Tat-Sab_{KIM1} peptide had decreased caspase activity following treatment with chemotherapy agents as compared to cells treated with 1 μ M Tat-Scramble or Tat-Sab_{KIMIL-A} (Figure 3.6E).

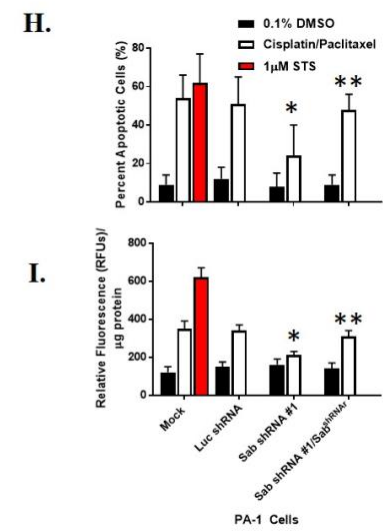
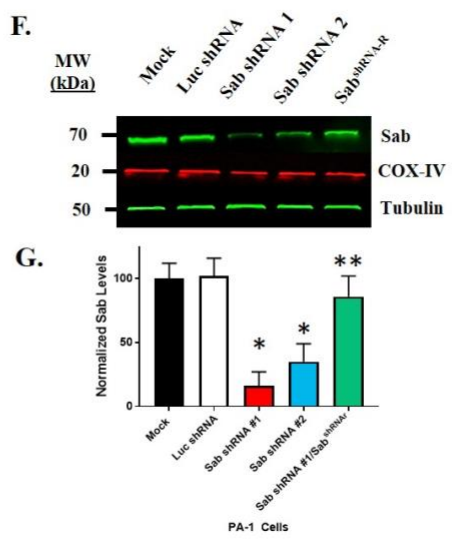
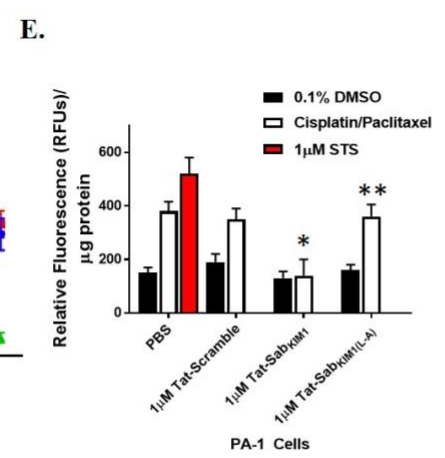
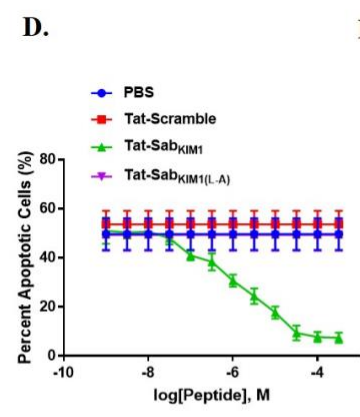
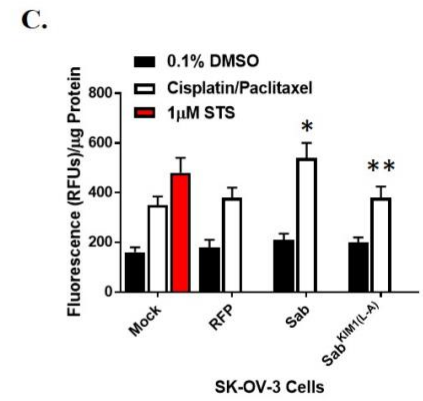
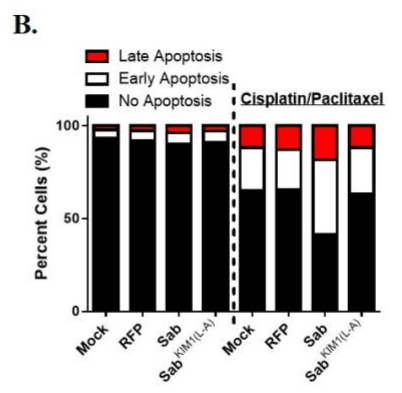
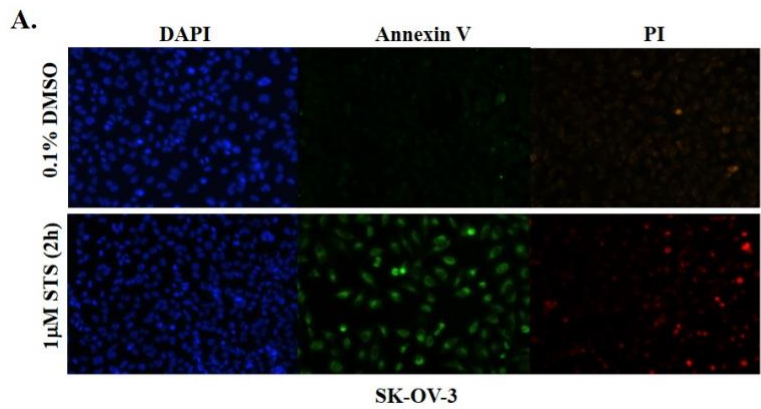


FIGURE 3.6: Inhibiting Sab-mediated signaling in sensitive OC cells enhances resistance.

(A) Fluorescent microscopy of a TUNEL assay performed on SK-OV-3 cells treated with vehicle (0.1% DMSO) or 1 μ M STS for 2 hours. Cells were stained with DAPI for total cell number, while Annexin V and PI staining were used to detect early and late apoptosis respectively. (B) The TUNEL assays were scored by counting the fluorescent cells in a field of view, and based on fluorescence SK-OV-3 cells expressing either RFP, Sab, or Sab^{KIM1(L-A)} were assessed for apoptosis levels in the presence and absence of 25 μ M cisplatin and 10 μ M paclitaxel after 72 hours. (C) Caspase assays were performed using cell lysates obtained from SK-OV-3 cells expressing RFP, Sab, or Sab^{KIM1(L-A)} that were exposed to 1% DMSO, Cisplatin/Paclitaxel for 72 hours, or 1 μ M STS for 24 hours. (D) Chemosensitive PA-1 cells with high Sab expression were surveyed for apoptosis using TUNEL assays in the presence and absence of 0.25 μ M cisplatin and 0.1 μ M paclitaxel after 72 hours in the presence of increasing concentrations of Tat-Scramble, Tat-Sab_{KIM1}, or Tat-Sab_{KIM1(L-A)} peptides. Both early and late apoptotic cells were scored in these experiments. (E) Caspase assays were used to assess the extent of apoptosis induced in PA-1 cells treated with cisplatin/paclitaxel and 1 μ M of either Tat-Scramble, Tat-Sab_{KIM1}, or Tat-Sab_{KIM1(L-A)} peptides. STS was used as a positive control for apoptosis. (F) To selectively impair Sab-mediated signaling in chemosensitive PA-1 cells, we used shRNA-mediated gene silencing of Sab. Luciferase-specific shRNAs were used as a negative control, while two Sab-specific shRNAs were used. Additionally, a version of Sab resistant to shRNA #1 was expressed in PA-1 cells treated with San shRNA #1 as a rescue control. (G) The levels of Sab were assessed by western blot analysis using COX-IV as a mitochondrial loading control and tubulin as a cellular loading control. (H) A TUNEL assay was performed to assess the levels of apoptosis in cells treated with Luc or Sab shRNAs and compared to a Sab rescue in PA-1 cells. (I) Caspase assays were employed to indicate the level of apoptosis in the PA-1 cells treated with shRNAs. An asterisk (*) is used to indicate studies with a p-value <0.01. A double asterisk (**) is used to demark differences between cell types and distinct treatments. Data are plotted as means and error bars represent the standard deviation among at least three biological replicates.

To confirm that the inhibition of apoptosis observed with the Tat-Sab_{KIM1} peptide was due to loss of Sab-mediated signaling, we silenced Sab expression in PA-1 cells using shRNAs specific for Sab (Figure 3.6F; quantified in Figure 3.6G). Cell death induction was restored in Sab-deficient PA-1 cells by ectopic expression of a shRNA-resistant Sab construct (Figure 3.6F and 3.6H) [35]. Additionally, silencing Sab expression in PA-1 cells impaired caspase activation when compared to cells expressing a control shRNA (Figure 3.6I), and expression of a shRNA-resistant Sab restore caspase activity following 0.25 μ M cisplatin and 0.10 μ M

paclitaxel treatment. Taken together, these results suggest that Sab facilitates signaling necessary to induce apoptosis in OC cells.

4. Discussion

Mitochondrial JNK signaling on the OMM scaffold protein Sab has been shown to be an instrumental event in the induction of mitochondria-induced cell death; furthermore, altering the concentration of Sab-mediated JNK signaling has been shown to affect chemosensitivity in tissues (brain and heart) and cancer cells. In our current study, we extend these observations by demonstrating that chemoresistant cancer cells have diminished Sab expression compared to normal tissue, and restoring or enhancing Sab levels on the OMM is critical to reestablishing proper apoptotic signaling in OC cell lines. Our analysis of six independent OC transcriptome analyses [38-43] found that Sab mRNA levels were reduced over 5-fold when compared to normal tissues (Figure 3.1, Table 3.1). Previous studies have demonstrated in various tissues and cell lines that diminished Sab-mediated signaling prevents apoptosis [33, 36, 47, 48, 50, 51]. To date, there are no published reports regarding the transcriptional regulation of Sab. It stands to reason that the decreased reliance on mitochondrial health status and the suppression of apoptotic mechanisms in cancer cells [19] may be partly responsible for the reduction in Sab expression. Indeed, we recently described that JNK-deficient murine embryonic fibroblasts (MEFs) had a significant decrease in Sab on the OMM compared to wild-type MEFs [35]. In our opinion, this would suggest that perturbations in signal transduction pathways, specifically those responsible for apoptosis, may be instrumental to the diminished Sab levels in OC.

Intriguingly, one OC patient from The Cancer Genome Atlas repository [42] had a Sab-overexpression phenotype; however, the genomic sequence of Sab from this patient possessed premature termination site, which truncated the protein at residue 379 (Sab is normally 455 amino acids in length). The loss of the C-terminal portion removes the two kinase interaction motifs (KIMs) responsible for mitochondrial MAPK signaling. Without the KIMs, it is unlikely that this Sab variant would have any impact on apoptotic induction, as previous studies have demonstrated that mutation of the KIMs that disrupt MAPK binding prevent the induction of cell death.

We demonstrated that the relative levels of Sab correlate to chemo-responsiveness in OC cells. Over-expression of Sab improved the chemosensitivity of resistant SK-OV-3 cells; meanwhile, inhibiting Sab-mediated signaling with the Tat-Sab_{KIM1} peptide or silencing Sab expression increased chemoresistance in vulnerable PA-1 cells (Figure 3.2 and 3.5). These effects were mediated by the relative levels of JNK on mitochondria. JNK signaling has long been implicated in apoptotic responses [52]. JNK signaling can contribute to apoptosis through the combination of nuclear and cytosolic/mitochondrial mechanisms.

The primary mitochondrial alteration facilitated by Sab-mediated JNK signaling in OC cells was the change in Bcl-2/BH3-only proteins at mitochondria (Figure 3 and 4). Previous research establishes this possibility, as JNK can directly phosphorylate Bcl-2 and BH3-only proteins affecting their functions and localizations [53]. We observed a marked decrease in mitochondrial Bcl-2 levels, an event previously noted in breast cancer cells treated with paclitaxel [54, 55]. Following stress, such as chemotherapy, JNK can phosphorylate Bcl-2 on Ser70 inducing its migration from the OMM [33, 56]. Furthermore,

JNK can impair Bcl-xL activity by phosphorylating Thr47 and Thr115 [45]. Enhancing the amount of Sab on the OMM would increase the concentration of activated JNK that could modify Bcl-2 proteins and hasten the impairment of anti-apoptotic mechanisms on mitochondria.

JNK can directly phosphorylate BH3-only proteins and increase their pro-apoptotic potential. During UV-induced apoptosis JNK has been shown to phosphorylate Bim and Bmf [24, 56, 57]. This phosphorylation causes Bim and Bmf to dissociate from dynein and myosin V motor complexes and activate Bax and Bak to initiate apoptosis. Furthermore, phosphorylation of Bim by JNK can complement JNK's phosphorylation of Bcl-2 and Bcl-xL because Bim can bind and neutralize Bcl-2 and Bcl-xL to promote apoptosis as well. Additionally, JNK can phosphorylate Bad on Ser128, which promotes apoptosis [58]. Bad, similar to Bim, can promote apoptosis by inhibiting Bcl-2 proteins. JNK can improve Bad activity by phosphorylating 14-3-3 ξ , which causes the release of Bad from the scaffold [59]. JNK can also affect the BH3-only proteins of the extrinsic pathway of apoptosis at the mitochondrial level. JNK can induce the cleavage of Bid, thereby elevating the levels of t-Bid, which will, in turn, activate Bax and Bak [60, 61]. During TNF- α -evoked apoptosis in HeLa cells, JNK activity induces a caspase 8-dependent cleavage of Bid that produces the product jBid that promotes the release of Smac/DIABLO [62]. In addition to the direct modulation of Bcl-2 function, mitochondrial JNK signaling facilitated by Sab would also enhance the activity of BH-3 only proteins contributing to apoptosis in OC cells treated with chemotherapy.

We have previously demonstrated that increasing Sab levels in mammalian cells can increase the vulnerability towards toxic agents. First, we demonstrated that the sub-chronic exposure to the chemosensitizer LY294002 increased Sab levels on the OMM, which led to an increase in mitochondrial JNK signaling and induction of apoptosis [35]. This data combined with our current study would suggest that increasing Sab levels would be a useful technique to improve chemo-responsiveness in cancer cells. However, we have recently reported that elevated Sab levels in the heart can increase the risk for cardiotoxicity following chemotherapy [36]. We show that artificially enhancing Sab in cardiomyocyte cell lines sensitized the cells to imatinib [14]. One may anticipate that targeted methods to selectively up-regulate Sab expression in OC tumors may be a safer approach to sensitize cancer cells than that of widespread Sab increase in the body.

We propose that Sab levels may be utilized better as a prognostic biomarker to guide the selection and magnitude of therapy for OC patients. Specifically, low Sab concentrations in a tumor biopsy or resection may suggest a more rigorous therapeutic regimen; whereby, high Sab levels may allow for a less ambitious and toxic approach to treating patients. Nonetheless, cancer, especially OC, are complex conditions and Sab concentrations may need to be considered in the cellular context of the tumor for choosing the most efficacious therapeutic approach. Because little is known regarding the regulation of Sab expression, future studies in our group will be focused on understanding the molecular mechanisms responsible for controlling Sab levels on the OMM.

Our current study reinforces the important role that scaffold proteins play in regulating the cell signaling responses, especially how scaffold proteins, such as Sab, can influence the

magnitude and outcomes at specific subcellular sites within cells. We demonstrate that increasing the concentration of a specific OMM scaffold protein can enhance signaling pathways on mitochondria and alter organelle and cellular physiology. Specifically, we have demonstrated that increasing Sab levels in OC cells increases mitochondrial JNK signaling and apoptotic priming, which enhances the vulnerability of OC cells to chemotherapy agents. Moreover, we uncovered that Sab levels are decreased in OC patient samples, and restoring Sab levels in OC cells with low Sab expression enhances chemoresponsiveness. Thus, assessing Sab expression in the context of genetic and histological testing, including dynamic BH3 profiling may be a useful prognostic tool for OC.

References

- 1 Parkin, D. M., Bray, F., Ferlay, J. and Pisani, P. (2005) Global Cancer Statistics, 2002. CA: A Cancer Journal for Clinicians. **55**, 74-108
- 2 Jemal, A., Siegel, R., Ward, E., Hao, Y., Xu, J., Murray, T. and Thun, M. J. (2008) Cancer Statistics, 2008. CA: A Cancer Journal for Clinicians. **58**, 71-96
- 3 Ledermann, J., Harter, P., Gourley, C., Friedlander, M., Vergote, I., Rustin, G., Scott, C., Meier, W., Shapira-Frommer, R., Safra, T., Matei, D., Macpherson, E., Watkins, C., Carmichael, J. and Matulonis, U. (2012) Olaparib Maintenance Therapy in Platinum-Sensitive Relapsed Ovarian Cancer. New England Journal of Medicine. **366**, 1382-1392
- 4 Gore, M. E., Fryatt, I., Wiltshaw, E. and Dawson, T. (1990) Treatment of relapsed carcinoma of the ovary with cisplatin or carboplatin following initial treatment with these compounds. Gynecologic Oncology. **36**, 207-211
- 5 Sandercock, J., Parmar, M. K. B., Torri, V. and Qian, W. (2002) First-line treatment for advanced ovarian cancer: paclitaxel, platinum and the evidence. Br J Cancer. **87**, 815-824

- 6 Yap, T. A., Carden, C. P. and Kaye, S. B. (2009) Beyond chemotherapy: targeted therapies in ovarian cancer. *Nat Rev Cancer*. **9**, 167-181
- 7 Placido, S. D., Scambia, G., Vagno, G. D., Naglieri, E., Lombardi, A. V., Biamonte, R., Marinaccio, M., Cartenì, G., Manzione, L., Febbraro, A., Matteis, A. d., Gasparini, G., Valerio, M. R., Danese, S., Perrone, F., Lauria, R., Laurentiis, M. D., Greggi, S., Gallo, C. and Pignata, S. (2004) Topotecan Compared With No Therapy After Response to Surgery and Carboplatin/Paclitaxel in Patients With Ovarian Cancer: Multicenter Italian Trials in Ovarian Cancer (MITO-1) Randomized Study. *Journal of Clinical Oncology*. **22**, 2635-2642
- 8 Bookman, M. A., Greer, B. E. and Ozols, R. F. (2003) Optimal therapy of advanced ovarian cancer: carboplatin and paclitaxel vs. cisplatin and paclitaxel (GOG 158) and an update on GOG0 182-ICON5. *International Journal of Gynecological Cancer*. **13**, 735-740
- 9 Spannuth, W. A., Sood, A. K. and Coleman, R. L. (2008) Angiogenesis as a strategic target for ovarian cancer therapy. *Nat Clin Prac Oncol*. **5**, 194-204
- 10 Mesiano, S., Ferrara, N. and Jaffe, R. B. (1998) Role of Vascular Endothelial Growth Factor in Ovarian Cancer. *The American Journal of Pathology*. **153**, 1249-1256
- 11 Matei, D., Emerson, R. E., Lai, Y. C., Baldrige, L. A., Rao, J., Yiannoutsos, C. and Donner, D. D. (2005) Autocrine activation of PDGFR[alpha] promotes the progression of ovarian cancer. *Oncogene*. **25**, 2060-2069
- 12 Matei, D., Chang, D. D. and Jeng, M.-H. (2004) Imatinib Mesylate (Gleevec) Inhibits Ovarian Cancer Cell Growth through a Mechanism Dependent on Platelet-Derived Growth Factor Receptor α and Akt Inactivation. *Clinical Cancer Research*. **10**, 681-690
- 13 Levine, D. A., Bogomolny, F., Yee, C. J., Lash, A., Barakat, R. R., Borgen, P. I. and Boyd, J. (2005) Frequent Mutation of the *PIK3CA* Gene in Ovarian and Breast Cancers. *Clinical Cancer Research*. **11**, 2875-2878
- 14 Obata, K., Morland, S. J., Watson, R. H., Hitchcock, A., Chenevix-Trench, G., Thomas, E. J. and Campbell, I. G. (1998) Frequent PTEN/MMAC Mutations in Endometrioid but not Serous or Mucinous Epithelial Ovarian Tumors. *Cancer Research*. **58**, 2095-2097
- 15 Wiener, J. R., Windham, T. C., Estrella, V. C., Parikh, N. U., Thall, P. F., Deavers, M. T., Bast, R. C., Mills, G. B. and Gallick, G. E. (2003) Activated Src Protein Tyrosine Kinase

- Is Overexpressed in Late-Stage Human Ovarian Cancers. *Gynecologic Oncology*. **88**, 73-79
- 16 Bryant, H. E., Schultz, N., Thomas, H. D., Parker, K. M., Flower, D., Lopez, E., Kyle, S., Meuth, M., Curtin, N. J. and Helleday, T. (2005) Specific killing of BRCA2-deficient tumours with inhibitors of poly(ADP-ribose) polymerase. *Nature*. **434**, 913-917
 - 17 Kalli, K. R., Oberg, A. L., Keeney, G. L., Christianson, T. J. H., Low, P. S., Knutson, K. L. and Hartmann, L. C. (2008) Folate receptor alpha as a tumor target in epithelial ovarian cancer. *Gynecologic Oncology*. **108**, 619-626
 - 18 Gibbs, D. D., Theti, D. S., Wood, N., Green, M., Raynaud, F., Valenti, M., Forster, M. D., Mitchell, F., Bavetsias, V., Henderson, E. and Jackman, A. L. (2005) BGC 945, a Novel Tumor-Selective Thymidylate Synthase Inhibitor Targeted to α -Folate Receptor-Overexpressing Tumors. *Cancer Research*. **65**, 11721-11728
 - 19 Hanahan, D. and Weinberg, R. A. (2011) Hallmarks of cancer: the next generation. *Cell*. **144**, 646-674
 - 20 Chappell, N. P., Teng, P.-n., Hood, B. L., Wang, G., Darcy, K. M., Hamilton, C. A., Maxwell, G. L. and Conrads, T. P. (2012) Mitochondrial Proteomic Analysis of Cisplatin Resistance in Ovarian Cancer. *Journal of Proteome Research*. **11**, 4605-4614
 - 21 Ara, G., Kusumoto, T., Korbut, T. T., Cullere-Luengo, F. and Teicher, B. A. (1994) *cis*-Diamminedichloroplatinum(II) Resistant Human Tumor Cell Lines Are Collaterally Sensitive to PtCl₄(Rh-123)₂: Evidence for Mitochondrial Involvement. *Cancer Research*. **54**, 1497-1502
 - 22 Montero, J., Sarosiek, Kristopher A., DeAngelo, Joseph D., Maertens, O., Ryan, J., Ercan, D., Piao, H., Horowitz, Neil S., Berkowitz, Ross S., Matulonis, U., Jänne, Pasi A., Amrein, Philip C., Cichowski, K., Drapkin, R. and Letai, A. (2015) Drug-Induced Death Signaling Strategy Rapidly Predicts Cancer Response to Chemotherapy. *Cell*. **160**, 977-989
 - 23 Chonghaile, T. N., Sarosiek, K. A., Vo, T.-T., Ryan, J. A., Tammareddi, A., Moore, V. D. G., Deng, J., Anderson, K. C., Richardson, P., Tai, Y.-T., Mitsiades, C. S., Matulonis, U. A., Drapkin, R., Stone, R., DeAngelo, D. J., McConkey, D. J., Sallan, S. E., Silverman, L., Hirsch, M. S., Carrasco, D. R. and Letai, A. (2011) Pretreatment Mitochondrial Priming Correlates with Clinical Response to Cytotoxic Chemotherapy. *Science*. **334**, 1129-1133

- 24 Letai, A., Bassik, M. C., Walensky, L. D., Sorcinelli, M. D., Weiler, S. and Korsmeyer, S. J. (2002) Distinct BH3 domains either sensitize or activate mitochondrial apoptosis, serving as prototype cancer therapeutics. *Cancer Cell*. **2**, 183-192
- 25 Shamas-Din, A., Brahmabhatt, H., Leber, B. and Andrews, D. W. (2011) BH3-only proteins: Orchestrators of apoptosis. *Biochimica et Biophysica Acta (BBA) - Molecular Cell Research*. **1813**, 508-520
- 26 Ryan, J. A., Brunelle, J. K. and Letai, A. (2010) Heightened mitochondrial priming is the basis for apoptotic hypersensitivity of CD4+ CD8+ thymocytes. *Proceedings of the National Academy of Sciences*. **107**, 12895-12900
- 27 Ryan, J. and Letai, A. (2013) BH3 profiling in whole cells by fluorimeter or FACS. *Methods*. **61**, 156-164
- 28 Letai, A. G. (2008) Diagnosing and exploiting cancer's addiction to blocks in apoptosis. *Nat Rev Cancer*. **8**, 121-132
- 29 Certo, M., Del Gaizo Moore, V., Nishino, M., Wei, G., Korsmeyer, S., Armstrong, S. A. and Letai, A. (2006) Mitochondria primed by death signals determine cellular addiction to antiapoptotic BCL-2 family members. *Cancer Cell*. **9**, 351-365
- 30 Chandel, N. S. (2014) Mitochondria as signaling organelles. *BMC Biology*. **12**, 34
- 31 Bender, T. and Martinou, J.-C. (2013) Where Killers Meet—Permeabilization of the Outer Mitochondrial Membrane during Apoptosis. *Cold Spring Harbor Perspectives in Biology*. **5**
- 32 Brunelle, J. K. and Letai, A. (2009) Control of mitochondrial apoptosis by the Bcl-2 family. *J Cell Sci*. **122**, 437-441
- 33 Chambers, J. W., Cherry, L., Laughlin, J. D., Figuera-Losada, M. and LoGrasso, P. V. (2011) Selective inhibition of mitochondrial JNK signaling achieved using peptide mimicry of the Sab kinase interacting motif-1 (KIM1). *ACS Chem Biol*. **6**, 808-818
- 34 Chambers, J. W. and LoGrasso, P. V. (2011) Mitochondrial c-Jun N-terminal kinase (JNK) signaling initiates physiological changes resulting in amplification of reactive oxygen species generation. *J Biol Chem*. **286**, 16052-16062

- 35 Chambers, T. P., Portalatin, G. M., Paudel, I., Robbins, C. J. and Chambers, J. W. (2015) Sub-chronic administration of LY294002 sensitizes cervical cancer cells to chemotherapy by enhancing mitochondrial JNK signaling. *Biochem Biophys Res Commun.* **463**, 538-544
- 36 Chambers, T. P., Santiesteban, L., Gomez, D. and Chambers, J. W. (2017) Sab mediates mitochondrial dysfunction involved in imatinib mesylate-induced cardiotoxicity. *Toxicology.* **382**, 24-35
- 37 Rhodes, D. R., Kalyana-Sundaram, S., Mahavisno, V., Varambally, R., Yu, J., Briggs, B. B., Barrette, T. R., Anstet, M. J., Kincead-Beal, C., Kulkarni, P., Varambally, S., Ghosh, D. and Chinnaiyan, A. M. (2007) Oncomine 3.0: genes, pathways, and networks in a collection of 18,000 cancer gene expression profiles. *Neoplasia.* **9**, 166-180
- 38 Adib, T. R., Henderson, S., Perrett, C., Hewitt, D., Bourmpoulia, D., Ledermann, J. and Boshoff, C. (2004) Predicting biomarkers for ovarian cancer using gene-expression microarrays. *Br J Cancer.* **90**, 686-692
- 39 Bonome, T., Levine, D. A., Shih, J., Randonovich, M., Pise-Masison, C. A., Bogomolny, F., Ozbun, L., Brady, J., Barrett, J. C., Boyd, J. and Birrer, M. J. (2008) A Gene Signature Predicting for Survival in Suboptimally Debulked Patients with Ovarian Cancer. *Cancer Research.* **68**, 5478-5486
- 40 Hendrix, N. D., Wu, R., Kuick, R., Schwartz, D. R., Fearon, E. R. and Cho, K. R. (2006) Fibroblast Growth Factor 9 Has Oncogenic Activity and Is a Downstream Target of Wnt Signaling in Ovarian Endometrioid Adenocarcinomas. *Cancer Research.* **66**, 1354-1362
- 41 Lu, K. H., Patterson, A. P., Wang, L., Marquez, R. T., Atkinson, E. N., Baggerly, K. A., Ramoth, L. R., Rosen, D. G., Liu, J., Hellstrom, I., Smith, D., Hartmann, L., Fishman, D., Berchuck, A., Schmandt, R., Whitaker, R., Gershenson, D. M., Mills, G. B. and Bast, R. C. (2004) Selection of Potential Markers for Epithelial Ovarian Cancer with Gene Expression Arrays and Recursive Descent Partition Analysis. *Clinical Cancer Research.* **10**, 3291-3300
- 42 Network, T. C. G. A. R. (2011) Integrated genomic analyses of ovarian carcinoma. *Nature.* **474**, 609-615
- 43 Yoshihara, K., Tajima, A., Komata, D., Yamamoto, T., Kodama, S., Fujiwara, H., Suzuki, M., Onishi, Y., Hatae, M., Sueyoshi, K., Fujiwara, H., Kudo, Y., Inoue, I. and Tanaka, K. (2009) Gene expression profiling of advanced-stage serous ovarian cancers distinguishes

- novel subclasses and implicates ZEB2 in tumor progression and prognosis. *Cancer Science*. **100**, 1421-1428
- 44 Aoki, H., Kang, P. M., Hampe, J., Yoshimura, K., Noma, T., Matsuzaki, M. and Izumo, S. (2002) Direct activation of mitochondrial apoptosis machinery by c-Jun N-terminal kinase in adult cardiac myocytes. *J Biol Chem*. **277**, 10244-10250
- 45 Kharbanda, S., Saxena, S., Yoshida, K., Pandey, P., Kaneki, M., Wang, Q., Cheng, K., Chen, Y. N., Campbell, A., Sudha, T., Yuan, Z. M., Narula, J., Weichselbaum, R., Nalin, C. and Kufe, D. (2000) Translocation of SAPK/JNK to mitochondria and interaction with Bcl-x(L) in response to DNA damage. *J Biol Chem*. **275**, 322-327
- 46 Chauhan, D., Li, G., Hideshima, T., Podar, K., Mitsiades, C., Mitsiades, N., Munshi, N., Kharbanda, S. and Anderson, K. C. (2003) JNK-dependent release of mitochondrial protein, Smac, during apoptosis in multiple myeloma (MM) cells. *J Biol Chem*. **278**, 17593-17596
- 47 Nijboer, C. H., Bonestroo, H. J., Zijlstra, J., Kavelaars, A. and Heijnen, C. J. (2013) Mitochondrial JNK phosphorylation as a novel therapeutic target to inhibit neuroinflammation and apoptosis after neonatal ischemic brain damage. *Neurobiol Dis*. **54**, 432-444
- 48 Win, S., Than, T. A., Min, R. W. M., Aghajan, M. and Kaplowitz, N. (2016) c-Jun N-terminal kinase mediates mouse liver injury through a novel Sab (SH3BP5)-dependent pathway leading to inactivation of intramitochondrial Src. *Hepatology*. **63**, 1987-2003
- 49 Schroeter, H., Boyd, C. S., Ahmed, R., Spencer, J. P., Duncan, R. F., Rice-Evans, C. and Cadenas, E. (2003) c-Jun N-terminal kinase (JNK)-mediated modulation of brain mitochondria function: new target proteins for JNK signalling in mitochondrion-dependent apoptosis. *Biochem J*. **372**, 359-369
- 50 Win, S., Than, T. A., Fernandez-Checa, J. C. and Kaplowitz, N. (2014) JNK interaction with Sab mediates ER stress induced inhibition of mitochondrial respiration and cell death. *Cell Death Dis*. **5**, e989
- 51 Win, S., Than, T. A., Han, D., Petrovic, L. M. and Kaplowitz, N. (2011) c-Jun N-terminal kinase (JNK)-dependent acute liver injury from acetaminophen or tumor necrosis factor (TNF) requires mitochondrial Sab protein expression in mice. *J Biol Chem*. **286**, 35071-35078

- 52 Tournier, C., Hess, P., Yang, D. D., Xu, J., Turner, T. K., Nimnual, A., Bar-Sagi, D., Jones, S. N., Flavell, R. A. and Davis, R. J. (2000) Requirement of JNK for Stress- Induced Activation of the Cytochrome c-Mediated Death Pathway. *Science*. **288**, 870-874
- 53 Dhanasekaran, D. N. and Reddy, E. P. (2008) JNK signaling in apoptosis. *Oncogene*. **27**, 6245-6251
- 54 Srivastava, R. K., Mi, Q.-S., Hardwick, J. M. and Longo, D. L. (1999) Deletion of the loop region of Bcl-2 completely blocks paclitaxel-induced apoptosis. *Proceedings of the National Academy of Sciences*. **96**, 3775-3780
- 55 Yamamoto, K., Ichijo, H. and Korsmeyer, S. J. (1999) BCL-2 Is Phosphorylated and Inactivated by an ASK1/Jun N-Terminal Protein Kinase Pathway Normally Activated at G2/M. *Molecular and Cellular Biology*. **19**, 8469-8478
- 56 Lei, K., Nimnual, A., Zong, W. X., Kennedy, N. J., Flavell, R. A., Thompson, C. B., Bar-Sagi, D. and Davis, R. J. (2002) The Bax subfamily of Bcl2-related proteins is essential for apoptotic signal transduction by c-Jun NH(2)-terminal kinase. *Mol Cell Biol*. **22**, 4929-4942
- 57 Marani, M., Tenev, T., Hancock, D., Downward, J. and Lemoine, N. R. (2002) Identification of Novel Isoforms of the BH3 Domain Protein Bim Which Directly Activate Bax To Trigger Apoptosis. *Molecular and Cellular Biology*. **22**, 3577-3589
- 58 Donovan, N., Becker, E. B. E., Konishi, Y. and Bonni, A. (2002) JNK Phosphorylation and Activation of BAD Couples the Stress-activated Signaling Pathway to the Cell Death Machinery. *Journal of Biological Chemistry*. **277**, 40944-40949
- 59 Tsuruta, F., Sunayama, J., Mori, Y., Hattori, S., Shimizu, S., Tsujimoto, Y., Yoshioka, K., Masuyama, N. and Gotoh, Y. (2004) JNK promotes Bax translocation to mitochondria through phosphorylation of 14-3-3 proteins. *The EMBO Journal*. **23**, 1889-1899
- 60 Sarosiek, Kristopher A., Chi, X., Bachman, John A., Sims, Joshua J., Montero, J., Patel, L., Flanagan, A., Andrews, David W., Sorger, P. and Letai, A. (2013) BID Preferentially Activates BAK while BIM Preferentially Activates BAX, Affecting Chemotherapy Response. *Molecular Cell*. **51**, 751-765

- 61 Madesh, M., Antonsson, B., Srinivasula, S. M., Alnemri, E. S. and Hajnóczky, G. (2002) Rapid Kinetics of tBid-induced Cytochrome c and Smac/DIABLO Release and Mitochondrial Depolarization. *Journal of Biological Chemistry*. **277**, 5651-5659
- 62 Deng, Y., Ren, X., Yang, L., Lin, Y. and Wu, X. (2003) A JNK-Dependent Pathway Is Required for TNF α -Induced Apoptosis. *Cell*. **115**, 61-70
- 63 Chambers, J. W., Pachori, A., Howard, S., Ganno, M., Hansen, D., Jr., Kamenecka, T., Song, X., Duckett, D., Chen, W., Ling, Y. Y., Cherry, L., Cameron, M. D., Lin, L., Ruiz, C. H. and Lograsso, P. (2011) Small Molecule c-jun-N-terminal Kinase (JNK) Inhibitors Protect Dopaminergic Neurons in a Model of Parkinson's Disease. *ACS Chem Neurosci*. **2**, 198-206
- 64 Laughlin, John D., Nwachukwu, Jerome C., Figuera-Losada, M., Cherry, L., Nettles, Kendall W. and LoGrasso, Philip V. (2012) Structural Mechanisms of Allostery and Autoinhibition in JNK Family Kinases. *Structure*. **20**, 2174-2184
- 65 Vo, T. T., Ryan, J., Carrasco, R., Neubergh, D., Rossi, D. J., Stone, R. M., Deangelo, D. J., Frattini, M. G. and Letai, A. (2012) Relative mitochondrial priming of myeloblasts and normal HSCs determines chemotherapeutic success in AML. *Cell*. **151**, 344-355
- 66 Allen, R. T., Hunter Iii, W. J. and Agrawal, D. K. (1997) Morphological and biochemical characterization and analysis of apoptosis. *Journal of Pharmacological and Toxicological Methods*. **37**, 215-228
- 67 Anuradha, C. D., Kanno, S. and Hirano, S. (2001) Oxidative damage to mitochondria is a preliminary step to caspase-3 activation in fluoride-induced apoptosis in HL-60 cells. *Free Radical Biology and Medicine*. **31**, 367-373
- 68 Kluck, R. M., Bossy-Wetzell, E., Green, D. R. and Newmeyer, D. D. (1997) The release of cytochrome c from mitochondria: a primary site for Bcl-2 regulation of apoptosis. *Science*. **275**

Chapter 5

SAB CONCENTRATIONS INDICATE CHEMOTHERAPEUTIC SUSCEPTIBILITY IN UTERINE CANCER CELLS

1. Introduction

Uterine cancer (UC), the most common gynecological cancer in developed countries [1], is a malignancy of the uterus that commonly arises in the endometrium as adenocarcinoma [2]. There are approximately 55,000 new cases of UC each year, which accounts for ~3.3% of new cancer cases and the prevalence of UC is increasing [1]. UC patients have an 81.7% 5-year survival rate; accordingly, the UC survival rate drops to 16.9% for metastatic disease [3]. Treatment options for uterine cancer include surgery with radiotherapy and chemotherapy [4, 5]. Because of the favorable survival rate, the underlying causes of treatment resistance in UC have not been extensively investigated. However, metastatic UC is typified by treatment resistance [6]; specifically, there is substantial chemoresistance toward megestrol acetate, the approved drug for treatment of UC [7]. Additionally, UC is often a disease of older women, whereby, most UC diagnoses are made between the ages of 45 and 75 years of age [8]. Thus, safer therapeutic alternatives may need to be considered due to the increased likelihood of toxic off-target effects in older patients [8]. Consequently, understanding the molecular mechanisms driving UC oncogenesis and resistance will be instrumental in developing rational therapies targeting unique aspects of UC pathophysiology to develop more efficacious and safer UC treatments.

Mitochondria are highly integrated organelles that regulate a myriad of cellular processes including cell death [9]. Paramount to mitochondrial apoptotic events are the Bcl-2 family of proteins, which control the cell death potential of mitochondria [10]. BH3-only proteins,

members of the Bcl-2 family, facilitate apoptotic programming by sequestering the pro-survival Bcl-2 proteins and mediating the formation of the Bax-Bak pore [11]. The formation of the Bax-Bak pore causes mitochondrial outer membrane permeabilization (OMMP), which allows for the release of pro-apoptotic components from the mitochondria (*i.e.* cytochrome c, endonuclease G, etc.) [12, 13]. Recently, studies have demonstrated that the levels of BH3-only proteins correlate to chemo-responsiveness [14-19]; wherein, high BH3-only levels conferred chemo-sensitivity due to elevated OMMP, while low BH3-only levels corresponded to chemo-resistance *in vitro* and *in vivo* [20-24]. Further, chemical induction of BH3-only proteins in chemo-resistant cells improved the chemo-responsiveness of several cancer cell types [18, 20]. However, the mechanism responsible for enhanced BH3-only levels in certain cancers remains elusive.

Recently, we demonstrated that the chemosensitizer LY294002 [25] altered mitochondrial signaling to enhance the effectiveness of radiotherapy and chemotherapeutic agents [25-27]. In cervical cancer cells (HeLa cells), administration of low-dose LY294002 increased the concentration of a mitochondrial scaffold protein Sab, which facilitated chemosensitization [28]. Previously, Sab-mediated signaling events have been linked to mitochondrial dysfunction and the induction of apoptosis in numerous cell types and under a myriad of conditions [29-34]. Sab facilitates c-Jun N-terminal Kinase (JNK) signaling on the outer mitochondrial membrane (OMM) [29, 35, 36]. Specifically, activated JNK isoforms can interact with one of two kinase interaction motifs (KIM1/2) near the C-terminus of Sab, and ablation of essential residues in the KIM binding sites or use of KIM-

motif mimicry can prevent JNK translocation to mitochondria along with subsequent organelle dysfunction and apoptosis [28, 29, 35-37]. Mitochondrial JNK signaling induces apoptosis through the manipulation of Bcl-2 family proteins via posttranslational modifications [29, 38-43]. The magnitude of local JNK signaling on Bcl-2 proteins in tumors determines the capacity of individual cells to induce apoptosis [44, 45]. Furthermore, chemotherapeutic agents have been shown to be potent inducers of mitochondrial JNK signaling events [28, 40, 46, 47]. Based on these studies, enhancing JNK signaling on mitochondria could be a means to improve therapeutic responsiveness in UC patients.

Because the abundance of scaffold proteins at specific subcellular sites dictate the biological outcomes of signaling events [48-50], the goal of the current study is to determine if changes in Sab concentrations affect mitochondrial physiology and the induction of apoptosis in UC cells. To investigate this possibility, we performed secondary data analysis of existing gene expression studies from patients with UC. After observing that Sab levels were reduced in UC patient samples with advanced and recurring disease, we assessed mitochondrial physiology in a metastatic-derived (AN-3-Ca) and a primary site-derived (SKUT-1) cell line. We found that Sab-levels were increased in the primary site line compared to the metastatic line. This difference was reflected by the resistance of An-3-Ca cells to common chemotherapeutic agents. The AN-3-Ca resistance to chemotherapy was mitigated by overexpressing Sab in the cells; contrariwise, silencing Sab in chemosensitive SKUT-1 cells promote resistance to chemotherapy agents. After

observing this evidence, these results suggest that alteration of Sab expression in late-stage UC may be responsible for chemoresistance.

2. Materials and methods

Gene Expression Analysis: Secondary data analysis was performed to determine the relative levels of Sab expression in UC. The expression of Sab (SH3-binding protein 5; SH3BP5) was examined using the OncoPrint database (<http://www.oncoPrint.org>) in October 2017 [51]. By querying available endometrial cancer datasets that included Sab, we compared experimental data from normal and malignant tissue. The data were compiled across the independent studies. Data are presented as mean fold changes between endometrial cancer and control samples or distinct types of endometrial cancers.

Materials: AN-3-Ca (HTB-111) and SKUT-1 (HTB-114) cells were obtained from American Type Culture Collection (Manassas, VA), and metabolic testing reagents were acquired from Seahorse Biosciences (Boston, MA). Antibodies were procured from Cell Signaling Technologies (Danvers, MA) unless indicated otherwise. Chemotherapeutic agents and general laboratory supplies were purchased from Fisher Scientific (Pittsburgh, PA) unless alternatively noted below. Near-infrared detection reagents were purchased from Li-Cor Biosciences.

Cell Culture: AN-3-Ca and SKUT-1 cells were grown in Eagle Minimum Essential Medium (EMEM) supplemented with 10% fetal bovine serum (FBS), 100U/ml penicillin, 10µg/mL streptomycin, and 5µg/mL plasmocin (Invivogen). The cells were cultured at

37°C under humidity with 5% CO₂. The cells were counted using the TC10 counter (BioRad) in the presence of Trypan blue.

Determining IC₅₀ for drugs: To examine the relative effectiveness of drugs towards a particular cell line, we calculated IC₅₀ for drugs in AN-3-Ca and SKUT-1 cells [28]. Cells were plated in a black-walled 96-well plate at a density of 2.0x10⁵ cells per well and grown overnight. We tested common and existing chemotherapeutic agents for UC; this group of compounds included megestrol acetate, ABT-737, cisplatin, doxorubicin, mitomycin C, and paclitaxel. The cells were treated with increasing concentrations of the drug (ranging from 0.1nM to 100µM on a log₁₀ scale) for 72 hours and were then washed, fixed, and stained with TO-PRO-3 for 45 minutes at room temperature. The plate was imaged using the Odyssey CLx imager (Li-Cor Biosciences), the fluorescence of each well was determined using the ImageStudio 2.0 software (Li-Cor Biosciences), and IC₅₀s were calculated using the GraphPad Prism7© software.

Western blot analysis: Protein analysis from cells was performed as described in our previous works [28-30]. Briefly, AN-3-Ca and SKUT-1 cells were plated in either 6-well plates or 35-mm² dishes. Following treatments, cells were washed twice in phosphate buffered saline (PBS; 137mM NaCl, 2.7mM KCl, 10mM Na₂HPO₄, and 1.8mM KH₂PO₄) and lysed in radioimmunoprecipitation assay buffer (RIPA; 50mM Tris-HCl, pH 8.0, 150mM NaCl, 1% Nonidet P-40, 0.5% deoxycholate, 0.1% SDS) supplemented with 1mM phenylmethanesulfonyl fluoride (PMSF) and Halt Protease and Phosphatase Inhibitor Cocktails (Thermo Scientific). Cells were incubated while gently rocking at 4°C for five

minutes, and then transferred to a sterile micro-centrifuge tube. After two minutes on ice, cell disruption was completed using sonication. The lysate was cleared by centrifugation at $14,000 \times g$ for 15 minutes. The protein in the cell lysates was quantified using a BCA kit (Pierce BCA Protein Assay Kit) in clear 96-well plates according to the manufacturer's protocol using the Biotek Synergy H1 Microplate Reader. Proteins were then resolved by SDS-PAGE and transferred onto low fluorescence PVDF membranes. Membranes were placed in blocking buffer comprised of PBS supplemented with either 5% non-fat milk (for standard blots) or 5% bovine serum albumin (BSA; for phosphor-specific blots) and incubated for at least one hour at room temperature (RT) or overnight at 4°C. The membranes were incubated in PBS containing 0.1% Tween 20 (PBST) and either 5% non-fat milk or BSA in the presence of primary antibodies for at least 2.5 hours (RT) or overnight (4°C) while gently rocking. Primary antibodies specific for Sab (Novus Biologics, #H00009467-M01), Bcl-2 (Cell Signaling Technologies (CST), 2870), Bcl-xL (CST, 2764), Mcl-1 (CST, 5453), Bad (CST, 9239), Bik (CST, 4592), Bim (CST, 2933), Bid (CST, 2002), PUMA (CST, 12450), Bax (CST, 5023), Bak (CST, 12105) Actin (CST, 4970), and α -tubulin (CST, 2144) were used at dilutions of 1:1000 for these studies. Membranes were washed three times for five minutes in PBST. Membranes were incubated with secondary antibodies in the appropriate blocking buffer at a ratio of 1:20,000 for one hour at RT gently rocking. The following secondary antibodies were used in the experiments below: IRDye 680RD Goat anti-Rabbit (926-32211) and IRDye 800CW Goat anti-Mouse (926-68070) (Licor Biosciences). Membranes were again washed three times

for five minutes in PBST. Membranes were analyzed using fluorescence detection using the Odyssey CLx near infrared scanner (Licor Biosciences). The corresponding bands on the western blots were quantified and normalized using the Image Studio 2.0 software (Licor Biosciences). The fluorescence of specific bands of interest were divided by the fluorescence of the loading control band to equilibrate signal strength and loading. The resulting signal was then normalized by dividing the signals from treated samples by respective untreated or normal tissue control signals for each experiment.

Metabolic Analysis: Cellular metabolism was assessed by measuring the extracellular acidification rate (ECAR) and the oxygen consumption rate (OCR) of UC cells using the Seahorse Biosciences XF-96 extracellular flux analyzer [52]. Cells were plated in XF-96 analyzer plates at 1.0×10^4 cells per well and treated as described below. Basal glycolysis rates (ECAR) were achieved by supplementing glucose-free assay with 10mM glucose (Glc). After 10 minutes, the ECAR was measured; simultaneously, OCR was measured to determine the amount of glucose oxidation in each treatment group. Then 1.0 μ M oligomycin was added to inhibit ATP-dependent respiration and induce maximum glycolysis (or ECAR). While treatment with 100 μ M 2-DOG was used to impair glucose utilization and oxidation. For assessing oxygen consumption and substrate oxidation, cells were placed in nutrient-free media, and OCR was measured before injection of either 10mM glucose or 5mM glutamine. Then, a mitochondrial respiratory profile was created. Briefly, basal OCR was measured for 20 minutes; next, cells were treated with 1 μ M oligomycin for 10 minutes, and then OCR was measured again to determine ATP-

independent respiration rates. Following that measurement, 1 μ M uncoupler (FCCP) was added for 10 minutes, and then maximum OCR was measured. Finally, 1 μ M of rotenone and antimycin A was added for 10 minutes to completely inhibit mitochondrial respiration, and OCR was measured to assess the amount of non-mitochondrial respiration. From these measurements, we derived respiratory parameters, including spare respiratory capacity as previously described. All rates were calculated from a minimum of six wells per experiment. Data were either normalized to cell number.

Manipulation of Sab Expression: We transiently transfected UC cells with plasmids designed to express Sab (pLOC:Sab), red fluorescent protein (RFP; pLOC:RFP), or a Sab mutant lacking MAPK binding motifs (pLOC:Sab^{KIML/A}) to evaluate the impact of increasing Sab levels. Plasmid DNA and FugeneHD (Promega) were combined in Optimem (Invitrogen) at a ratio of 1:6 and incubated for 15 minutes at RT before addition to culture. Eight hours after the addition of the transfection complex to media, the media was exchanged. Protein levels were assessed by western blot analysis at 72 hours post-transfection only cells demonstrating more than four-fold increases in Sab levels were used. To decrease Sab expression, SKUT-1 cells were transiently transfected with pLKO.1 plasmids containing shRNAs either a luciferase-specific shRNA (control) or a shRNA for Sab that demonstrated over 85% silencing in 72 hours. Ectopic expression of a shRNA-resistant form of Sab (previously described in (Chambers, TP, 2015)) was used to rescue Sab levels in SKUT-1 cells silencing Sab. Briefly, 1.5×10^4 cells were plated in a 96-well plate, or 1.5×10^5 cells were plated a day before transfection in 35-mm dishes for

experiments. Plasmids were mixed with FugeneHD (Promega) at a 6:1 ratio per manufacturer's recommendations and added to cells for up to 72 hours. Protein levels were determined by western blotting as described above.

Replicates and Statistics: Biochemical and other cellular measures were done with a minimum of six experimental replicates. Mitochondrial and protein analysis experiments were performed on a minimum of three biological replicates. To determine statistical significance, Mann-Whitney analysis was employed for significance between treatments and a Wilcoxon match pairs test was used to compare groups. One-way analysis of variance (ANOVA) was used to compare data across studies. Statistical significance is indicated by an asterisk in figures in which the P-value is less than 0.05. Data are displayed in figures as means with error bars representing plus and minus one standard deviation.

3. Results

3.1. Sab expression is diminished in late-stage uterine cancer and recurrent disease.

To determine if changes in Sab levels may occur in UC, we used existing studies of endometrial cancer gene expression from the Oncomine repository [51]. We segregated these data into clinical stage first to determine if Sab concentrations changed during progression of the disease. In Figure 4.1A, Sab expression is significantly decreased (nearly 6-fold) in Stage 4 samples, but not in the other stages of the disease. Similarly, our analysis of recurrent tumors versus patient samples from non-recurrent disease, demonstrate that Sab levels are markedly decreased (approximately 4-fold) in recurrent tumors compared to

non-recurrent (Figure 5.1B). In long-term recurrent disease, Sab mRNA levels are even lower (Figure 5.1B) at five years. This data suggest that Sab expression is diminished in advanced and recurrent UC.

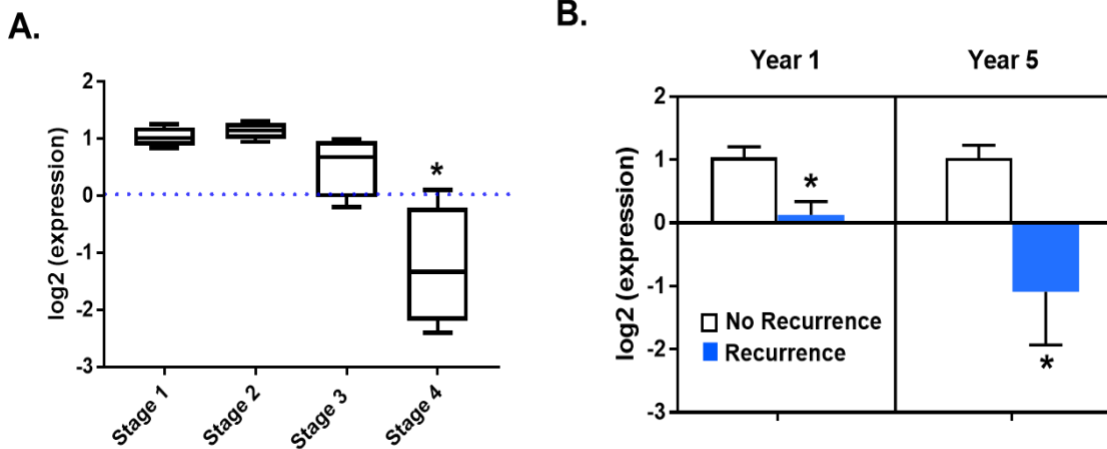


Figure 4.1: Secondary analysis of Sab expression from uterine cancer microarray studies. (A) The amount of Sab mRNA was examined from previous studies, and the patient samples were segregated based on the reported stage of the cancer. The distinct types of uterine cancer were grouped into clinical classifications. An asterisk (*) indicates a difference as determined by one-way Analysis of variance (ANOVA). (B) For samples with available data regarding the recurrence of disease, Sab expression levels were assessed in regards to disease recurrence at one and five years. An asterisk (*) indicates a difference between non-recurring and recurring tumors according to the Wilcoxon matched pairs test. Data are displayed as means with error bars representing plus and minus one standard deviation.

3.2. Metastatic AN-3-Ca cells have reduced chemosensitivity:

Because of the difference in Sab expression observed in Stage 4 disease, we performed comparisons of primary site and metastatic UC cell types. We obtained SKUT-1 and AN-3-Ca cells that were derived from primary site and metastatic tumors, respectively. First, we assessed the relative chemosensitivity of the two lines to observe potential differences

using a battery of chemotherapeutic agents. Each drug reflects a different mode of death induction in cancer cells providing insight into potential defects in cell death signaling. In Table 4.1, the IC₅₀s for megestrol acetate, ABT-737, cisplatin, doxorubicin, mitomycin C, and paclitaxel are presented. The metastasis-derived AN-3-Ca cell line consistently required more drug to induce cell death compared to primary site-derived SKUT-1 cells.

3.3. SKUT-1 cells and AN-3-Ca cells are metabolically distinct:

Because the trend in the IC₅₀ data may suggest a difference in the induction of apoptosis, a mitochondrial process, we examined whether mitochondrial function differed between the two lines. Using respirometry, we measured the respiratory profile of the two cell lines and found that AN-3-Ca cells had a greater oxygen consumption rate (OCR) than SKUT-1 cells (Figure 4.2A). This was reflected by higher basal respiration (Figure 4.2B) and a greater respiratory capacity (Figure 4.2C) when compared to SKUT-1 cells. Additionally, AN-3-Ca cells had a higher incidence of uncoupling than SKUT-1 cells (Figure 4.2D), and overall, AN-3-Ca cells had a greater OCR/ECAR ratio (Figure 4.2E). Next, we analyzed the metabolic parameters related to glycolysis in the two cell lines by assessing the extracellular acidification rate (ECAR) (Figure 4.2F). We found that SKUT-1 cells had a greater rate of glycolysis than AN-3-Ca cells (Figure 4.2G). Additionally, when 1 μM oligomycin was added to achieve maximum glycolysis, it was found that the

Table 4.1: IC₅₀ values for Common Chemotherapy agents for UC cell lines

Drug	AN-3-Ca	SK-UT-1
Megestrol Acetate	21.3 ± 5.1 μM	6.1 ± 2.7 μM
ABT-737	8.6 ± 1.8 μM	0.48 ± 0.2 μM
Cisplatin	12.8 ± 3.4 μM	4.9 ± 2.1 μM
Doxorubicin	0.09 ± 0.02 μM	0.03 ± 0.01 μM
Mitomycin C	0.63 ± 0.2 μM	0.10 ± 0.04 μM
Paclitaxel	0.01 ± 0.06 μM	0.003 ± 0.001 μM

Note: Values were compiled for and calculated using three distinct cell viability assays.

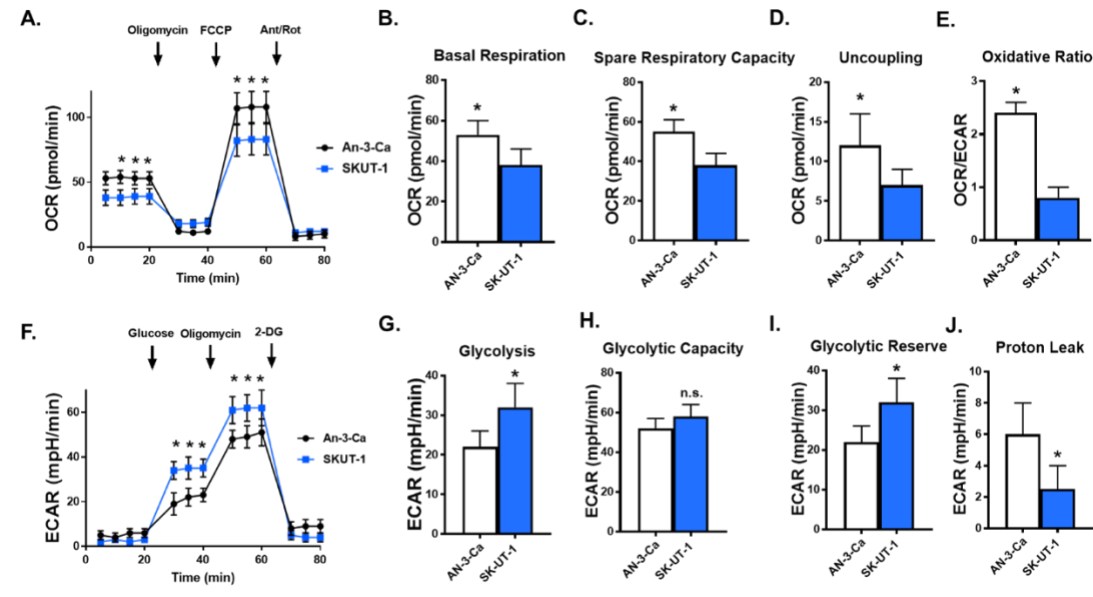


Figure 4.2: Mitochondrial metabolism differs between AN-3-Ca and SKUT1 cells. (A) Respiratory profile of AN-3-CA and SKUT-1 cells was measured using the Seahorse XF-96 extracellular flux analyzer. B. Basal respiration, C. Spare respiratory capacity, D. Uncoupling, E. Oxidative ratio, F. Extracellular acidification rate, G. Glycolysis, H. Glycolytic Capacity, I. Glycolytic reserve, J. Proton leak were measured. Data are displayed as means with error bars representing plus and minus one standard deviation.

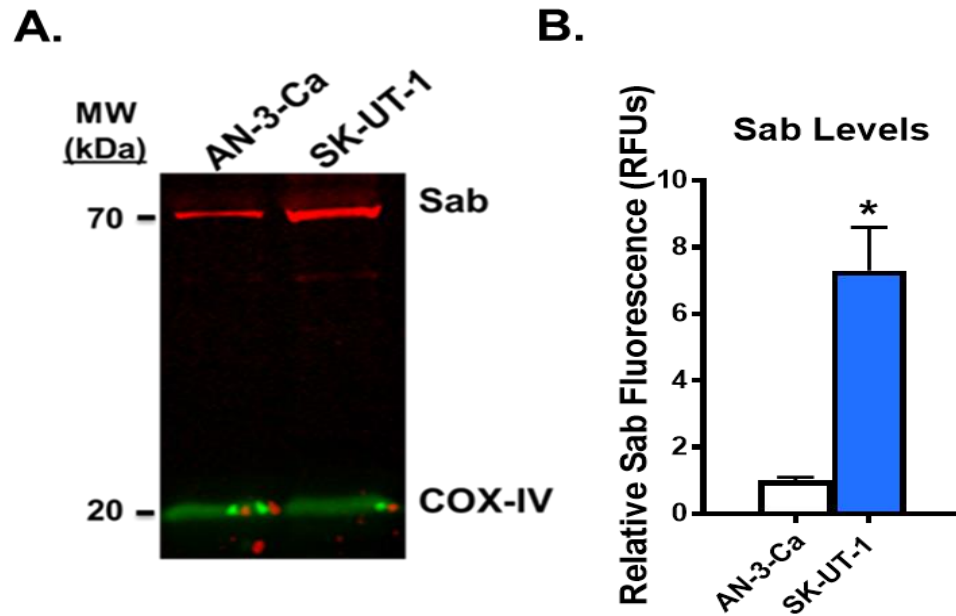


Figure 4.3: Sab concentrations differ between metastatic AN-3-Ca cells and primary site SKUT-1 cells. (A) A representative western blot analysis of AN-3-Ca and SKUT-1 cells to assess the relative levels of Sab on mitochondria. COX-IV was used as a mitochondrial loading control. (B) Quantification of four replicate analysis was performed using Image Studio 2.0. An asterisk (*) indicates a difference ($P < 0.05$) between cell lines as determined by a Mann-Whitney test. Data are displayed as means with error bars representing plus and minus one standard deviation.

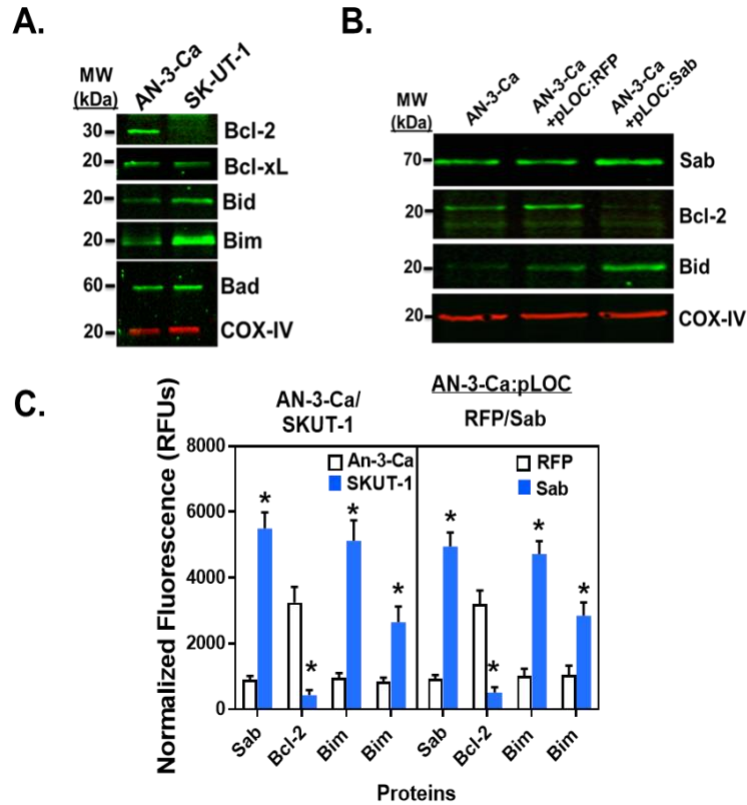


Figure 4.4: Increasing Sab concentrations restore chemosensitivity in AN-3-Ca cells. (A) Western blot analysis of AN-3-Ca and SKUT-1 cells to assess the relative levels of Bcl-2 protein levels. COX-IV was used as a mitochondrial loading control. (B) Ectopic expression of either RFP or Sab was assessed by western blot analysis. Additionally, Bcl-2 and Bim levels were measured with COX-IV serving as an organelle loading control. (C) Quantification of the changes in Sab, Bcl-2, Bim, and Bid were performed using Image Studio 2.0. Differences ($P < 0.05$) between paired samples was determined with a Wilcoxon matched pairs test, which are indicated by an asterisk (*). Data are displayed as means with error bars representing plus and minus one standard deviation.

two cell lines had a similar capacity for glycolysis (Figure 4.2H); however, SKUT-1 cells had a greater glycolytic reserve (Figure 4.2I).

Intriguingly, AN-3-Ca cells had a greater proton leak than SKUT-1 cells (Figure 4.2J). Taken together, the studies suggest that AN-3-Ca cells and SKUT-1 cells have distinct mitochondrial metabolic profiles.

3.4 AN-3-Ca cells have diminished Sab concentrations:

Because our previous work demonstrated that Sab-mediated events could affect chemo-responsiveness and metabolism in human cancers, we measured the relative abundance of Sab in the primary-site-derived SKUT-1 cells and metastatic AN-3-Ca cell lines. In Figure 4.3A, western blot analyses revealed a significant increase in Sab concentrations in the SKUT-1 cells compared to AN-3-Ca cells. The relative Sab fluorescence in these cells was normalized to the mitochondrial loading control, cyclo-oxygenase IV (COX-IV), a component of respiratory complex IV. Using semi-quantitative analysis, we found that AN-3-Ca cells had ~8-fold less Sab than SKUT-1 cells (Figure 4.3B).

3.5 AN-3-Ca cells have increased anti-apoptotic Bcl-2 proteins resulting from diminished Sab levels:

Because of the chemo-responsive and metabolic differences along with the distinct Sab concentrations between the two cells, we assessed the expression of hallmark Bcl-2 proteins in AN-3-Ca and SKUT-1 cells. The specific apoptotic proteins we examined were the anti-apoptotic Bcl-2 family proteins: Bcl-2 and Bcl-xL. We also looked at pro-apoptotic BH3-only family proteins: Bid, Bim, Bad. In Figure 4A, AN-3-Ca have higher anti-apoptotic Bcl-2 concentrations (Bcl-2, Bcl-XL) and lower pro-apoptotic Bcl-2 protein

levels (Bid, Bim, and Bad) compared to SKUT-1 cells (quantified in Figure 4.4C). To test whether the shift in Bcl-2 proteins in AN-3-Ca cells was due to diminished Sab concentrations, we overexpressed Sab or red fluorescent protein (RFP) in AN-3-Ca cells to determine the effect on Bcl-2 protein levels (Figure 4.4B). Increasing the relative abundance of Sab in AN-3-Ca cells resulted in a significant decrease in Bcl-2 protein levels that was not observed in cells expressing RFP (Figure 4.4B). Furthermore, elevating Sab concentrations in AN-3-Ca cells increased the relative abundance of Bim, an effect that was not found in RFP-expressing AN-3-Ca cells (Figure 4.3B). This occurred without a significant change in mitochondrial protein levels, as indicated by COX-IV detection (Figure 4.3B). To determine whether increasing Sab altered the susceptibility of AN-3-Ca cells to chemotherapeutic agents, we examined cell viability following treatment with the previously introduced chemotherapeutic agents (Table 5.2). AN-3-Ca cells overexpressing cells were significantly more susceptible to chemotherapy agents than cells expressing RFP or non-transfected AN-3-Ca cells (Table 4.2). Collectively, these results demonstrate that increasing Sab levels alters the chemosensitivity of UC cells by manipulating Bcl-2 family protein levels on mitochondria.

3.6 Silencing Sab expression in SKUT-1 cells induces chemoresistance:

To examine if altering Sab expression impacted the sensitivity of primary-site derived cells to chemotherapy agents, we introduced a plasmid into SKUT-1 cells that expressed either

Table 4.2: IC₅₀ values for Chemotherapy agents in AN-3-Ca cells with increasing Sab expression.

Drug	AN-3-Ca	pLOC:RFP	pLOC:Sab
Megestrol Acetate	21.3 ± 5.1 μM	19.8 ± 6.7 μM	8.8 ± 3.1 μM
ABT-737	8.6 ± 1.8 μM	9.4 ± 2.1 μM	2.6 ± 1.3 μM
Cisplatin	12.8 ± 3.4 μM	15.5 ± 4.3 μM	2.9 ± 0.9 μM
Doxorubicin	0.09 ± 0.02 μM	0.11 ± 0.04 μM	0.01 ± 0.01 μM
Mitomycin C	0.63 ± 0.20 μM	0.84 ± 0.22 μM	0.15 ± 0.09 μM
Paclitaxel	0.01 ± 0.06 μM	0.02 ± 0.008 μM	0.02 ± 0.004 μM

Note: Data are presented in mean plus/minus the standard deviation from the mean for no less than six replicate experiments.

a control (luciferase-specific) small-hairpin RNA (shRNA) or a Sab-specific shRNA. We assessed the ability of the shRNAs to affect Sab abundance after 72 hours; wherein, the Sab shRNA, but not the control shRNA, reduced Sab levels to a concentration comparable to AN-3-Ca cells (Figure 4.5A). These differences were quantified in Figure 4.5B. To determine if silencing Sab expression, impaired JNK translocation to mitochondria, we purified mitochondria from cells that were treated with 0.01% DMSO or 25μM staurosporine (STS) to induce JNK translocation to mitochondria. In the presence of DMSO, JNK did not become activated or translocate to mitochondria in either cell line or the presence of the shRNAs

We expressed a shRNA-resistant version of Sab as a potential rescue for Sab-mediated events (Figure 4.5C). However, the addition of STS triggered JNK translocation to mitochondria in SKUT-1 cells, as well as in SKUT-1 cells expressing the control and Sab shRNAs (Figure 4.5C, bottom panel). The relative abundance of mitochondrial JNK (P-

JNK) corresponded to the levels of Sab in each cell type (Figure 4.5C), which was quantified as (Figure 4.5C, top panel).

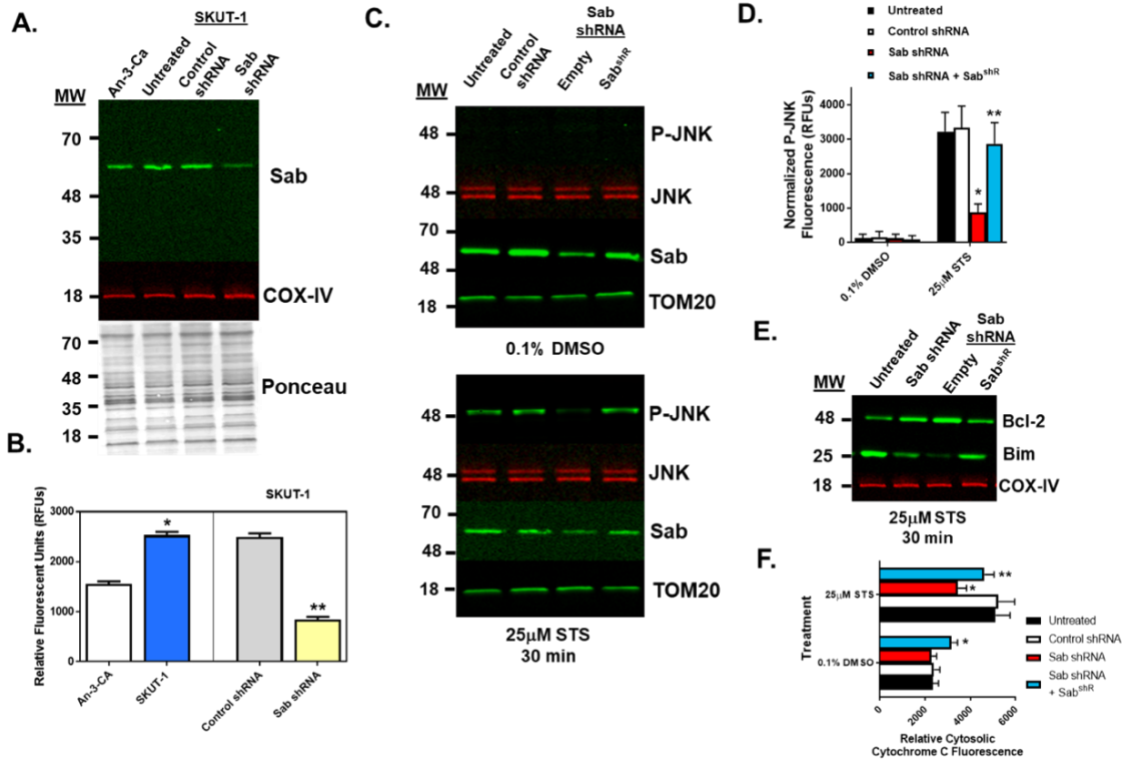


Figure 4.5: Silencing Sab in SKUT-1 cells make them chemoresistant. (A) Western blot analysis of AN-3-Ca and SKUT-1 after silencing Sab in SKUT-1 cell to assess Sab levels. COX-IV was used as a mitochondrial loading control. (B) Quantification of Sab. (C) Western blot analysis of active JNK in SKUT-1 cells after silencing of Sab. (D) Quantification of P-JNK was performed using the Image Studio 2.0 Software. Differences ($P < 0.05$) between paired samples were determined using a Wilcoxon matched pairs test, which are indicated by an asterisk (*). (E) Western blot analysis of Bcl-2 and Bim in SKUT-1 cells after silencing of Sab. (F) Relative cytosolic cytochrome C released. Data are displayed as means with error bars representing plus and minus one standard deviation.

well to demonstrate that there was significantly less mitochondrial JNK in SKUT-1 cells silencing Sab and rescued by expressing the shRNA-resistant Sab (Figure 4.5D). We also examined critical JNK-regulated Bcl-2 proteins, Bcl-2, Bim, and Bid, in the presence and absence of the Sab shRNA. Following STS-exposure, Bcl-2 levels decreased in SKUT-1 cells, but not in cells expressing the Sab shRNA (Figure 4.5E). Mitochondrial Bcl-2 was restored by expressing the shRNA-resistant Sab (Figure 4.5E). Contrariwise, the concentrations of Bim and Bid increased following STS treatment in SKUT-1 cells, but not in cells with the shRNA for Sab (Figure 4.5E). Again, the matriculation of Bim and Bid to mitochondria was rescued by expressing the shRNA-resistant form of Sab in SKUT-1 cells (Figure 4.5E). To determine if the changes in Sab levels affected the apoptotic potential in SKUT-1 cells, we measured the amount of cytosolic cytochrome c following treatment with STS in SKUT-1 cells with and without Sab-mediated signaling. Again, silencing Sab results in less cytosolic cytochrome c release into the cytosol following STS-treatment, and introducing the shRNA-resistant Sab restores the induction of apoptosis in SKUT-1 cells (Figure 4.5F). These data reiterate that Sab is a crucial element of apoptotic signaling in UC cells.

To determine if indeed reducing Sab levels corresponds to chemoresistance, we examined the toxicity of chemotherapeutic agents in SKUT-1 cells expressing either the control or Sab shRNAs. We found that silencing Sab made SKUT-1 cells significantly less sensitive to chemotherapeutic agents (Table 4.3). Thus, the defects in apoptosis corresponded to diminished chemo-responsiveness in SKUT-1 cells. These data demonstrate that Sab-

mediated signaling is crucial to cell death induction in UC cells and decreased Sab levels may in part be responsible for the treatment-resistant disease.

Table 4.3. IC₅₀ values for chemotherapy agents in SKUT-1 cells with diminished Sab expression.

Drug	Control shRNA	Sab shRNA
Megestrol Acetate	24.3 ± 6.4 μM	81.2 ± 11.4 μM
ABT-737	8.9 ± 1.2 μM	38.3 ± 7.9 μM
Cisplatin	13.1 ± 2.9 μM	31.5 ± 9.3 μM
Doxorubicin	0.08 ± 0.03 μM	0.23 ± 0.11 μM
Mitomycin C	0.65 ± 0.15 μM	1.94 ± 0.62 μM
Paclitaxel	0.02 ± 0.03 μM	0.10 ± 0.04 μM

Note: Data are presented in mean plus/minus the standard deviation from the mean for no less than six replicate experiments.

4. Discussion

Late-stage UCs are typified by a poor survival rate; specifically, metastatic UC has only a 16.9% survival [1]. Because the risk factors are commonplace: obesity, high blood pressure, and diabetes mellitus, it's important to address the low survival of metastatic cancer [7]. Our previous work has shown that mitochondrial JNK signaling on the scaffold protein Sab is a critical mediator of apoptosis in gynecological cancers cells [28, 29]. Furthermore, in Chapter 3, we showed that diminished Sab levels contribute to chemoresistance in ovarian cancer. Herein, we used patient-derived data and cellular studies to demonstrate the consequences of diminished Sab-mediated signaling in UC. Our results demonstrate that Sab expression is down-regulated in UC and restoring Sab levels

on mitochondria restores apoptotic induction. These studies provides unique insight into the mechanisms driving resistance in late-stage UC.

Our secondary data analysis of Sab expression in UC patient samples revealed that Sab mRNA levels were decreased significantly in late-stage and recurrent disease (Figure 4.1). While this reflects our previous observation in ovarian cancer, we did not segregate the ovarian patient data into clinical stages nor did we consider recurrence. The late decrease in Sab transcripts in advanced disease suggests that the change in Sab expression is in response to the progressive pathology of the disease. Our previous work demonstrates that mitochondrial JNK signaling, and by extension the expression of Sab, is highly responsive to mitochondrial toxins [28, 53, 54]. Since mitochondrial dysfunction is necessary for oncogenesis [55], one can postulate that Sab expression may be diminished as cancer cells switch to glycolysis and minimize their reliance on mitochondria [56]. Additionally, it is possible that prolonged mitochondrial dysfunction could habituate stress signaling failing to recognize mitochondrial damage and activate stress responses like mitochondrial JNK signaling. Regardless, the transcriptional regulation of Sab in gynecological cancers remains a topic of active investigation in our group.

To examine the role of Sab-mediated signaling in UC physiology, we employed a primary-site derived cell line (SKUT-1) and a metastatic-derived cell line (AN-3-Ca) to investigate early and late-stage UC. Initially, we found that AN-3-Ca cells had greater mitochondrial metabolism than SKUT-1 (Figure 2), which would suggest greater integrity of mitochondrial membrane potential. This was realized when we discovered that AN-3-Ca

cells had a higher concentration of Bcl-2 on the mitochondrial surface [57, 58]. This would suggest that the outer membrane of the mitochondria was more intact than the SKUT-1 cells, which may in part explain the higher levels of respiration. The greater oxidative potential of metastatic UC cells may also be necessary to generate ROS needed for invasion [59]. Although we have previously shown that Sab can contribute to ROS amplification [53], it is likely that the significant levels of uncoupling and proton leak in AN-3-Ca cells (Figure 2) suggest a level of mitochondrial dysfunction that may be sufficient to generate the levels of ROS needed for metastasis.

SKUT-1 cells were found to be more glycolytic, which is the hallmark metabolic feature of cancers [55]. This may also be partly explained by the increased levels of Sab in older patients. Specifically, in the aging brain, mitochondrial JNK signaling has been shown to impair the activity of pyruvate dehydrogenase reducing the amount of glucose oxidation [60, 61]. Alternatively, JNK signaling has been shown to influence a myriad of metabolic signaling [62]. One mechanism JNK signaling could employ is to phosphorylate Bcl-2 proteins and alter their functions. Bcl-2 proteins have been shown to contribute to metabolic flux in mammalian cells [63, 64], and altering their mitochondrial functions could contribute to this outcome.

The predominant impact of diminished Sab levels appears to be on the induction of apoptosis. UC cells with low Sab levels had increased anti-apoptotic Bcl-2 proteins and were resistant to chemotherapeutic agents; alternatively, cells with high Sab levels or restoring Sab levels increased the levels of pro-apoptotic BH3-only proteins on

mitochondria resulting in greater sensitivity to chemotherapeutic drugs. The specific change was a decrease in Bcl-2 levels on mitochondria and an increase in Bim and Bid. These drugs are well-established JNK targets [38], and the manipulation of these proteins occurs either at mitochondria or via JNK activity on the common scaffold 14-3-3 [65]. Mitochondrial JNK is a potent inducer of apoptosis following cytosolic stress, so increasing the magnitude of mitochondrial JNK signaling could greatly enhance apoptotic responses in cancer cells. However, this should be considered with caution, since elevating mitochondrial JNK signaling can induce off-target effects such as cardiotoxicity of chemotherapy agents [30]. This is of particular concern in older patients, which is the largest population of UC patients [3].

These studies demonstrate that diminished Sab-mediated signaling in advanced UC can contribute to apoptotic resistance. Consequently, the concentration of Sab in tumors could be used as a prognostic to determine the relative dose of chemotherapy needed to treat a UC patient; alternatively, therapeutic approaches aimed at increasing Sab-mediated signaling could be potent chemosensitizing agents if their actions can be limited to cancer cells. We propose that investigation of Sab in more cell lines and in patient-derived xenograft models are needed to validate Sab as a prognostic marker or therapeutic target.

References

- 1 Ferlay, J., Soerjomataram, I., Dikshit, R., Eser, S., Mathers, C., Rebelo, M., Parkin, D. M., Forman, D. and Bray, F. (2015) Cancer incidence and mortality worldwide: sources, methods and major patterns in GLOBOCAN 2012. *Int J Cancer*. **136**, E359-386
- 2 Morice, P., Leary, A., Creutzberg, C., Abu-Rustum, N. and Darai, E. (2016) Endometrial cancer. *Lancet*. **387**, 1094-1108
- 3 Siegel, R. L., Miller, K. D. and Jemal, A. (2016) Cancer statistics, 2016. *CA: A Cancer Journal for Clinicians*. **66**, 7-30
- 4 Group, S. G. O. C. P. E. C. W., Burke, W. M., Orr, J., Leitao, M., Salom, E., Gehrig, P., Olawaiye, A. B., Brewer, M., Boruta, D., Herzog, T. J., Shahin, F. A. and Society of Gynecologic Oncology Clinical Practice, C. (2014) Endometrial cancer: a review and current management strategies: part II. *Gynecol Oncol*. **134**, 393-402
- 5 Group, S. G. O. C. P. E. C. W., Burke, W. M., Orr, J., Leitao, M., Salom, E., Gehrig, P., Olawaiye, A. B., Brewer, M., Boruta, D., Vilella, J., Herzog, T., Abu Shahin, F. and Society of Gynecologic Oncology Clinical Practice, C. (2014) Endometrial cancer: a review and current management strategies: part I. *Gynecol Oncol*. **134**, 385-392
- 6 McMeekin, D. S., Filiaci, V. L., Thigpen, J. T., Gallion, H. H., Fleming, G. F. and Rodgers, W. H. (2007) The relationship between histology and outcome in advanced and recurrent endometrial cancer patients participating in first-line chemotherapy trials: A Gynecologic Oncology Group study. *Gynecologic Oncology*. **106**, 16-22
- 7 Makker, V., Green, A. K., Wenham, R. M., Mutch, D., Davidson, B. and Miller, D. S. (2017) New therapies for advanced, recurrent, and metastatic endometrial cancers. *Gynecologic Oncology Research and Practice*. **4**, 19
- 8 Hecht, J. L. and Mutter, G. L. (2006) Molecular and Pathologic Aspects of Endometrial Carcinogenesis. *Journal of Clinical Oncology*. **24**, 4783-4791

- 9 Labbé, K., Murley, A. and Nunnari, J. (2014) Determinants and Functions of Mitochondrial Behavior. *Annual Review of Cell and Developmental Biology*. **30**, 357-391
- 10 Kale, J., Osterlund, E. J. and Andrews, D. W. (2017) BCL-2 family proteins: changing partners in the dance towards death. *Cell Death And Differentiation*. **25**, 65
- 11 Strasser, A. and Vaux, D. L. (2017) Viewing BCL2 and cell death control from an evolutionary perspective. *Cell Death And Differentiation*. **25**, 13
- 12 Hsu, Y.-T., Wolter, K. G. and Youle, R. J. (1997) Cytosol-to-membrane redistribution of Bax and Bcl-X_L during apoptosis. *Proceedings of the National Academy of Sciences*. **94**, 3668-3672
- 13 Mikhailov, V., Mikhailova, M., Degenhardt, K., Venkatachalam, M. A., White, E. and Saikumar, P. (2003) Association of Bax and Bak Homo-oligomers in Mitochondria: Bax REQUIREMENT FOR Bak REORGANIZATION AND CYTOCHROME_c RELEASE. *Journal of Biological Chemistry*. **278**, 5367-5376
- 14 Brunelle, J. K. and Letai, A. (2009) Control of mitochondrial apoptosis by the Bcl-2 family. *J Cell Sci*. **122**, 437-441
- 15 Certo, M., Del Gaizo Moore, V., Nishino, M., Wei, G., Korsmeyer, S., Armstrong, S. A. and Letai, A. (2006) Mitochondria primed by death signals determine cellular addiction to antiapoptotic BCL-2 family members. *Cancer Cell*. **9**, 351-365
- 16 Letai, A., Bassik, M. C., Walensky, L. D., Sorcinelli, M. D., Weiler, S. and Korsmeyer, S. J. (2002) Distinct BH3 domains either sensitize or activate mitochondrial apoptosis, serving as prototype cancer therapeutics. *Cancer Cell*. **2**, 183-192
- 17 Letai, A. G. (2008) Diagnosing and exploiting cancer's addiction to blocks in apoptosis. *Nat Rev Cancer*. **8**, 121-132

- 18 Ryan, J. and Letai, A. (2013) BH3 profiling in whole cells by fluorimeter or FACS. *Methods*. **61**, 156-164
- 19 Ryan, J. A., Brunelle, J. K. and Letai, A. (2010) Heightened mitochondrial priming is the basis for apoptotic hypersensitivity of CD4+ CD8+ thymocytes. *Proceedings of the National Academy of Sciences*. **107**, 12895-12900
- 20 Chonghaile, T. N., Sarosiek, K. A., Vo, T.-T., Ryan, J. A., Tammareddi, A., Moore, V. D. G., Deng, J., Anderson, K. C., Richardson, P., Tai, Y.-T., Mitsiades, C. S., Matulonis, U. A., Drapkin, R., Stone, R., DeAngelo, D. J., McConkey, D. J., Sallan, S. E., Silverman, L., Hirsch, M. S., Carrasco, D. R. and Letai, A. (2011) Pretreatment Mitochondrial Priming Correlates with Clinical Response to Cytotoxic Chemotherapy. *Science*. **334**, 1129-1133
- 21 Davids, M. S., Deng, J., Wiestner, A., Lannutti, B. J., Wang, L., Wu, C. J., Wilson, W. H., Brown, J. R. and Letai, A. (2012) Decreased mitochondrial apoptotic priming underlies stroma-mediated treatment resistance in chronic lymphocytic leukemia. *Blood*. **120**, 3501-3509
- 22 Montero, J., Sarosiek, Kristopher A., DeAngelo, Joseph D., Maertens, O., Ryan, J., Ercan, D., Piao, H., Horowitz, Neil S., Berkowitz, Ross S., Matulonis, U., Jänne, Pasi A., Amrein, Philip C., Cichowski, K., Drapkin, R. and Letai, A. (2015) Drug-Induced Death Signaling Strategy Rapidly Predicts Cancer Response to Chemotherapy. *Cell*. **160**, 977-989
- 23 Sarosiek, Kristopher A., Chi, X., Bachman, John A., Sims, Joshua J., Montero, J., Patel, L., Flanagan, A., Andrews, David W., Sorger, P. and Letai, A. (2013) BID Preferentially Activates BAK while BIM Preferentially Activates BAX, Affecting Chemotherapy Response. *Molecular Cell*. **51**, 751-765
- 24 Vo, T. T., Ryan, J., Carrasco, R., Neuberg, D., Rossi, D. J., Stone, R. M., Deangelo, D. J., Frattini, M. G. and Letai, A. (2012) Relative mitochondrial priming of myeloblasts and normal HSCs determines chemotherapeutic success in AML. *Cell*. **151**, 344-355
- 25 Rosenzweig, K. E., Youmell, M. B., Palayoor, S. T. and Price, B. D. (1997) Radiosensitization of human tumor cells by the phosphatidylinositol3-kinase

- inhibitors wortmannin and LY294002 correlates with inhibition of DNA-dependent protein kinase and prolonged G2-M delay. *Clinical Cancer Research*. **3**, 1149-1156
- 26 Zhong, H., Chiles, K., Feldser, D., Laughner, E., Hanrahan, C., Georgescu, M.-M., Simons, J. W. and Semenza, G. L. (2000) Modulation of Hypoxia-inducible Factor 1 α Expression by the Epidermal Growth Factor/Phosphatidylinositol 3-Kinase/PTEN/AKT/FRAP Pathway in Human Prostate Cancer Cells: Implications for Tumor Angiogenesis and Therapeutics. *Cancer Research*. **60**, 1541-1545
- 27 Mitsuuchi, Y., Johnson, S. W., Selvakumaran, M., Williams, S. J., Hamilton, T. C. and Testa, J. R. (2000) The Phosphatidylinositol 3-Kinase/AKT Signal Transduction Pathway Plays a Critical Role in the Expression of p21^{WAF1/CIP1/SDI1} Induced by Cisplatin and Paclitaxel. *Cancer Research*. **60**, 5390-5394
- 28 Chambers, T. P., Portalatin, G. M., Paudel, I., Robbins, C. J. and Chambers, J. W. (2015) Sub-chronic administration of LY294002 sensitizes cervical cancer cells to chemotherapy by enhancing mitochondrial JNK signaling. *Biochem Biophys Res Commun*. **463**, 538-544
- 29 Chambers, J. W., Cherry, L., Laughlin, J. D., Figuera-Losada, M. and Lograsso, P. V. (2011) Selective inhibition of mitochondrial JNK signaling achieved using peptide mimicry of the Sab kinase interacting motif-1 (KIM1). *ACS chemical biology*. **6**, 808-818
- 30 Chambers, T. P., Santiesteban, L., Gomez, D. and Chambers, J. W. (2017) Sab mediates mitochondrial dysfunction involved in imatinib mesylate-induced cardiotoxicity. *Toxicology*. **382**, 24-35
- 31 Court, N. W., Kuo, I., Quigley, O. and Bogoyevitch, M. A. (2004) Phosphorylation of the mitochondrial protein Sab by stress-activated protein kinase 3. *Biochem Biophys Res Commun*. **319**, 130-137
- 32 Win, S., Than, T. A., Fernandez-Checa, J. C. and Kaplowitz, N. (2014) JNK interaction with Sab mediates ER stress induced inhibition of mitochondrial respiration and cell death. *Cell Death Dis*. **5**, e989

- 33 Win, S., Than, T. A., Han, D., Petrovic, L. M. and Kaplowitz, N. (2011) c-Jun N-terminal kinase (JNK)-dependent acute liver injury from acetaminophen or tumor necrosis factor (TNF) requires mitochondrial Sab protein expression in mice. *J Biol Chem.* **286**, 35071-35078
- 34 Win, S., Than, T. A., Min, R. W. M., Aghajan, M. and Kaplowitz, N. (2016) c-Jun N-terminal kinase mediates mouse liver injury through a novel Sab (SH3BP5)-dependent pathway leading to inactivation of intramitochondrial Src. *Hepatology.* **63**, 1987-2003
- 35 Wiltshire, C., Gillespie, D. A. and May, G. H. (2004) Sab (SH3BP5), a novel mitochondria-localized JNK-interacting protein. *Biochem Soc Trans.* **32**, 1075-1077
- 36 Wiltshire, C., Matsushita, M., Tsukada, S., Gillespie, D. A. and May, G. H. (2002) A new c-Jun N-terminal kinase (JNK)-interacting protein, Sab (SH3BP5), associates with mitochondria. *Biochem J.* **367**, 577-585
- 37 Barr, R. K., Boehm, I., Attwood, P. V., Watt, P. M. and Bogoyevitch, M. A. (2004) The critical features and the mechanism of inhibition of a kinase interaction motif-based peptide inhibitor of JNK. *The Journal of biological chemistry.* **279**, 36327-36338
- 38 Dhanasekaran, D. N. and Reddy, E. P. (2008) JNK signaling in apoptosis. *Oncogene.* **27**, 6245-6251
- 39 Donovan, N., Becker, E. B. E., Konishi, Y. and Bonni, A. (2002) JNK Phosphorylation and Activation of BAD Couples the Stress-activated Signaling Pathway to the Cell Death Machinery. *Journal of Biological Chemistry.* **277**, 40944-40949
- 40 El Fajoui, Z., Toscano, F., Jacquemin, G., Abello, J., Scoazec, J. Y., Micheau, O. and Saurin, J. C. (2011) Oxaliplatin sensitizes human colon cancer cells to TRAIL through JNK-dependent phosphorylation of Bcl-xL. *Gastroenterology.* **141**, 663-673
- 41 Hunot, S., Vila, M., Teismann, P., Davis, R. J., Hirsch, E. C., Przedborski, S., Rakic, P. and Flavell, R. A. (2004) JNK-mediated induction of cyclooxygenase 2 is required

for neurodegeneration in a mouse model of Parkinson's disease. *Proc Natl Acad Sci U S A.* **101**, 665-670

- 42 Kharbanda, S., Saxena, S., Yoshida, K., Pandey, P., Kaneki, M., Wang, Q., Cheng, K., Chen, Y. N., Campbell, A., Sudha, T., Yuan, Z. M., Narula, J., Weichselbaum, R., Nalin, C. and Kufe, D. (2000) Translocation of SAPK/JNK to mitochondria and interaction with Bcl-x(L) in response to DNA damage. *The Journal of biological chemistry.* **275**, 322-327
- 43 Lee, J. J., Lee, J. H., Ko, Y. G., Hong, S. I. and Lee, J. S. (2010) Prevention of premature senescence requires JNK regulation of Bcl-2 and reactive oxygen species. *Oncogene.* **29**, 561-575
- 44 Wagner, E. F. and Nebreda, A. R. (2009) Signal integration by JNK and p38 MAPK pathways in cancer development. *Nature reviews. Cancer.* **9**, 537-549
- 45 Fey, D., Halasz, M., Dreidax, D., Kennedy, S. P., Hastings, J. F., Rauch, N., Munoz, A. G., Pilkington, R., Fischer, M., Westermann, F., Kolch, W., Kholodenko, B. N. and Croucher, D. R. (2015) Signaling pathway models as biomarkers: Patient-specific simulations of JNK activity predict the survival of neuroblastoma patients. *Sci Signal.* **8**, ra130
- 46 Ito, Y., Mishra, N. C., Yoshida, K., Kharbanda, S., Saxena, S. and Kufe, D. (2001) Mitochondrial targeting of JNK/SAPK in the phorbol ester response of myeloid leukemia cells. *Cell Death Differ.* **8**, 794-800
- 47 Zhang, Z. B., Jiang, X. G., Liang, Z. Q. and Gu, Z. L. (2012) Arsenic trioxide inhibits the growth of human glioma stem cells through activating the JNK pathway. *Molecular & Cellular Toxicology.* **8**, 187-193
- 48 Dhanasekaran, D. N., Kashef, K., Lee, C. M., Xu, H. and Reddy, E. P. (2007) Scaffold proteins of MAP-kinase modules. *Oncogene.* **26**, 3185-3202
- 49 Good, M. C., Zalatan, J. G. and Lim, W. A. (2011) Scaffold Proteins: Hubs for Controlling the Flow of Cellular Information. *Science.* **332**, 680-686

- 50 Zeke, A., Lukács, M., Lim, W. A. and Reményi, A. (2009) Scaffolds: interaction platforms for cellular signalling circuits. *Trends in Cell Biology*. **19**, 364-374
- 51 Rhodes, D. R., Kalyana-Sundaram, S., Mahavisno, V., Varambally, R., Yu, J., Briggs, B. B., Barrette, T. R., Anstet, M. J., Kincaid-Beal, C., Kulkarni, P., Varambally, S., Ghosh, D. and Chinnaiyan, A. M. (2007) Oncomine 3.0: genes, pathways, and networks in a collection of 18,000 cancer gene expression profiles. *Neoplasia*. **9**, 166-180
- 52 Wu, M., Neilson, A., Swift, A. L., Moran, R., Tamagnine, J., Parslow, D., Armistead, S., Lemire, K., Orrell, J., Teich, J., Chomicz, S. and Ferrick, D. A. (2007) Multiparameter metabolic analysis reveals a close link between attenuated mitochondrial bioenergetic function and enhanced glycolysis dependency in human tumor cells. *Am J Physiol Cell Physiol*. **292**, C125-136
- 53 Chambers, J. W. and LoGrasso, P. V. (2011) Mitochondrial c-Jun N-terminal kinase (JNK) signaling initiates physiological changes resulting in amplification of reactive oxygen species generation. *J Biol Chem*. **286**, 16052-16062
- 54 Chambers, J. W., Pachori, A., Howard, S., Iqbal, S. and LoGrasso, P. V. (2013) Inhibition of JNK Mitochondrial Localization and Signaling Is Protective against Ischemia/Reperfusion Injury in Rats. *Journal of Biological Chemistry*. **288**, 4000-4011
- 55 Hanahan, D. and Weinberg, R. A. (2011) Hallmarks of cancer: the next generation. *Cell*. **144**, 646-674
- 56 Vander Heiden, M. G., Cantley, L. C. and Thompson, C. B. (2009) Understanding the Warburg effect: the metabolic requirements of cell proliferation. *Science*. **324**, 1029-1033
- 57 Adams, J. M. and Cory, S. (2007) The Bcl-2 apoptotic switch in cancer development and therapy. *Oncogene*. **26**, 1324-1337
- 58 DeBerardinis, R. J., Mancuso, A., Daikhin, E., Nissim, I., Yudkoff, M., Wehrli, S. and Thompson, C. B. (2007) Beyond aerobic glycolysis: transformed cells can

engage in glutamine metabolism that exceeds the requirement for protein and nucleotide synthesis. *Proc Natl Acad Sci U S A.* **104**, 19345-19350

- 59 Yang, L., Moss, T., Mangala, L. S., Marini, J., Zhao, H., Wahlig, S., Armaiz-Pena, G., Jiang, D., Achreja, A., Win, J., Roopaimoole, R., Rodriguez-Aguayo, C., Mercado-Uribe, I., Lopez-Berestein, G., Liu, J., Tsukamoto, T., Sood, A. K., Ram, P. T. and Nagrath, D. (2014) Metabolic shifts toward glutamine regulate tumor growth, invasion and bioenergetics in ovarian cancer
- 60 Zhou, Q., Lam, P. Y., Han, D. and Cadenas, E. (2008) c-Jun N-terminal kinase regulates mitochondrial bioenergetics by modulating pyruvate dehydrogenase activity in primary cortical neurons. *J Neurochem.* **104**, 325-335
- 61 Zhou, Q., Lam, P. Y., Han, D. and Cadenas, E. (2009) Activation of c-Jun-N-terminal kinase and decline of mitochondrial pyruvate dehydrogenase activity during brain aging. *FEBS Lett.* **583**, 1132-1140
- 62 Vallerie, S. N. and Hotamisligil, G. S. (2010) The role of JNK proteins in metabolism. *Sci Transl Med.* **2**, 60rv65
- 63 Danial, N. N. (2009) BAD: undertaker by night, candyman by day. *Oncogene.* **27**, S53
- 64 Gross, A. and Katz, S. G. (2017) Non-apoptotic functions of BCL-2 family proteins. *Cell Death And Differentiation.* **24**, 1348
- 65 Vogt, P. K., Jiang, H. and Aoki, M. (2005) Triple Layer Control: Phosphorylation, Acetylation and Ubiquitination of FOXO Proteins. *Cell Cycle.* **4**, 908-913

Chapter 5

A HIGH-THROUGHPUT ASSAY TO SCREEN FOR COMPOUNDS ELEVATING SAB CONCENTRATIONS IN CHEMO-RESISTANT HUMAN OVARIAN CANCER CELLS.

1. Introduction

With a mortality rate of approximately 55%, ovarian cancer (OC) is the deadliest gynecological malignancy due to the high level of recurrent and therapeutic resistant disease. The risk of developing recurrent OC in a woman's lifetime is 1 in 79 and risk of dying from invasive OC is 1 in 109, which highlights the seriousness of OC [1, 2]. Even though numerous treatments are available for OC, the recurrence and resistance to available therapies is a substantial problem for effectively treating patients. Thus, there is a need for more advanced treatments that target the unique aspects of OC biology in recurrent and resistant cases for complete, efficacious management of OC.

Sab (SH3-binding protein 5, SH3BP5) is an outer mitochondrial scaffold protein that facilitates signal transduction events at the organelle-cell interface [3, 4]. Specifically, the interaction between Sab and the c-Jun N-terminal kinase (JNK) leads to inhibition of mitochondrial respiration, generation of reactive oxygen species, and the onset of mitochondrial dysfunction [5-7]. The JNK-Sab interaction (Mito-JNK signaling) is a crucial component of the intrinsic-apoptotic cell death following many toxic insults including chemotherapy agents [8-11]. Furthermore, inhibiting JNK or selectively targeting the JNK-Sab interactions protects various cell types from mitochondrial dysfunction and cell death [5, 6, 12-17]. Chambers et al. demonstrated that interfering with the JNK-Sab interaction blocks JNK-mediated Bcl-2 phosphorylation and emigration from the outer mitochondrial membrane [5]. Lastly, in different models of human disease, Mito-JNK signaling is essential for mitochondrial dysfunction and apoptosis [5, 6, 12-15, 17].

Enhanced Mito-JNK signaling has been linked to an increased capacity to induce apoptosis in cells with elevated Sab concentrations on mitochondria [6, 18]. Thus, increasing Sab levels was exploited as a strategy to enhance the efficacy of chemotherapeutic agents in drug-resistant cancer cells. LY294002 is an inhibitor of the PI3K signaling pathway, and it is used to improve chemotherapeutic efficacy [6, 18]. We observed an increase in Sab concentrations on the outer mitochondrial membrane with sub-chronic low dose treatment of LY294002, which caused the increase in the mitochondrial JNK level during stress. Elevated Sab resulted in a decrease in IC₅₀ values of commonly used chemotherapeutic drugs, cisplatin, and paclitaxel [18]. However, the concentration of LY294002 was higher than physiologically-relevant drug concentrations [19]. As discussed in Chapter 3, the level of Sab expression corresponded to apoptotic priming and drug efficacy in ovarian cancer (OC) cell lines. Furthermore, we observed that increasing Sab levels enhances pro-apoptotic Mito-JNK signaling in OC (Chapter 3) and endometrial (Chapter 4) cells. Clinically, gene expression (microarray) data from the Oncomine repository shows that Sab expression is diminished significantly in OC tumors compared to normal tissue controls. The low levels of Sab in patients also corresponded to disease resistance and poor survival as well. Hence, we propose that therapeutics aimed at increasing Sab levels in gynecological cancers can be used to improve chemotherapeutic efficacy in treatment-resistant gynecological cancers.

Our studies in OC demonstrate that Sab may be a biomarker for apoptotic priming and chemo-sensitivity. Small molecules capable of increasing Sab levels in chemoresistant

cancer cells can render these cells sensitive to established therapies, which represents a new, innovative venue for treating gynecological malignancies. Molecular target-based therapy is considered a new approach for designing and prioritizing OC treatments, and Sab may represent a potential target for these efforts. Moreover, small molecules affecting Sab expression will provide unique insight into mechanisms of OC resistance and regulation of mitochondrial physiology and JNK signaling.

To determine if Sab expression could be modulated by small molecules, we developed a highly-specific and reproducible In-cell western (ICW) assay, a quantitative immunofluorescence-based technique used to detect protein levels [20], to detect the relative levels of Sab in chemoresistant OC cells. After determining antibody specificity, a small panel of 80 compounds was used to identify compounds that induced Sab expression over 72 hours. We found that mitochondrial toxins and estrogens were the most potent inducers of Sab expression, while cyclic AMP analogs and inducers of protein kinase A (PKA) signaling significantly impaired Sab levels. Each compound class was verified in cell culture with conventional western blot analysis; RT-PCR analysis of Sab expression did not always correlate to Sab levels. After validation, the ICW was used to screen a scaffold ranking plate (over 50 compound classes) and a positional scanning library (over 3,000 individual compounds) from the Torrey Pines Institute for Molecular Studies. We identified seven (7) distinct scaffolds that significantly elevated Sab expression in chemoresistant SK-OV-3 cells. From the two best scaffold families, we screened over 900 compounds, and more than forty of those compounds increased Sab-expression. Also,

greater than 20 compounds were robustly lethal to SK-OV-3 and may represent new therapeutic classes to treat resistant diseases. We propose that the Sab ICW is a robust approach to survey small molecules for impacts on Sab protein levels in cells.

2. Methods

2.1. Cells and Tissue Culture

Human HeLa, Hek-293T, and HepG2 cells were cultured in Dulbecco's Minimal Essential Media (DMEM) containing 10% fetal bovine serum (FBS), 100U/ml Penicillin, 10µg/ml streptomycin and 5µg/ml plasmocin. Human SK-OV-3 (ATCC HTB-77) ovarian carcinoma cells were grown in McCoy's 5A (Thermo-Fisher Scientific #SH30200.01) media supplemented with 10% fetal bovine serum (FBS), 100U/ml Penicillin, 100g/ml streptomycin and 5µg/ml plasmocin under normal cell culture conditions (at 37°C and 5% CO₂). Cells were grown to approximately 80% confluency were trypsinized using TrypLE Express (Life Technologies #12604-013) and counted with the TC10 cell counter (Bio-Rad) using trypan blue exclusion dye.

2.2 Antibody Validation and Optimization

The Sab monoclonal antibody (Novus Biologics #H00009467-M01) was validated using cell lines with varying levels of Sab expression. We isolated a HEK-293T clone that did not express Sab (based on RT-PCR for Sab transcripts), and this line, called HEK-293T-381 ("Sab null"), was used as a negative control. Additionally, we used shRNAs (described in Chapter 3) to reduce Sab-expression; meanwhile, pLOC:Sab was used to increase Sab

levels in HeLa cells. Western blots were performed on these cell lines to make sure that the Sab antibody only detected Sab protein in human cells [5, 6, 18].

2.3 In-Cell Western

After optimization of cell number, reagent concentrations, and assay volumes, we developed the following protocol for the Sab ICW. Black walled clear bottom 96 well plate (Thermo Scientific #H2861653050) was seeded with a 200 μ l mixture of trypsinized cells and media, with a count of 20,000 cells per well. Three hours after plating cells were treated with either 1 μ M of known compounds for 72 hours or 50 μ g/ml for compounds in scaffold ranking and lead discovery for 16 hours at normal cell culture conditions. Cells were fixed with 4% paraformaldehyde (Santa Cruz Biotechnology #SC-281692) for 20 minutes at room temperature (RT).

The cells were quenched with 100mM glycine for 5 minutes at RT. Cells were permeabilized using phosphate-buffered saline (PBS) with 0.2% Triton X-100, gently rocking for 20 minutes at RT. After permeabilization, the cells were blocked with 150 μ l of LI-COR blocking buffer (LI-COR Biosciences, 927-40100), gently rocking the plate for 90 minutes at RT. Sab antibody was diluted in blocking buffer at a ratio of 1:1000 and 100 μ l of this solution was added to each well. The plate was incubated on a rocker for 2.5 hours at RT and then washed with 100 μ l of PBST (PBS+0.1% Tween-20) for 5 minutes rocking at RT. This was repeated five times. A 1:800 ratio of anti-mouse secondary antibody (IRDye 800CW anti-mouse, LI-COR Biosciences, 926-32210) and 1:1000 ratio of 1mM of TO-PRO-3 (Invitrogen) were diluted in blocking buffer to make the secondary

antibody solution. Cells were incubated with 100µl of secondary antibody solution in each well for 45 minutes gently rocking at RT. The plate was washed five times with PBST. The wash buffer was removed, and the plate was scanned in Odyssey scanner, and the protein expression was quantified using the LI-COR In-cell western analysis in the Image Studio 2.0 (LI-Cor). Compounds that induced robust cell death, as indicated by a complete loss of TO-PRO-3 fluorescence, were noted, but these compounds were not included in our analysis of Sab expression. Instead, lethal compounds were checked for toxicity in HEK-293T cells to determine if the cell death was selective towards SK-OV-3 cells. A list of known compounds (and their classifications) used for optimization and primary testing can be found in Table 5.1.

2.4 Drug Treatments for Validation

To determine if drugs identified in the ICW screen did indeed affect Sab levels in SK-OV-3 cells, we plated 2.5×10^6 SK-OV-3 cells in the wells of two replicate six-well plate. Each well of the plate was then either left untreated or treated with 0.1% dimethylsulfoxide (DMSO) or 0.01µM, 0.1µM, 1µM, or 10µM of the identified compound. The cells grew in these conditions for 72 hours.

2.5 Validation of Sab Levels

From the cell cultures described above, one plate was used to harvest RNA according to the Qiagen RNEasy Kit protocol, and a second plate was lysed and used for traditional western blot analysis. Cells were lysed, and proteins were quantified according to our previous studies (see Chapter 3). The RNA was used for RT-PCR analysis to evaluate if

the compound affected Sab expression, while the cell lysates samples were used to assess the impact of Sab protein levels. RT-PCR data were normalized to the relative levels of housekeeping genes, actin, glyceraldehyde-3-phosphate dehydrogenase (GAPDH), pyruvate kinase (PK), lactate dehydrogenase (LDH), and ATP synthase subunit F1 α . Protein levels were normalized to tubulin for cellular analyses, while VDAC was used as a mitochondrial normalization control. In the absence of another Sab antibody recognizing a distinct epitope, we used relative JNK translocation to mitochondria to determine if JNK levels were increased or decreased following particular drug treatments in response to cytotoxic stress. Briefly, cells were grown in three (3) 150mm² plates and exposed to candidate compounds at a non-toxic dose for 72 hours. The cells were then exposed to 25 μ M Anisomycin for 45 minutes. Mitochondria were isolated using our established protocol (see references). Mitochondria were lysed using RIPA and analyzed for western blot analysis for the relative levels of JNK. Results were quantified using the Image Studio 2.0 software.

2.6 Assessment of Cell Viability and Chemotherapeutic Efficacy

We performed dynamic BH3-profiling, determined the IC₅₀ values for cisplatin and paclitaxel, and assessed relative cell viability using a panel of assays in the presence of cisplatin/paclitaxel after 72 hours of exposure to the identified compounds to evaluate the impact on drug efficacy. The methods for measuring IC₅₀ values and cytotoxicity assessments were described in the previous chapters.

2.7 Statistics

Cell-based measures and traditional western blotting data were analyzed by performing Mann-Whitney U Tests for direct comparisons, and analysis of variance was performed to compare multiple compounds. For studies involving cell-based screening, assay quality was determined using a Z' calculation of positive (Sab-overexpressing cells) and negative controls (Sab-silenced cells) using the equation described in [21]. The Z' was interpreted in regards to the coefficient of variation (CV) for specific cells. Only measures with >15% between basal measures and positive and negative controls were considered for use. Valid assay parameters were considered those that had a Z' score >0.675 and CV greater than 50%. Reproducibility was determined between measures using a Tukey post-hoc analysis.

3. Results

3.1 Development of a reliable ICW to detect Sab levels in human cell lines and OC cells.

To develop our in-cell western (ICW) approach, we selected an antibody previously used in our lab to monitor Sab levels in cell lysates and tissue homogenates. To be sure that the antibody would be selective enough for use in a high-throughput screening assay, we measured the antibodies specificity in cell lines that did not express Sab (HEK-293T-381 – Sab-null), HEK-293T, and HEK-293 cells overexpressing Sab (pLOC: Sab) and silencing Sab (pLKO.1:shSab). Accordingly, the antibody did not detect the anticipated Sab band nor any additional bands in the Sab null cells (Figure 5.1). While different levels of Sab

were found in HEK-293T, and HEK-293T cells with increased and decreased Sab expression (Figure 5.1). COX-IV was used to demonstrate equal loading of mitochondrial

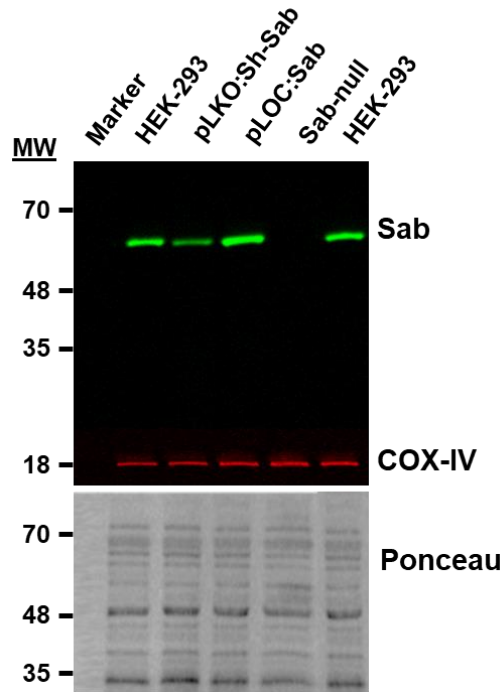


Figure 5.1: Validation of the Sab-specific antibody for assay development A western blot analysis of HEK-293T cells was performed with an antibody (Novus Biologicals) specific for human Sab. The HEK-293T cells were transfected with plasmids for silencing Sab (pLKO:shSab), which expressed a Sab shRNA, and pLOC:Sab, a plasmid that over-expressed Sab. A HEK-293T clone that did not express Sab (Sab null) was used as a negative control. An extended membrane image is presented to demonstrate the minimal non-specific binding of the antibody. COX-IV was used as a mitochondrial loading control, while Ponceau S was used to demonstrate equal loading among cell types.

Proteins and Ponceau staining of membranes were used as a loading control (Figure 5.1).

After validating the reliability of the antibody, we optimized cell conditions to develop an assay that provided a sufficient dynamic range between Sab null and Sab overexpressing HEK-293T cells. In Figure 5.2, we demonstrate the signal distribution of the in-cell western

in the different HEK-293T types. The assay has a dynamic range of 10-fold on a log scale which is a large dynamic range for a high-throughput assay.

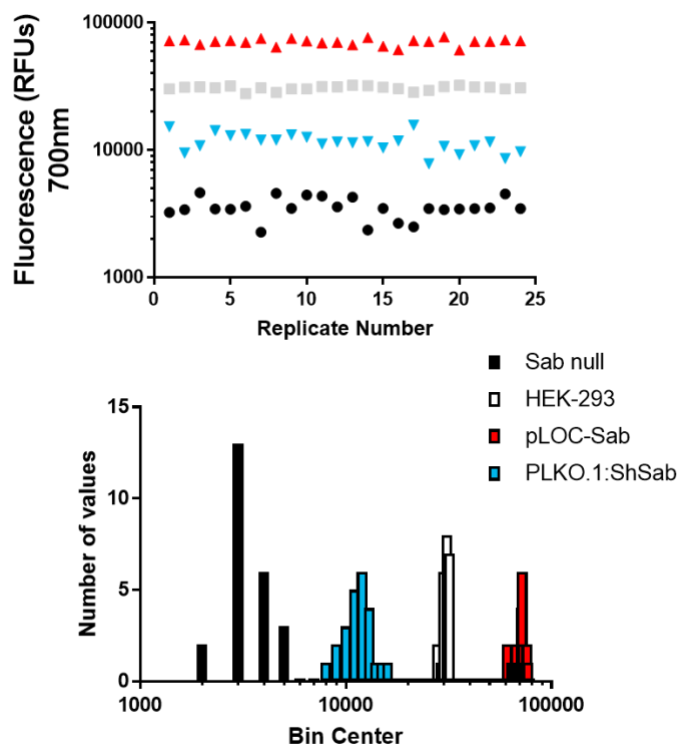


Figure 5.2: Optimizing the ICW for detection of distinct levels of Sab in cells. (top panel) The ICW was performed in a 96-well plate, and the Sab-related fluorescence was determined using the Odyssey CLx imager. Repeated measures (20) were performed for each cell type with 16 blank wells. (Bottom panel) Sab fluorescence distributions were plotted for each condition, and a Z' score was calculated to be 0.76 between Sab-null and normal HEK-293T cells suggesting a strong assay.

3.2 Pilot studies reveal that mitochondrial toxins and estrogens increase Sab expression.

To determine if Sab levels could be manipulated by pharmacological agents, we used a small pool (62) of compounds from the LOPAC 1280 library that were known to impact

mitochondrial physiology and cellular kinase cascades to examine to impact on Sab levels. We plated 12,000 HEK-293T cells in a 96-well plate and treated with compounds at a 10-fold dilution from manufacturer's preparation. We performed the ICW at 72 hours post-treatment. The data were analyzed, and Sab-fluorescence was normalized to viable cells

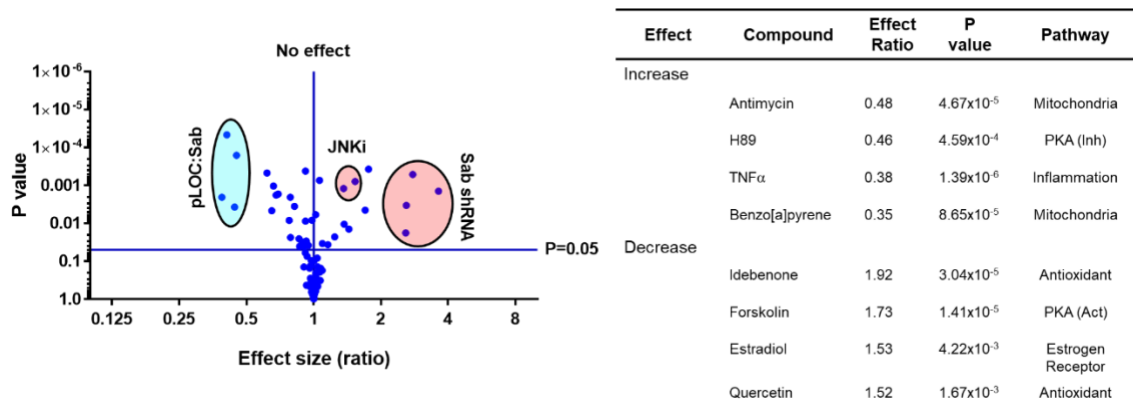


Figure 5.3: A preliminary screen to examine Sab levels following pharmacological treatments. (left) Normalized Sab fluorescence was plotted, and the relative change with respect to controls was plotted on a volcano plot. Assay controls for Sab-expression, such as over-expression, silencing, and JNK inhibitors are highlighted. (right) A table summarizing the compounds that increased and decreased Sab levels in HEK-293T cells. The P-value and pathways are noted to the right of the compound effect ratio.

by TO-PRO-3 staining. The data were plotted on a volcano plot to observe Sab concentration trends (Figure 5.3).

The compounds responsible for the accumulation of Sab in cells were mitochondrial toxins, such as antimycin and benzo[α]pyrene, and inflammatory compounds, like TNF- α . Alternatively, antioxidants were found to decrease Sab levels in cells. Intriguingly, estrogen metabolites were also found to decrease Sab levels. Intriguingly, PKA modulators were potent effectors of Sab levels; wherein, inhibition of PKA by H89 increased Sab

concentrations, while activation of PKA by forskolin decreased Sab levels. This preliminary screen indicated that the ICW is a valid tool to detect changes in Sab abundance in cells and identify compounds that affect Sab concentrations.

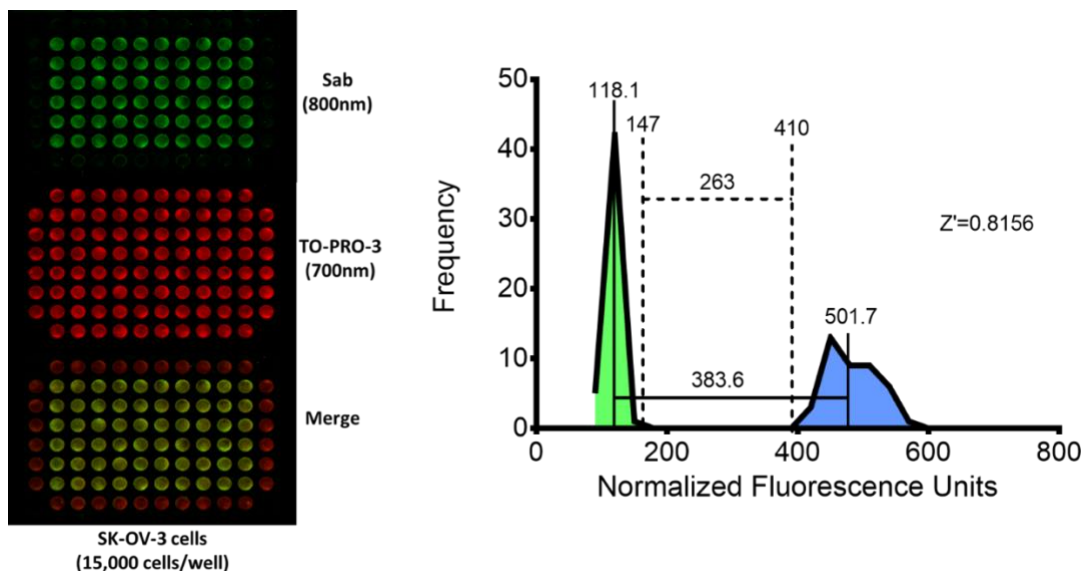


Figure 5.4: A redeveloped ICW for Sab detection in chemoresistant SK-OV-3 cells. (left) A representative validation assay for SK-OV-3 cells. (right) The Z' score calculation for four (4) replicate assay. A high Z' score of 0.8156 was achieved indicating a strong assay.

3.3 Examination of the scaffold ranking library from Torrey Pines Institute for Molecular Studies (TPIMS). To identify compounds that could increase Sab levels in chemoresistant OC cells, we re-optimized the assay for SK-OV-3 cells (see Chapter 3). The redeveloped assay is shown in Figure 5.4.

To determine if pharmacological agents could increase Sab levels in SK-OV-3 cells, we took the most potent Sab enhancers from our preliminary screen and used those molecules to assess the feasibility of elevating Sab in resistant OC cells. In Figure 5.5, H89,

LY294002, antimycin, rotenone, oligomycin, and hydrogen peroxide (H₂O₂) were exposed to SK-OV-3 cells at increasing doses for up to 72 hours, and the Sab ICW was performed. All of the compounds except oligomycin increased Sab expression in SK-OV-3 cells (Figure 5.5). This result confirms that Sab levels can be increased by pharmacological agents in SK-OV-3 cells.

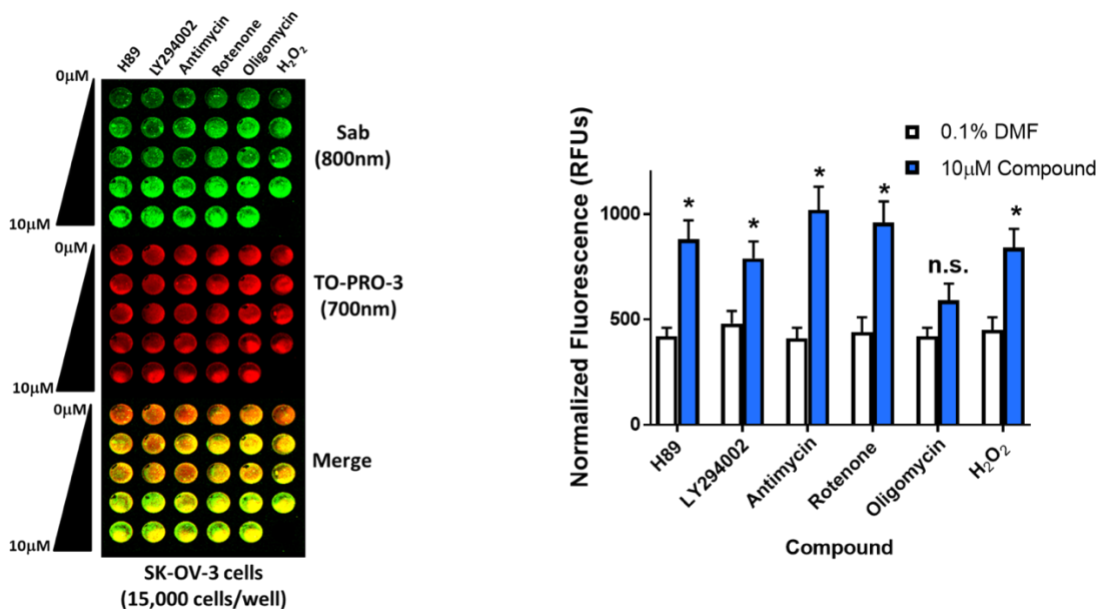


Figure 5.5: A feasibility screen for detecting changes in Sab levels in SK-OV-3 cells. (left) A representative assay in SK-OV-3 cells using compounds known to enhance Sab levels in HEK-293T cells. We plated 15,000 cells per well and treated them with increasing concentrations of drugs for up to 72 hours. The Sab ICW was performed after treatment. (right) The quantification of three replicate assays was performed with Sab fluorescence normalized to TO-PRO-3 staining. One-way ANOVAs were performed to identify significant differences as indicated by an * (P<0.05). Data are displayed as means with error bars representing plus and minus one standard deviation.

Next, we utilized a scaffold-ranking and positional-scanning library from the Torrey Pines Institute for Molecular Studies (TPIMS, Port St. Lucie, FL) to identify new compounds that could increase Sab concentrations in chemoresistant OC cells. We screened ~50

scaffold families in a randomized plate from TPIMS. We plated the cells and treated with compound families from TPIMS for 48 hours and applied the Sab ICW. Two separate screens were performed per batch (Figure 5.6A), and after the assay we applied our statistical parameters to identify prospective compound families (Figure 5.6B & 5.6C).

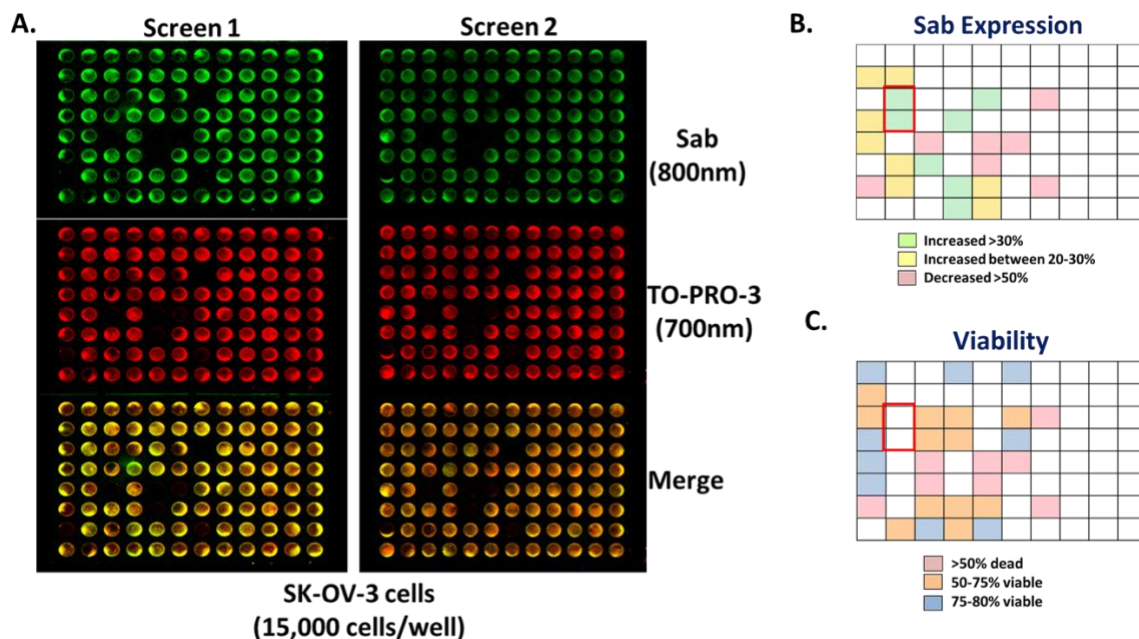


Figure 5.6: A scaffold ranking screen and compound criteria for the TPIMS library. (A) A representative screen in SK-OV-3 cells using compounds from TPIMS. We plated 15,000 cells per well and treated them with increasing concentrations of drugs for 48 hours. The Sab ICW was performed after treatment. (B) The quantification criteria for assessing Sab levels and (C) viability by TO-PRO-3 staining.

The screen netted seven (7) compound families that could be viable compounds for elevating Sab expression in chemoresistant OC cells. We took those compounds and we assayed the compounds in the ICW to validate the compounds as Sab inducers. In Figure

5.7, the secondary screen is shown, and a spaghetti plot shows that one group elevated Sab expression significantly, and that family was 1661, suggesting it may be a useful chemosensitizer.

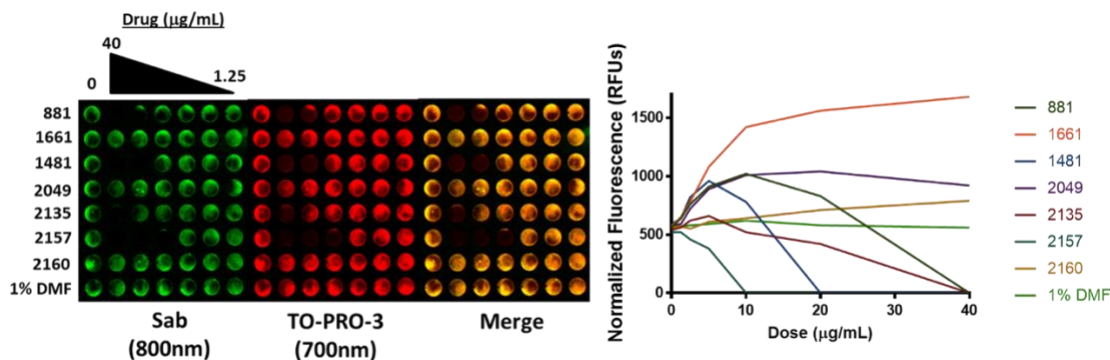


Figure 5.7: A positional scanning screen to identify best-in-class compounds from the TPIMS library. (left) A representative screen in SK-OV-3 cells using compound families from TPIMS. We plated 15,000 cells per well and treated them with increasing concentrations of drugs for 48 hours. The Sab ICW was performed after treatment. (right) Quantification of the assay illustrates the increase with Sab fluorescence in response drug dose.

Lastly, we evaluated family 1661 in SK-OV-3 cells to determine if the compound elevated Sab and to assess the impact on viability. We performed a dose-dependent ICW for compound family 1661, and we found that the compound family did increase Sab expression in a dose-dependent manner and had limited impact on viability in a physiologically relevant dose range (Figure 5.8A). These measures are quantified in Figure 5.8B. We then treated SK-OV-3 with 1661 at increasing concentrations in two replicate preparation from TPIMS. In these studies (Figure 5.8C), Sab levels increase in a dose-dependent manner without impacting mitochondrial protein concentration (indicated by COX-IV levels). Ponceau staining was used as a loading control. These results demonstrate

that family 1661 could be a potent enhancer of Sab protein levels in chemoresistant OC cells or OC tumors.

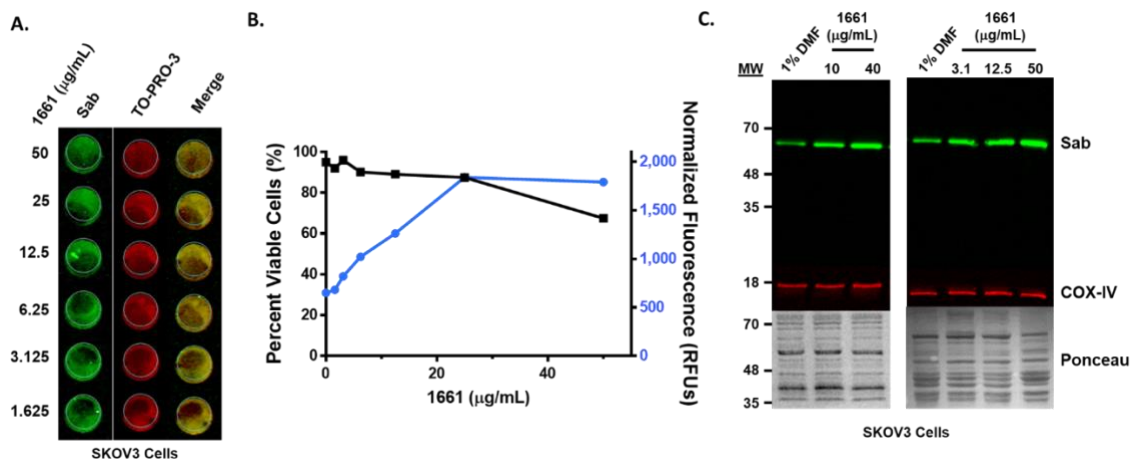


Figure 5.8: Evaluation of family 1661 in SK-OV-3 cells. A. Dose-dependent ICW for family 1661. B. Quantification of A. C. SK-OV-3 cells were treated with increasing dose of compound family 166. Sab level increases in a dose-dependent manner. Data are displayed as means with error bars representing plus and minus one standard deviation.

4. Discussion

The ability to predict tumor-specific vulnerabilities to therapeutic regimes will be an invaluable resource aiding personalized medical efforts, and such technologies will improve patient outcomes associated with ovarian cancer. In the current work, we describe a high-throughput technique to quantify the Sab concentrations in human cell lines with the aim of identifying compounds capable of increasing Sab levels to improve chemotherapeutic efficacy. This approach has many advantages over traditional way to quantify protein expression. Western blotting has been used as a major approach to quantify protein expression; however, this high-throughput ICW is advantageous over low-

throughput WB. WB is labor-intensive and time-consuming. There is a requirement of more resources, i.e., more cells and more compounds or drugs, however, with this approach, the experiment can be done in one well of a microplate, which saves time and resources. There is a 100-fold decrease in volume in micro-plate compared to the experiment done in Petri-dishes [20]. As we have screened scaffold of compounds, this approach was very useful for detection of Sab-level. During western blotting, while lysing the cells, we use different detergents, and this might interfere with the protein detection, however, in ICW assay we detect the protein within the cell without interfering with its expression. With the fixation step, there might be a change in fluorescence signal. We used 4% PFA in PBS with less fluorescence property [20]. We also experimented without using the fixation agent and didn't observe a significant difference in fluorescence signal with or without fixation. The approach that we developed uses TO-PRO-3 for antibody normalization which is a preferred method [22]. TO-PRO-3 is a DNA staining dye and is used to normalize the number of cells. TO-PRO-3 stains the live cells, hence it also detects the cytotoxicity of the compound under screening. Because of the availability of two separate lasers and two different fluorescence channel in Odyssey Imager, we could detect two different targets, the antigen of our interest (Sab) and TO-PRO-3 dye. The fluorescent antibody is detected at 800nm channel while the TO-PRO-3 stain is detected at 700nm channel. The emission spectra are separated by 100nm, showing minimum interference in the signal.

As suggested by Chen et al., antibody specificity is critical for validation of ICW assay. We observed a single band of Sab in western blotting, showing the specificity of Sab in SKOV-3 cells [22]. The antibody is highly specific, as we do not see any alternate bands (Figure 5.1), which makes it an ideal candidate for assay development. More importantly, the specificity of the antibody provided an opportunity for a large dynamic range (Figure 5.2). This 10-fold change will permit the identification of robust as well as modest modulation of Sab concentrations in cells, which will be essential to elucidate the regulation of Sab in different tissues and cell types. More importantly, a range of effective compounds can be identified for use in OC studies; whereby, a modest, non-toxic adjustment in Sab levels may be required to restore apoptotic capacity.

The demonstration that Sab levels could be altered by pharmacological agents was crucial to establishing our assay (Figures 5.3 and 5.5) because if we could not manipulate Sab with chemicals, the only other option would be through gene therapy approaches, which are not ready for clinical use. It was interesting that manipulation of PKA signaling had such a profound effect on Sab levels. This observation is interesting in part because mitochondrial PKA signaling has been shown to sustain mitochondrial health and improve cell survival [23-28]. These are the opposite effects of mitochondrial JNK signaling. It is interesting to conjecture that protective PKA signaling may post-translationally impair detrimental Sab-mediated events in human cells. Alternatively, enhanced Sab mediated signaling may be required to disengage the protection of PKA in apoptotic cells. The relationship of these two signaling pathways is ongoing in our lab.

A potent enhancer of Sab levels were mitochondrial toxins. Indeed, we have shown that mitochondrial JNK signaling is responsive to mitochondrial stress and JNK signaling regulates Sab expression [7, 18]. This data suggests that the upregulation of Sab following mitochondrial damage may be a stress response rather than an abortive mechanism. Similarly, TNF- α is a potent activator of JNK signaling during inflammation, and JNK is responsible for activation transcriptional responses in immune responses; however, the role of mitochondrial JNK in this regard is still unknown [29]. Further studies will be needed to determine the physiological role of mitochondrial JNK signaling on Sab.

The presence of estradiol as a negative regulator of Sab levels was equally interesting because estrogen has been shown to regulate AP-1 transcription, a target activated by JNK. Also, estrogen has been shown to prevent neurodegeneration in Parkinson's models where our work has demonstrated that Sab-mediated JNK signaling drives neuron loss in the substantia nigra [15, 30-32]. Alternatively, estrogen has been shown to induce JNK-mediated apoptosis in cancer cells [33, 34]. It is likely the impact of estrogen signaling on JNK-mediated processes will be cell type and tissue-specific; thus, elucidating the impact of estrogen signaling on Sab levels in OC cells will be important since estrogen can be used as hormone therapy in gynecological cancers [35-37].

We used this technique to screen the compounds that could increase Sab expression in SKOV-3 cells. As mentioned previously, increasing Sab expression sensitizes the cancer cells for chemotherapeutic agents [18]. We were looking for compounds that would increase the Sab expression with less cytotoxic effect, eventually causing less harm to

normal cells (Figure 7). Our screening strategy was to find the compounds that would increase the Sab expression by 30% with least effect on the viability of the cells. As shown in Figure 5.4, the assay was highly reproducible with the screening of same compounds. We identified a compound family 1661 that will be the topic of ongoing development for use in preclinical OC models. Regardless of the outcome of 1661, we have developed an assay that can be used to screen existing chemical as possible agents to improve chemotherapeutic efficacy in chemoresistant OC cells.

References:

- 1 Ferlay, J., Soerjomataram, I., Dikshit, R., Eser, S., Mathers, C., Rebelo, M., Parkin, D. M., Forman, D. and Bray, F. (2015) Cancer incidence and mortality worldwide: sources, methods and major patterns in GLOBOCAN 2012. *Int J Cancer*. **136**, E359-386
- 2 Siegel, R. L., Miller, K. D. and Jemal, A. (2016) Cancer statistics, 2016. *CA: A Cancer Journal for Clinicians*. **66**, 7-30
- 3 Wiltshire, C., Gillespie, D. A. and May, G. H. (2004) Sab (SH3BP5), a novel mitochondria-localized JNK-interacting protein. *Biochem Soc Trans*. **32**, 1075-1077
- 4 Wiltshire, C., Matsushita, M., Tsukada, S., Gillespie, D. A. and May, G. H. (2002) A new c-Jun N-terminal kinase (JNK)-interacting protein, Sab (SH3BP5), associates with mitochondria. *Biochem J*. **367**, 577-585
- 5 Chambers, J. W., Cherry, L., Laughlin, J. D., Figuera-Losada, M. and Lograsso, P. V. (2011) Selective inhibition of mitochondrial JNK signaling achieved using peptide mimicry of the Sab kinase interacting motif-1 (KIM1). *ACS chemical biology*. **6**, 808-818

- 6 Chambers, T. P., Santiesteban, L., Gomez, D. and Chambers, J. W. (2017) Sab mediates mitochondrial dysfunction involved in imatinib mesylate-induced cardiotoxicity. *Toxicology*. **382**, 24-35
- 7 Chambers, J. W. and LoGrasso, P. V. (2011) Mitochondrial c-Jun N-terminal kinase (JNK) signaling initiates physiological changes resulting in amplification of reactive oxygen species generation. *J Biol Chem*. **286**, 16052-16062
- 8 Dhanasekaran, D. N. and Reddy, E. P. (2008) JNK signaling in apoptosis. *Oncogene*. **27**, 6245-6251
- 9 El Fajoui, Z., Toscano, F., Jacquemin, G., Abello, J., Scoazec, J. Y., Micheau, O. and Saurin, J. C. (2011) Oxaliplatin sensitizes human colon cancer cells to TRAIL through JNK-dependent phosphorylation of Bcl-xL. *Gastroenterology*. **141**, 663-673
- 10 Ito, Y., Mishra, N. C., Yoshida, K., Kharbanda, S., Saxena, S. and Kufe, D. (2001) Mitochondrial targeting of JNK/SAPK in the phorbol ester response of myeloid leukemia cells. *Cell Death Differ*. **8**, 794-800
- 11 Zhang, Z. B., Jiang, X. G., Liang, Z. Q. and Gu, Z. L. (2012) Arsenic trioxide inhibits the growth of human glioma stem cells through activating the JNK pathway. *Molecular & Cellular Toxicology*. **8**, 187-193
- 12 Win, S., Than, T. A., Fernandez-Checa, J. C. and Kaplowitz, N. (2014) JNK interaction with Sab mediates ER stress induced inhibition of mitochondrial respiration and cell death. *Cell death & disease*. **5**, e989
- 13 Win, S., Than, T. A., Han, D., Petrovic, L. M. and Kaplowitz, N. (2011) c-Jun N-terminal kinase (JNK)-dependent acute liver injury from acetaminophen or tumor necrosis factor (TNF) requires mitochondrial Sab protein expression in mice. *The Journal of biological chemistry*. **286**, 35071-35078
- 14 Win, S., Than, T. A., Min, R. W. M., Aghajan, M. and Kaplowitz, N. (2016) c-Jun N-terminal kinase mediates mouse liver injury through a novel Sab (SH3BP5)-dependent pathway leading to inactivation of intramitochondrial Src. *Hepatology*. **63**, 1987-2003

- 15 Chambers, J. W., Howard, S. and LoGrasso, P. V. (2013) Blocking c-Jun N-terminal kinase (JNK) translocation to the mitochondria prevents 6-hydroxydopamine-induced toxicity in vitro and in vivo. *J Biol Chem.* **288**, 1079-1087
- 16 Coffey, E. T. (2014) Nuclear and cytosolic JNK signalling in neurons. *Nat Rev Neurosci.* **15**, 285-299
- 17 Nijboer, C. H., Bonestroo, H. J., Zijlstra, J., Kavelaars, A. and Heijnen, C. J. (2013) Mitochondrial JNK phosphorylation as a novel therapeutic target to inhibit neuroinflammation and apoptosis after neonatal ischemic brain damage. *Neurobiology of disease.* **54**, 432-444
- 18 Chambers, T. P., Portalatin, G. M., Paudel, I., Robbins, C. J. and Chambers, J. W. (2015) Sub-chronic administration of LY294002 sensitizes cervical cancer cells to chemotherapy by enhancing mitochondrial JNK signaling. *Biochem Biophys Res Commun.* **463**, 538-544
- 19 Rosenzweig, K. E., Youmell, M. B., Palayoor, S. T. and Price, B. D. (1997) Radiosensitization of human tumor cells by the phosphatidylinositol3-kinase inhibitors wortmannin and LY294002 correlates with inhibition of DNA-dependent protein kinase and prolonged G2-M delay. *Clinical Cancer Research.* **3**, 1149-1156
- 20 EGORINA, E. M., SOVERSHAEV, M. A. and ØSTERUD, B. (2006) In-Cell Western assay: a new approach to visualize tissue factor in human monocytes. *Journal of Thrombosis and Haemostasis.* **4**, 614-620
- 21 Altekar, M., Homon, C. A., Kashem, M. A., Mason, S. W., Nelson, R. M., Patnaude, L. A., Yingling, J. and Taylor, P. B. (2006) Assay Optimization: A Statistical Design of Experiments Approach. *JALA: Journal of the Association for Laboratory Automation.* **11**, 33-41
- 22 Chen, H., Kovar, J., Sissons, S., Cox, K., Matter, W., Chadwell, F., Luan, P., Vlahos, C. J., Schutz-Geschwender, A. and Olive, D. M. (2005) A cell-based immunocytochemical assay for monitoring kinase signaling pathways and drug efficacy. *Analytical Biochemistry.* **338**, 136-142

- 23 Beene, D. L. and Scott, J. D. (2007) A-kinase anchoring proteins take shape. *Curr Opin Cell Biol.* **19**, 192-198
- 24 Dagda, R. K., Gusdon, A. M., Pien, I., Strack, S., Green, S., Li, C., Van Houten, B., Cherra, S. J., 3rd and Chu, C. T. (2011) Mitochondrially localized PKA reverses mitochondrial pathology and dysfunction in a cellular model of Parkinson's disease. *Cell Death Differ.* **18**, 1914-1923
- 25 De Rasmio, D., Panelli, D., Sardanelli, A. M. and Papa, S. (2008) cAMP-dependent protein kinase regulates the mitochondrial import of the nuclear encoded NDUFS4 subunit of complex I. *Cell Signal.* **20**, 989-997
- 26 Dickey, A. S. and Strack, S. (2011) PKA/AKAP1 and PP2A/Bbeta2 regulate neuronal morphogenesis via Drp1 phosphorylation and mitochondrial bioenergetics. *J Neurosci.* **31**, 15716-15726
- 27 Kim, H., Scimia, M. C., Wilkinson, D., Trelles, R. D., Wood, M. R., Bowtell, D., Dillin, A., Mercola, M. and Ronai, Z. A. (2011) Fine-tuning of Drp1/Fis1 availability by AKAP121/Siah2 regulates mitochondrial adaptation to hypoxia. *Mol Cell.* **44**, 532-544
- 28 Merrill, R. A., Dagda, R. K., Dickey, A. S., Cribbs, J. T., Green, S. H., Usachev, Y. M. and Strack, S. (2011) Mechanism of neuroprotective mitochondrial remodeling by PKA/AKAP1. *PLoS Biol.* **9**, e1000612
- 29 Weston, C. R. and Davis, R. J. (2007) The JNK signal transduction pathway. *Curr Opin Cell Biol.* **19**, 142-149
- 30 Srivastava, S., Weitzmann, M. N., Cenci, S., Ross, F. P., Adler, S. and Pacifici, R. (1999) Estrogen decreases TNF gene expression by blocking JNK activity and the resulting production of c-Jun and JunD. *The Journal of Clinical Investigation.* **104**, 503-513
- 31 Saunders-Pullman, R., Gordon-Elliott, J., Parides, M., Fahn, S., Saunders, H. R. and Bressman, S. (1999) The effect of estrogen replacement on early Parkinson's disease. *Neurology.* **52**, 1417-1417

- 32 Chambers, J. W., Pachori, A., Howard, S., Ganno, M., Hansen, D., Jr., Kamenecka, T., Song, X., Duckett, D., Chen, W., Ling, Y. Y., Cherry, L., Cameron, M. D., Lin, L., Ruiz, C. H. and Lograsso, P. (2011) Small Molecule c-jun-N-terminal Kinase (JNK) Inhibitors Protect Dopaminergic Neurons in a Model of Parkinson's Disease. *ACS Chem Neurosci.* **2**, 198-206
- 33 Altiok, N., Koyuturk, M. and Altiok, S. (2007) JNK pathway regulates estradiol-induced apoptosis in hormone-dependent human breast cancer cells. *Breast Cancer Research and Treatment.* **105**, 247-254
- 34 Domitrovic, R. (2011) The Molecular Basis for the Pharmacological Activity of Anthocyanins. *Current Medicinal Chemistry.* **18**, 4454-4469
- 35 Group, S. G. O. C. P. E. C. W., Burke, W. M., Orr, J., Leitao, M., Salom, E., Gehrig, P., Olawaiye, A. B., Brewer, M., Boruta, D., Herzog, T. J., Shahin, F. A. and Society of Gynecologic Oncology Clinical Practice, C. (2014) Endometrial cancer: a review and current management strategies: part II. *Gynecol Oncol.* **134**, 393-402
- 36 Group, S. G. O. C. P. E. C. W., Burke, W. M., Orr, J., Leitao, M., Salom, E., Gehrig, P., Olawaiye, A. B., Brewer, M., Boruta, D., Villella, J., Herzog, T., Abu Shahin, F. and Society of Gynecologic Oncology Clinical Practice, C. (2014) Endometrial cancer: a review and current management strategies: part I. *Gynecol Oncol.* **134**, 385-392
- 37 McMeekin, D. S., Filiaci, V. L., Thigpen, J. T., Gallion, H. H., Fleming, G. F. and Rodgers, W. H. (2007) The relationship between histology and outcome in advanced and recurrent endometrial cancer patients participating in first-line chemotherapy trials: A Gynecologic Oncology Group study. *Gynecologic Oncology.* **106**, 16-22

Chapter 6
CONCLUSION

The goal of this research project was to identify and characterize molecular events responsible for therapeutic resistance in gynecological cancers. Our rationale was that once mechanisms driving resistance and recurrence are known therapeutic approaches can be developed to target these events. Our previous research has focused on how changes in mitochondrial signaling influence the susceptibility of mammalian cells toward cytotoxic stimuli. Specifically, we have reported that increasing Sab-mediated signaling sensitizes cells to stressors in a JNK dependent manner. The result of this change in mitochondrial signaling is a lower threshold for the induction of apoptosis. Thus, we hypothesized that diminished Sab expression in gynecological cancers might contribute to chemotherapeutic resistance in late-stage disease. To see if this was the case, we examined gene expression data from patients and manipulated Sab expression in ovarian and uterine cancer cells to determine how Sab-mediated events impacted the chemoresponsiveness of cancer cells. Ultimately, we found that decreased Sab levels in gynecological cancer cell lines prevent proper induction of apoptosis, and restoring Sab levels resulting in improved chemosensitization. Finally, we used a high-throughput approach to identify pharmacological agents capable of increasing Sab levels in chemoresistant ovarian cancer cells. Future studies will revolve around elucidating the impact of Sab levels on gynecological cancers in preclinical models.

A summary of the primary findings from each of the project aims can be found below.

First, we identified a decrease in Sab expression using microarray data obtained from ovarian cancer patient tumors. Ovarian cancer cell lines were obtained and characterized based on the relative abundance of Sab and the relative responsiveness to chemotherapeutic drugs. We found that the cell lines expressing low levels of Sab were resistant to these chemotherapeutic drugs while the cell lines with a high level of Sab showed responsiveness to chemotherapeutic drugs. Sab levels were then manipulated by ectopic expression or gene silencing, which changes the magnitude of mitochondrial JNK signaling in ovarian cancer cells. Cells expressing a high level of Sab are primed for apoptosis, which means these cells have a higher level of pro-apoptotic BH3-only proteins and low level of anti-apoptotic Bcl-2 proteins. Hence our result suggests, Sab level reflects the concentration of BH3 only proteins. Dynamic BH3-profiling can determine chemoresponsiveness in cancer cells. Sab profiling along with dynamic BH3-profiling can be used as a combined approach to predict chemoresponsiveness in the ovarian cancer patient.

Second, we examined the impact of Sab levels on chemosusceptibility in uterine cancer. Analysis of patient samples revealed that Sab expression was diminished in advanced and recurrent uterine cancers. We used two different cell lines; a primary-site derived cell line with high Sab levels and a metastatic-derived cell line with low Sab expression. We assessed mitochondrial physiology and apoptotic capacity in these cells and found that low

Sab concentrations in the metastatic cell line corresponded to elevated respiration and proton leak, which was accompanied by elevated levels of anti-apoptotic Bcl-2 proteins. Uterine cancer cells with elevated Sab concentrations were more glycolytic and had a greater abundance of pro-apoptotic BH3-only proteins. Like ovarian cancer cells, uterine cancer cells with a higher level of Sab were sensitive to chemotherapeutic drugs and had higher expression of pro-apoptotic BH3 only proteins.

Finally, we surmised that pharmacological agents capable of elevating Sab concentrations could be used to prime gynecological cancer cells for apoptosis and lower the dose of chemotherapy. Not only could this approach improve the effectiveness of existing drugs, but the lower dose would mean that there would be less of a chance for off-target toxicity. To identify chemicals capable of increasing Sab in resistant cancer cells, we developed an in-cell western method to detect the relative abundance of Sab cancer cells. The approach was validated in HEK-293T cells where it was found that mitochondrial toxins and inhibitors of PKA were potent enhancers of Sab levels. The in-cell western was then applied to chemoresistant ovarian cancer cells and screened against a scaffold ranking library from the Torrey Pines Institute for Molecular Studies. We found promising compounds capable of increasing Sab levels in SK-OV-3 cells. Thus, the Sab in-cell western can be used as a method of screening compounds for novel therapies or to determine the relative responsiveness of patient cancers to specific therapies. Detecting the level of Sab in patients' tumor would help to determine the dose and efficacy of

chemotherapeutic drugs. We propose this technique can be a useful tool in personalized medicine.

The main limitation of our study is the use of cell lines instead of patient-derived tumors. The cell lines might not be representative of tumor cells from patients. Cell lines may develop additional mutations during adaptation to culture conditions, and additional genetic variations (i.e., epigenetic changes) not representative of the real cancer cells. Additionally, the cell lines used in our studies were from different patients and distinct genetic backgrounds. These difference may also explain the differences in Sab-levels rather than mechanisms responsible for oncogenesis; likewise, these discrete differences among cell lines may also explain the susceptibility to chemotherapeutic agents. Thus, increasing Sab levels may be a means to lower the chemosensitivity of all cells and the phenomenon may not be specific to gynecological cancers. Further, recent studies preliminarily conclude that stem cells within tumors may be responsible for chemoresistance. Because we did not use stem cells from gynecological tumors, we may have missed other factors contributing to chemoresistance. Thus, future studies will focus on the isolation and characterization of chemoresponsiveness from patient-derived samples.

Another concern is that increasing Sab levels in cells of distinct genetic background all enhanced the responsiveness of cells to chemotherapy agents. When viewed in light of our studies in cardiomyocytes demonstrating that increasing the levels of Sab enhances the

effect of toxic exposures, it appears as though increasing Sab levels could lower the apoptotic threshold for all cell types. This means that, if compounds were found that could increase Sab levels in gynecological cancers, the drugs would have to be selectively targeted to cancer cells to avoid off-target toxicities. This highlights the importance of characterizing Sab-mediated signaling in many tissues before delivering potential therapies to patients.

Another pitfall of our study is the sample size, for ovarian cancer study we have used four cell lines while for uterine cancer study only two cell lines. The number of cell lines is too small to derive any true conclusions regarding Sab-mediated signaling and chemoresistance in gynecological cancers. Again, future studies with more cell types of appropriate origins will be needed to ascertain the true relevance of Sab-mediated signaling changes in gynecological cancers.

Despite the limitations of the current study, our study opens a new avenue for connecting Sab-mediated OMM signaling to the physiology, prognosis, and treatment of gynecological cancers.

In closing, we have found that Sab levels indicate the relative apoptotic capacity in gynecological cancer cells and increasing Sab levels represents a unique approach to improve therapeutic outcomes in patients.

Appendices

Supplementary Information for Chapter 3

SUPPLEMENTAL FIGURE 1: Sab is not present in non-mitochondrial subcellular fractions from OC cell lines.

SUPPLEMENTAL FIGURE 2: Quantification of Phospho-JNK and JNK levels on untreated and STS-treated OC cell lines.

SUPPLEMENTAL FIGURE 3: Anisomycin stress induces mitochondrial JNK translocation, and demonstrates differences in mitochondrial JNK signaling among the four OC cell lines.

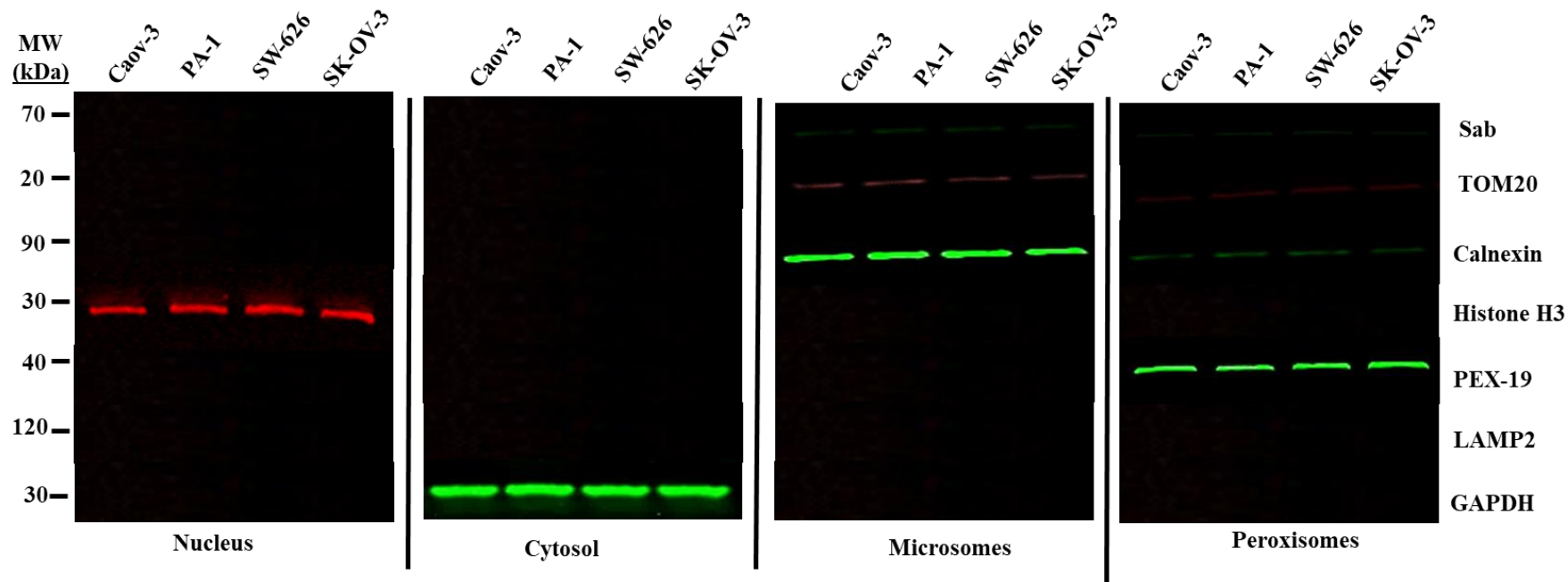
SUPPLEMENTAL FIGURE 4: TO-PRO-3 Assays were used to determine cellular IC₅₀ values for chemotherapeutic drugs.

SUPPLEMENTAL FIGURE 5: Correlation plots of IC₅₀ values for the four OC cell lines.

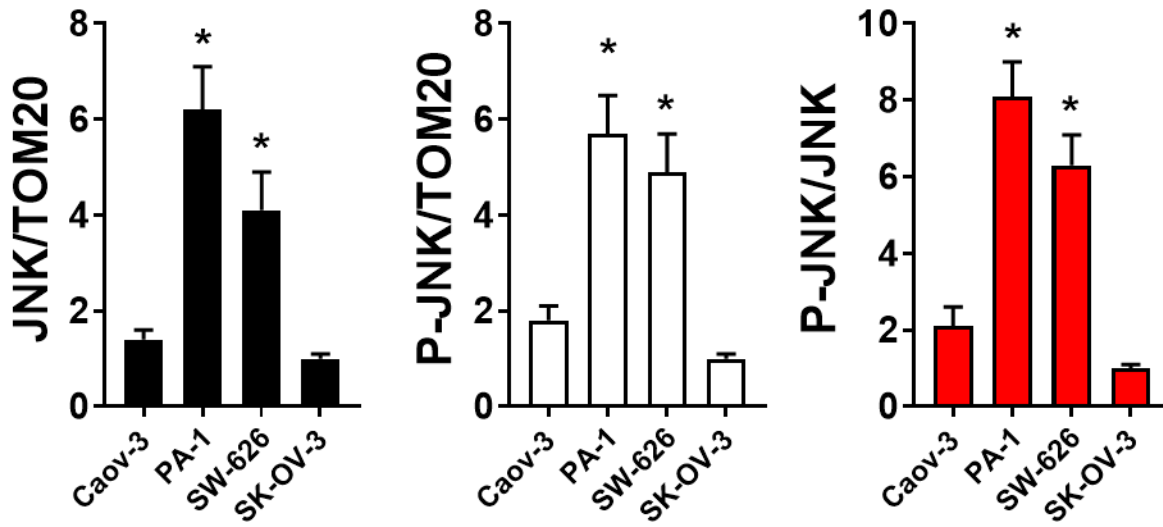
SUPPLEMENTAL FIGURE 6: Quantification of Bcl-2 and BH3-only western analysis of OC Cell Lines.

SUPPLEMENTAL FIGURE 7: Ectopic Expression of Sab in SK-OV-3 cells does not impact the cellular apoptosis profile.

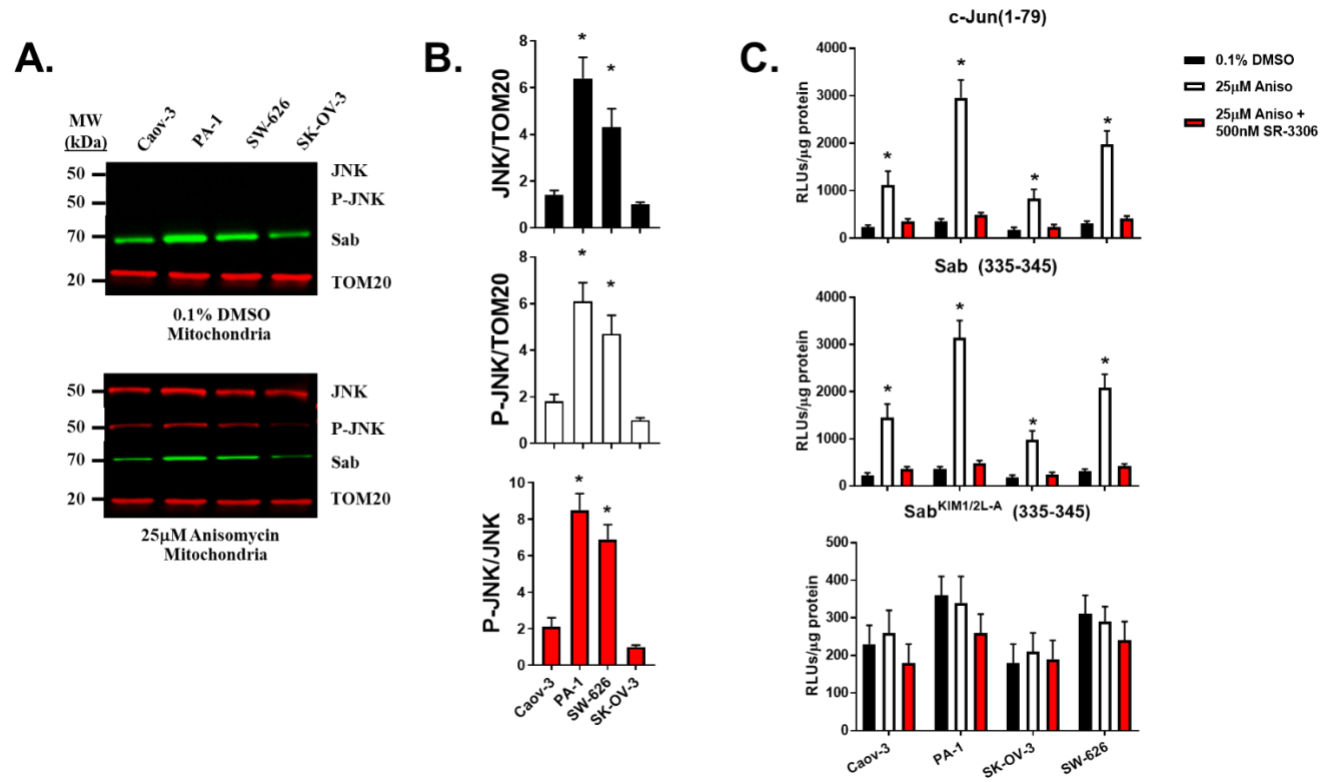
Supplemental Figure 1



Supplemental Figure 2

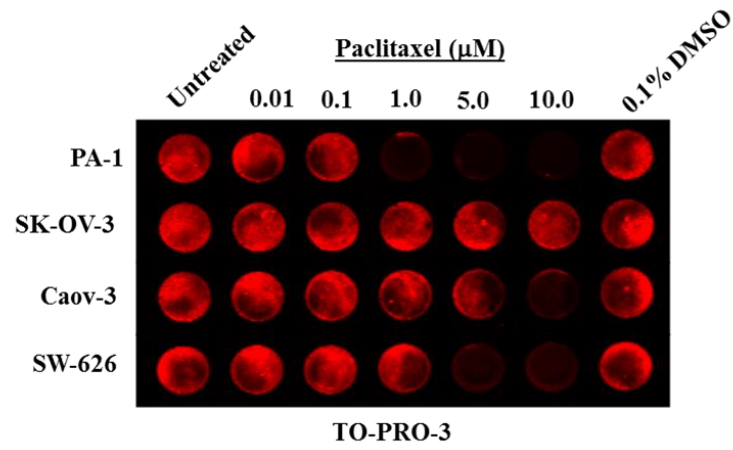


Supplemental Figure 3

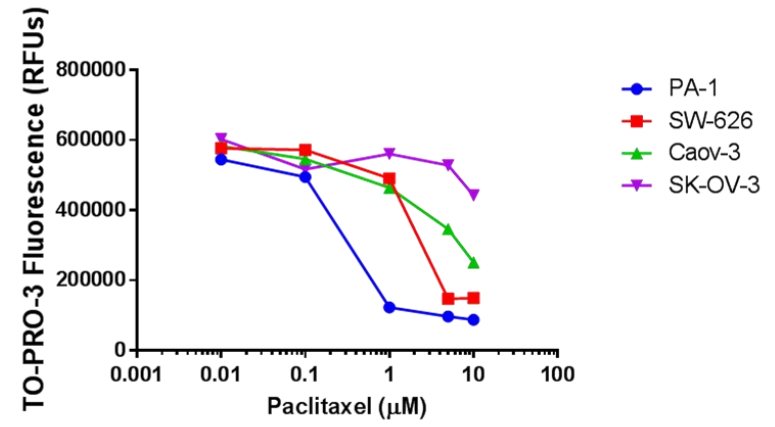


Supplemental Figure 4

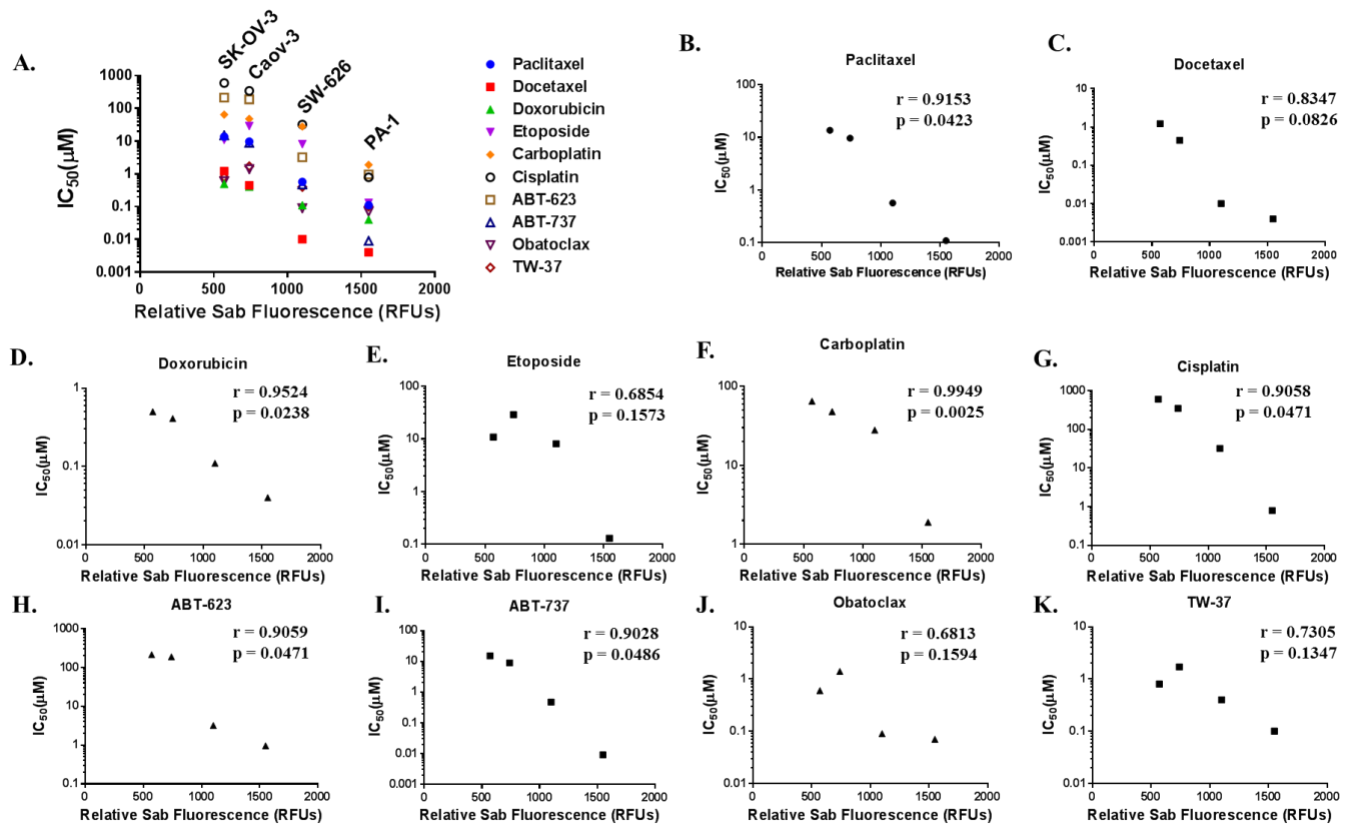
A.



B.

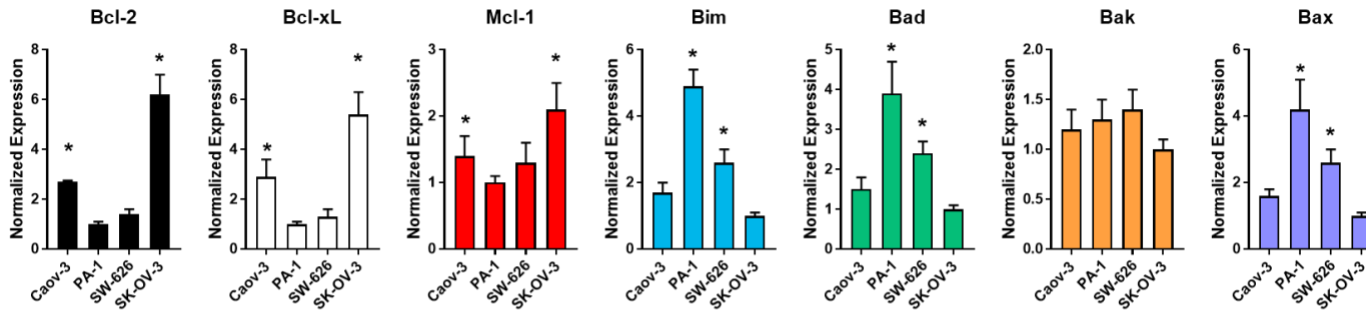


Supplemental Figure 5

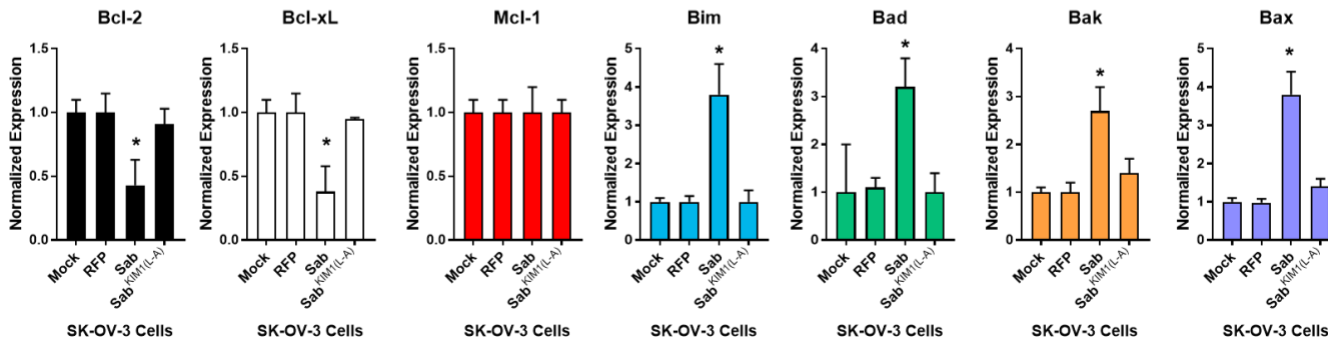


Supplemental Figure 6

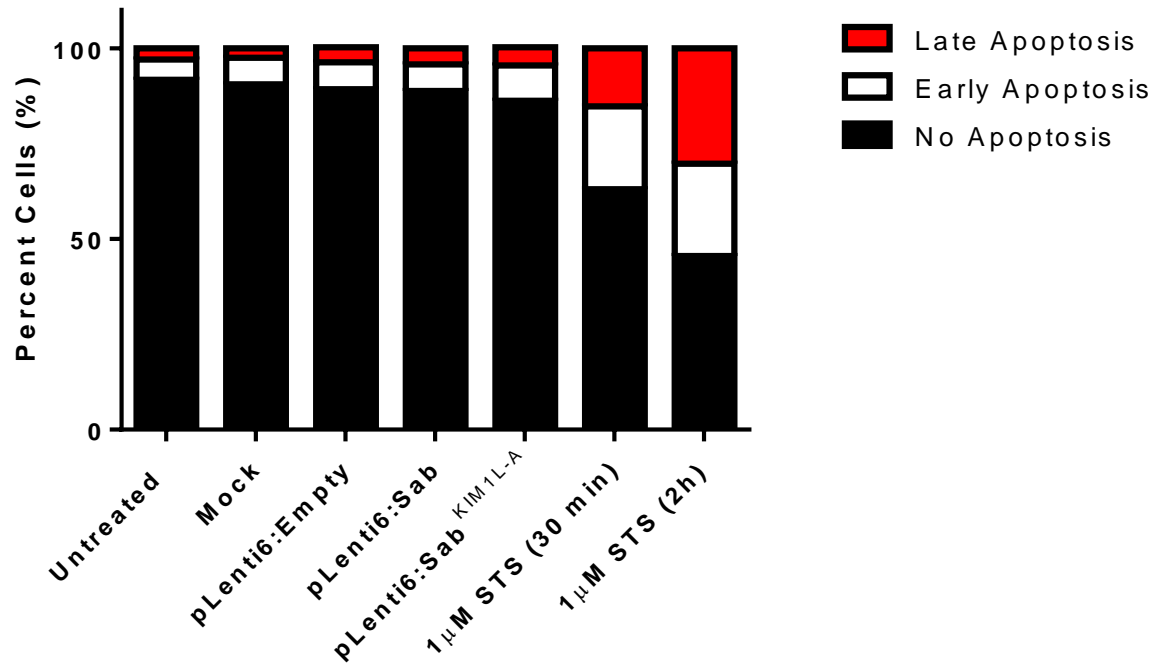
A. Ovarian Cancer Cell Lines (Figure 4)



B. Sab Over-expressing SK-OV-3 (Figure 5)



Supplemental Figure 7



VITA

IRU PAUDEL

Born, Kathmandu, Nepal

2003-2006

B.S., Microbiology
Tribhuvan University
Kathmandu, Nepal

2010

M.S., Medical Microbiology
Tribhuvan University
Kathmandu, Nepal

2012-2018

Doctoral Candidate
Herbert Wertheim College of Medicine
Florida International University
Miami, Florida

AWARDS AND HONORS

1. ASBMB Graduate Student and Post-Doctoral Travel Award, sponsored by the ASBMB (2015, 2016).
2. Winner, FIU scholarly forum graduate research poster competition 2017.

PUBLICATIONS and PRESENTATIONS

1. Paudel, I, and Chambers, JW. *Sab levels correlated to chemosensitivity in uterine cancer*. (Manuscript under preparation).
2. Paudel, I, and Chambers, JW. *High-throughput assay to detect Sab*. (Manuscript under preparation).
3. Paudel, I, Hernandez, SM, Portalatin, GD, Chambers, TP, Chambers, JW. *Sab Concentrations Indicate Chemotherapeutic Susceptibility in Ovarian Cancer Cell Lines*. Submitted to *Biochemical Journal*. (Under Review).
4. Pawitwar, SS, Dhar, S, Tiwari, S, Ojha, CR, Lapierre, J, Martins, K, Rodzinski, A, Parira, T, Paudel, I, Li, J, Dutta, RK. *Overview on the Currents status of Zika Virus Pathogenesis and Animal Related Research*. *Journal of Neuroimmune Pharmacology*. 2017:1-8.

5. Vanbellinghen, QP, Castellanos, A, Rodriguez-Silva, M, Paudel, I, Chambers, JW, Fernandez-Lima, FA. *Analysis of Chemotherapeutic Drug Delivery at the Single Cell Level Using 3D-MSI-TOF-SIMS*. *Journal of The American Society for Mass Spectrometry*. 2016 Dec 1; 27(12), 2033-2040.
6. Chambers, TP, Portalatin, GM, Paudel, I, Robbins, CJ, and Chambers, JW. *Sub-chronic administration of LY294002 sensitizes cervical cancer cells to chemotherapy by increasing mitochondrial JNK signaling*. *Biochemical Biophysical Communications (BBRC)*. 2015 Aug 7; 463(4):538-44.
7. Paudel, I and Chambers, JW. (Oral presentation). *Sab-mediated signaling influences mitochondrial dynamics*. United mitochondrial disease foundation (UMDF), Alexandria, VA. June 28-July 1, 2017.
8. Paudel, I and Chambers, JW. (Poster presentation). *Sab-mediated signaling regulates mitochondrial dynamics*. Graduate student's appreciation week (GSAW), Miami, FL. March 27-28, 2017.
9. Paudel, I and Chambers, JW. (Oral presentation). *Sab-mediated signaling regulates mitochondrial fission*. Herbert Wertheim College of Medicine 2016 Student Research Symposium and Annual Student and Faculty Awards at Florida International University, Miami, FL. April 28-29, 2016.
10. Paudel, I and Chambers, JW. (Poster presentation). *Sab-mediated signaling regulates mitochondrial fission*. Experimental Biology 2016 (EB 2016), San Diego, CA. April 2-6, 2016.
11. Paudel I, Giulianotti, MA, Welmaker, GS, and Chambers, JW. (Poster presentation). *Identification of novel ovarian cancer chemotherapies that target mitochondrial-cell communication*. Experimental Biology 2015 (EB2015), Boston, MA. March 29- April 3, 2015.
12. Paudel, I and Chambers, JW. *Targeting mitochondrial-cell communication to improve chemoresponse in ovarian cancer*. (Oral Presentation). Graduate student's appreciation week (GSAW), Miami, FL. April 6-7, 2015.
13. Paudel I, Giulianotti, MA, Welmaker, GS, and Chambers, JW. (Poster presentation). *Identification of novel ovarian cancer chemotherapies that target mitochondrial-cell communication*. Canesearch 2015, Miami, FL. March 4, 2015.

14. Paudel, I and Chambers, JW. *Targeting mitochondria for improvement of chemoresponse in ovarian cancer*. (Oral Presentation). Florida Drug Discovery Acceleration Program Collaborator Conference Torrey-Pines Institute of Molecular Studies, Port St. Lucie, FL. January 23, 2015.